

Die Rolle des Tumorsuppressorproteins Merlin bei der
Pathogenese von NF2-assoziiierter Polyneuropathie

Dissertation

**zur Erlangung des Doktorgrades
doctor rerum naturalium (Dr. rer. nat.)**

vorgelegt dem Rat der Medizinischen Fakultät der
Friedrich-Schiller-Universität Jena

Von Dr. med. Alexander Schulz, M.Sc.
Geboren am 30.11.1985 in Pößneck

Gutachter

1.

2.

3.

Tag der öffentlichen Verteidigung:

„Dies ist nicht das Ende. Es ist nicht einmal der
Anfang vom Ende. Aber es ist, vielleicht,
das Ende vom Anfang.“

Sir Winston Churchill

Abkürzungsverzeichnis

CMT	Charcot-Marie-Tooth
GAP	GTPase-Activating Protein (engl.)
GDI	GDP-Dissociation Inhibitor (engl.)
GDP	Guanosindiphosphat
GEF	Guanosine Triphosphate Exchange Factor (engl.)
GTP	Guanosintriphosphat
kDa	Kilodalton
KSP	Lysin(K)-Serin(S)-Prolin(P)
MRT	Magnetresonanztomographie
m/s	Meter pro Sekunde
N.	Nervus
NF2	Neurofibromatose Typ 2
nm	Nanometer
PNS	Peripheres Nervensystem
RhoA	Ras homolog gene family, member A (engl.)
ROCK	Rho-associated kinase (engl.)
ZNS	Zentrales Nervensystem

Inhaltsverzeichnis

1.	Zusammenfassung	1
2.	Einleitung	2
2.1.	Struktur und Funktion axonaler Fortsätze von Nervenzellen	2
2.2.	Allgemeine Einführung zu ‚Periphere Neuropathie‘	4
2.3.	Neurofilamente und das Zytoskelett von Axonen	6
2.4.	Die Erkrankung Neurofibromatose Typ 2	8
2.5.	Das Tumorsuppressorprotein Merlin	10
3.	Ziele der Arbeit	13
4.	Publizierte Originalarbeiten	14
4.1	„The role of merlin isoform 2 in neurofibromatosis type 2-associated polyneuropathy“ (Nature Neuroscience, 2013)	14
4.2.	„In vivo Electrophysiological Measurements on Mouse Sciatic Nerves“ (Journal of Visualized Experiments, 2014)	27
5.	Zur Veröffentlichung eingereichte Übersichtsarbeit	36
5.1.	„A neuronal function of the tumor suppressor protein merlin“ (Frontiers in Cellular Neuroscience, under review)	36
6.	Diskussion	60
7.	Ausblick	66
8.	Schlussfolgerungen	67
9.	Literatur- und Quellverzeichnis	68
10.	Lebenslauf	74
11.	Danksagung	77
12.	Ehrenwörtliche Erklärung	78

1. Zusammenfassung

Das autosomal-dominant vererbliche Tumorsyndrom Neurofibromatose Typ 2 (NF2) wird verursacht durch Mutationen im Tumorsuppressor-Gen *NF2*, das für das Protein Merlin codiert. Neben gutartigen Schwann-Zell-Tumoren, die das periphere und zentrale Nervensystem befallen können, leiden die meisten NF2-Patienten an peripherer Neuropathie. Diese Schädigung peripherer Nerven kann in Abwesenheit solcher Tumoren auftreten, die die Nerven komprimieren. Das legt eine Pathogenese unabhängig von der Entwicklung von Schwannommen nahe. Im Rahmen der vorliegenden Arbeit sollte daher untersucht werden, ob das Tumorsuppressorprotein Merlin eine bisher nicht charakterisierte Funktion in axonalen Fortsätzen von Nervenzellen hat, die das Auftreten von Neuropathien bei NF2-Patienten erklären kann.

Zur Bearbeitung dieser Fragestellung wurden primäre Kulturen von Nervenzellen, gentechnisch veränderte Mäuse sowie Nervenbiopsien von NF2-Patienten verwendet. Mithilfe dieser Ansätze konnte erarbeitet werden, dass eine spezielle, durch alternatives Spleißen entstandene Isoform des Proteins Merlin eine entscheidende Funktion zur Aufrechterhaltung der Struktur von Axonen besitzt. Merlin Isoform 2, das in axonalen Fortsätzen vorkommt, ist über eine definierte Signalkaskade in der Lage, die Phosphorylierung von Neurofilamenten zu bewirken; einem wichtigen Strukturprotein von Axonen. Eine reduzierte Phosphorylierung dieser Neuronen-spezifischen Zytoskelett-Proteine, die mit einer Reihe neurologischer Pathologien assoziiert ist, konnte im Nervengewebe von Mäusen nachgewiesen werden, bei denen diese spezielle Isoform von Merlin fehlt, sowie in Nervenbiopsien von NF2-Patienten. Dieser irreguläre Phosphorylierungszustand von Neurofilamenten wiederum führt zu einer veränderten, ultrastrukturellen Morphologie der betroffenen Axone.

Basierend auf den Daten dieser Arbeit kann postuliert werden, dass eine reduzierte oder fehlerhafte Expression von Merlin in Nervenzellen selbst die Entwicklung einer Neuropathie bewirken kann. Damit könnte auch erstmals mechanistisch erklärt werden, warum NF2-Patienten periphere Nervenschäden erleiden, die in Abwesenheit von Schwann-Zell-Tumoren auftreten können.

2. Einleitung

2.1. Struktur und Funktion axonaler Fortsätze von Nervenzellen

Nervenzellen im peripheren (PNS) und zentralen Nervensystem (ZNS) stellen hoch-polarisierte und komplexe, zelluläre Funktionseinheiten dar. Im Zuge seiner physiologischen Entwicklung sind vielfältige form- und gestaltprägende Schritte für die Funktionstüchtigkeit und Plastizität des Nervensystems notwendig. Neu generierte Nervenzellen migrieren von ihrem Entstehungsort zu ihrer Zielposition, bilden neuronale Fortsätze wie Axone und Dendriten, und etablieren synaptische Kontakte mit anderen Zellen. Um dabei einen suffizienten Informationsfluss zwischen zwei oder mehreren Nervenzellen zu gewährleisten, übertragen Neurone Signale nach Verarbeitung im Regelfall unidirektional vom dendritischen zum axonalen Pol der Zelle. Axonale Fortsätze von Nervenzellen können also als efferente Leitungsbahnen beschrieben werden, mit denen Neurone elektrische Signale zu anderen Zellen weiterleiten können, die zuvor im Dendritenbaum und Zellkörper integriert und verarbeitet wurden.

Axone als hochspezialisierten Zellfortsätze bedürfen während und nach ihrer Etablierung einer zeitlich und räumlich streng kontrollierten Regulierung von Zell-extrinsischen und -intrinsischen Signalen. Die Rho-Familie („Ras homolog gene family“) der kleinen G-Proteine, die als molekulare Schalter agieren, indem sie zwischen einem aktiven, GTP (Guanosintriphosphat)-beladenen und einem inaktiven, GDP (Guanosindiphosphat)-beladenen Zustand rotieren (Abbildung 1), sind hierbei wichtige, regulatorische Steuerelemente (Etienne-Manneville and Hall, 2002). Sie sind imstande, extrazelluläre Stimuli auf das Zytoskelett von Nervenzellen zu übertragen und haben so eine Schlüsselposition in der Regulation von neuronaler Morphogenese, Polarität, Fortsatzwachstum und Synaptogenese (Luo, 2000). Die bekanntesten Mitglieder dieser Familie sind die Proteine Cdc42 und Rac1, die das Ausbilden von Nervenzellfortsätzen begünstigen, sowie RhoA, das inhibierend auf das Wachstum von Neuriten wirkt (Nikolic, 2002). Welche Rolle allerdings diese kleinen G-Proteine bei der lebenslangen Aufrechterhaltung der Struktur von Axonen haben, ist bislang unvollständig verstanden.

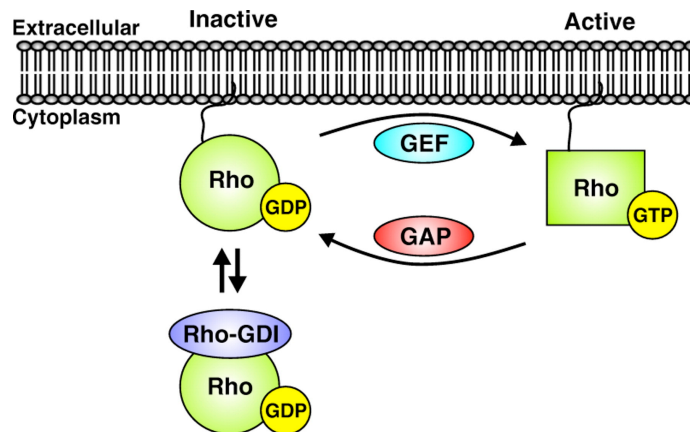


Abb. 1: Schematische Darstellung der GTP-abhängigen Aktivierung von G-Proteinen am Beispiel von Rho. GEF (Guanosine Triphosphate Exchange Factor), GAP (GTPase-Activating Protein) und Rho-GDI (GDP-Dissociation Inhibitor) sind hier als bekannte, regulierende Proteine jener Aktivierung aufgeführt (Huveneers and Danen, 2009).

Axone im PNS können hinsichtlich ihrer Faserqualitäten und Durchmesser kategorisiert werden (Tabelle 1). Dabei wird deutlich, dass der Durchmesser des Axons prinzipiell mit dem Grad der Myelinisierung korreliert, und dass diese wiederum die Nervenleitungsgeschwindigkeit der Nervenfasern determiniert, die mittels elektrophysiologischer Methoden bestimmt werden kann.

Tabelle 1: Klassifikation der Nervenfasern im PNS nach Erlanger und Gasser.
Modifiziert nach (Niesel and Van Aken, 2006)

Faserklasse	Myelinisierung	Axondurchmesser (µm)	Leitungsgeschwindigkeit (m/s)
A α	dick	15	75
A β	vorhanden	10	60
A γ	vorhanden	5	25
A δ	dünn	5	20
B	dünn	3	10
C	nicht vorhanden	1	1

Entsprechend dieser Einteilung und der sich daraus ableitenden Eigenschaften der jeweiligen Fasern ergibt sich eine sehr heterogene Verteilung von Axonen innerhalb eines peripheren Nerven und natürlich zwischen verschiedenen Nerven im PNS. In Abhängigkeit von seiner jeweiligen Funktion kann ein peripherer Nerv

motorische, sensible oder vegetative Fasern sowie eine bedarfsgerechte Kombination dieser drei Faserqualitäten beinhalten.

2.2. Allgemeine Einführung zu ‚Periphere Neuropathie‘

‚Periphere Neuropathie‘ ist eine Krankheitsbezeichnung für nicht-traumatische Funktionsschädigungen peripherer Nerven, die vielfältige Ursachen haben. Neuropathien peripherer Nerven können als eigenständige Entität oder im Rahmen von Systemerkrankungen auftreten. Tabelle 2 zeigt die vielfältigen Klassifikationsmöglichkeiten dieser heterogenen Krankheitsgruppe, die zu den häufigsten neurologischen Pathologien gehört (Brandt *et al.*, 2005).

Tabelle 2: Klassifikationsmöglichkeit peripherer Neuropathien
nach (England and Asbury, 2004)

Klassifikationskriterium	
Pathogenese	axonal; demyelinisierend; gemischte bzw. sekundäre Formen
Ätiologie	entzündlich; toxisch; metabolisch; infektiös; vaskulär; paraneoplastisch; autoimmun
Verteilung	symmetrisch; asymmetrisch; fokal; multifokal; distal; proximal
Ausprägung / Lokalisation	Mononeuropathie simplex (ein Nerv); Mononeuropathie multiplex (Schwerpunkt-Neuropathie); Polyneuropathie (mehrere bis viele Nerven)
Verlauf	akut; subakut; chronisch
Betroffene Faserqualität	motorisch; sensibel; autonom; gemischt

Im Falle krankhafter Veränderungen peripherer Nerven im Sinne einer peripheren Neuropathie können lediglich einzelne Faserqualitäten betroffen sein oder eine Mischung der verschiedenen, in Tabelle 1 aufgeführten Axon-Klassen. Dementsprechend unterschiedlich kann sich die Beschwerdesymptomatik bei Patienten darstellen (Reinhardt and Grehl, 2012). Die funktionelle

Beeinträchtigung von sensiblen Fasern kann zu Parästhesien und Sensibilitätsstörungen führen, die zumeist strumpf- oder handschuhförmig sowie symmetrisch auftreten. Außerdem ist – häufig als Frühsymptom – eine Störung des Vibrationsempfindens (Pallhypästhesie) festzustellen. Die Schädigung motorischer Fasern kann eine von distal nach proximal aufsteigende Hypo- bis Areflexie zur Folge haben, die schlussendlich in muskulärer Schwäche (Parese) mit begleitender Atrophie der Muskulatur enden kann. Darüber hinaus beklagt ein Großteil der Patienten, die an peripherer Neuropathie leiden, über eine variabel ausgeprägte Schmerzsymptomatik (neuropathischer Schmerz).

Bei der Diagnostik von neuropathischen Erkrankungen stehen eine ausführliche Anamnese und körperliche Untersuchung im Vordergrund, was durch elektrophysiologische Messungen und die Ermittlung spezieller Blutparameter zur Beurteilung der nutritiven Verhältnisse und / oder Schadstoffbelastung ergänzt wird (Diener and Weimar, 2012). Gegebenenfalls können Liquoruntersuchungen notwendig werden, die Aussagen über ein entzündliches Krankheitsgeschehen zulassen. Außerdem kann es in einigen Fällen hilfreich sein Nerv- und / oder Muskelbiopsien zu entnehmen, um Ausmaß und Verteilung struktureller Veränderungen zu evaluieren. Gewöhnlich wird für Nervenbiopsien wegen seines oberflächlichen Verlaufs und seiner rein sensorischen Faserqualitäten der N. suralis auf der Lateralseite eines Unterschenkels entnommen (McLeod, 2000).

Zu den mit großem Abstand häufigsten Ursachen für eine periphere Neuropathie zählen Diabetes mellitus Typ 1 und 2 sowie chronischer Alkoholabusus. Bedenkt man die Altersverteilung dieser beiden hauptsächlichen Ätiologien für die Entwicklung von Neuropathien erschließt sich auch die stark altersabhängige Prävalenz der peripheren Neuropathie: Während 2-3% der Gesamtbevölkerung daran leiden, ist sie bei etwa 8% der über 55-jährigen Menschen anzutreffen (Martyn and Hughes, 1997). Seltener Ursachen für periphere Neuropathie sind hingegen infektiöse, entzündliche, toxische oder genetische Ursachen.

Die häufigste erbliche Form von Neuropathien ist die Charcot-Marie-Tooth-Erkrankung (CMT), deren Prävalenz mit etwa 20–40 pro 100.000 Menschen angegeben wird (Pareyson and Marchesi, 2009). Innerhalb dieser Gruppe unterscheidet man anhand der Pathogenese Erkrankungen, die entweder auf einen demyelinisierenden Prozess (z.B. CMT1) oder einen axonalen Schaden

(z.B. CMT2) zurückzuführen sind (Berciano, 2011). Bei vielen dieser axonalen Formen von hereditären Neuropathien konnte man als Ursache mittlerweile Mutationen in axonalen Struktur- oder Transportproteinen nachweisen (Bennett and Chance, 2001).

2.3. Neurofilamente und das Zytoskelett von Axonen

Neurone als überwiegend post-mitotische Zellen gewährleisten über die gesamte Lebensspanne die Aufrechterhaltung sinnvoller synaptischer Verbindungen. Während die meisten anderen Körperzellen im Laufe der Zeit durch neugebildete Zellen ersetzt werden können, müssen die gleichen – in manchen Fällen bis zu einem Meter langen – axonalen Fortsätze über viele Dekaden hinweg intakt und funktionstüchtig bleiben. Um dies zu gewährleisten, benötigen alle Axone eine ebenso flexible und wie robuste Struktur.

Neurofilamente sind Neuronen-spezifische Intermediärfilamente (Liem and Messing, 2009) und bilden mit Aktinfilamenten und Mikrotubuli jeweils eine von drei Hauptklassen von Zytoskelett-Proteinen. Diese Klassen lassen sich unter anderem aufgrund ihrer mikroskopischen Größe im Querschnitt voneinander unterscheiden. Während Aktinfilamente einen Durchmesser von 7 nm aufweisen, sind Intermediärfilamente etwa 10 nm und Mikrotubuli etwa 25 nm dick. Dieser Umstand erleichtert auch die Identifikation von Zytoskelett-Proteine in elektronenmikroskopischen Aufnahmen (Abbildung 2).

Neurofilamente stellen den maßgeblichen strukturbestimmenden Bestandteil der axonalen Fortsätze von Nervenzellen dar. Gleichsam sind Neurofilamente in myelinisierten Axonen zahlenmäßig deutlich häufiger enthalten als Mikrotubuli (Hoffman *et al.*, 1984), was ihre Bedeutung für die strukturelle Integrität von Axonen mit großem Durchmesser nahelegt. Anomalien an bzw. von Neurofilamenten sind mit einer Vielzahl von neurologischen Erkrankungen im Menschen assoziiert, z.B. erbliche Neuropathien oder Amyotrophe Lateralsklerose (Perrot *et al.*, 2008). Sie sind generell aus drei verschiedenen Untereinheiten aufgebaut, die entsprechend ihres molekularen Gewichtes als NF-L („light“; 68 kDa), NF-M („medium“; 150 kDa) und NF-H („heavy“; 200 kDa) bezeichnet werden, und durch eigenständige Gene codiert werden. Mutationen in allen drei Neurofilament-codierenden Genen können axonale Schädigungen verursachen

und dann zu typischen neuropathischen Symptomen wie Schmerz, Sensibilitätsstörungen oder muskuläre Schwäche führen (England and Asbury, 2004).

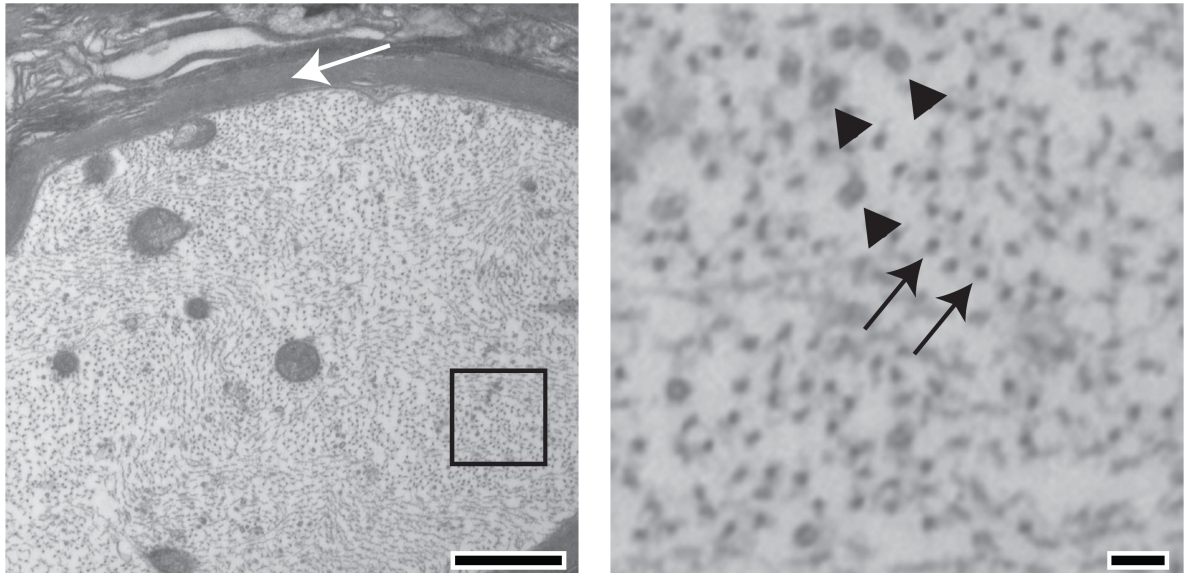


Abb. 2: Elektronenmikroskopische Aufnahmen eines myelinisierten Axons (Querschnitt durch den N. ischiadicus der Maus). Die Myelin-Scheide im linken Übersichtsbild ist durch einen weißen Pfeil gekennzeichnet (Maßstab Balken 500 nm). Das rechte Bild ist eine Vergrößerung des gekennzeichneten Bereiches im linken Bild (Maßstab Balken 50 nm). Einzelne Neurofilamente sind durch einen Pfeil, Mikrotubuli durch Pfeilspitzen gekennzeichnet (eigene Aufnahme).

Darüber hinaus bestimmen Neurofilamente direkt den Durchmesser von Axonen. Dies kann entweder durch Erhöhung der Transkriptionsaktivität und Proteinmenge (Zhu *et al.*, 1997) oder Phosphorylierungsvorgänge (de Waegh *et al.*, 1992) bewerkstelligt werden. Ein Neurofilament-Molekül kann dabei bis zu 50 Phosphorylierungsstellen tragen, sogenannte ‚KSP repeats‘ (Lysin-, Serin- und Prolin-reiche Proteinregionen), die durch eine Vielzahl bekannter Kinasen phosphoryliert werden können (Perrot *et al.*, 2008).

Biophysikalisch gleicht die Übertragung von Phosphatresten im Zuge von Phosphorylierungsprozessen der Addition von negativen Ladungen. Durch die Erhöhung von negativen Ladungen kommt es an gleichförmig orientierten Neurofilament-Molekülen zu erhöhten Abstoßungskräften untereinander. Dadurch kommt es zu einem Auseinanderweichen der Neurofilamente mit konsekutiver Vergrößerung des Durchmessers des jeweiligen Axons (de Waegh *et al.*, 1992).

Mit Hilfe von elektronenmikroskopischen Aufnahmen kann man diesen Abstand zwischen Neurofilamenten quantifizieren (engl. „interfilament distance“) und auf diese Weise eine qualitative Aussage über deren Phosphorylierungsgrad ermitteln (Abbildung 2).

2.4. Die Erkrankung Neurofibromatose Typ 2

Mutationen des Tumorsuppressor-Proteins Merlin verursachen das autosomal-dominante Tumorsyndrom Neurofibromatose Typ 2 (NF2) (Asthagiri *et al.*, 2009). Im Jahre 1993 konnte das dafür verantwortliche Gen *NF2* auf Chromosom 22q12 identifiziert werden (Rouleau *et al.*, 1993). NF2 zeichnet sich durch die Entwicklung von glialen Tumoren aus, die maßgeblich durch entartete Schwann-Zellen gebildet werden (Schwannome). Das klinisch bedeutsamste Charakteristikum der Erkrankung ist das Auftreten von Vestibularis-Schwannomen (Abbildung 3), das sich meist bilateral manifestiert und zu Schwerhörigkeit bzw. Taubheit führen kann (Baser *et al.*, 2003). NF2-Patienten leiden jedoch häufig auch an den Folgen benignen Schwann-Zell-Tumore im Bereich des Rückenmarks und peripherer Nerven. Grundsätzlich sind Mutationen im *NF2* Gen verantwortlich für nahezu sämtlich sporadisch auftretende Schwannome sowie für etwa 50 % der sporadischen Meningeome (Kim *et al.*, 2006).

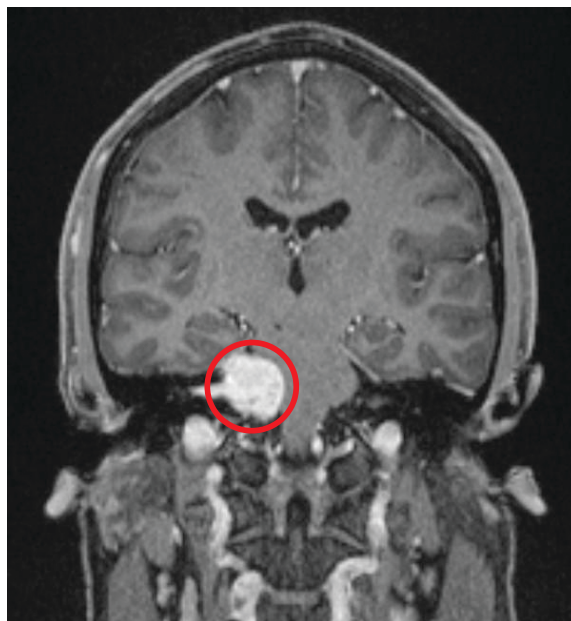


Abb. 3: Koronares Magnetresonanztomogramm (MRT) eines rechtsseitigen Vestibularis-Schwannoms (Dahnert, 2003).

Das erbliche Tumorsyndrom NF2 zeigt eine bemerkenswerte Bandbreite an klinischen Manifestationen. Neben krankheitstypischen Läsionen an Haut und Augen (z.B. Katarakt), weist ein Großteil der Betroffenen eine Schädigung peripherer Nerven (periphere Neuropathie) auf (Asthagiri *et al.*, 2009). Die Erkrankung NF2 hat eine Prävalenz von 1/25.000 und weist eine Penetranz von nahezu 100% auf (Evans *et al.*, 1992).

Entsprechend der Knudson-Hypothese bedarf es zur Tumorentwicklung der Inaktivierung beider Allele eines Tumorsuppressorgens (Knudson, 1971). Betroffenen Menschen fehlt üblicherweise ein funktionstüchtiges Allel entweder aufgrund einer Keimzellmutation oder einer *de novo* Mutation („first hit“). Später im Leben entwickeln sich dann aus denjenigen Zellen Tumore, die auch die Funktion des zweiten NF2 Allels im Sinne einer somatischen Mutation verloren haben („second hit“). Der Verlust der Heterozygotie (engl. „loss of heterozygosity“) (Thiagalingam *et al.*, 2001), der entscheidend für die Entwicklung von NF2-assoziierten Tumoren zu sein scheint (Stemmer-Rachamimov *et al.*, 1998), geschieht dabei oft durch den Verlust des gesamten Chromosoms 22, auf dem das NF2 Gen liegt (Lutchman and Rouleau, 1996).

Neben der Entwicklung benignen, glialer Tumoren, die ZNS und PNS betreffen können, entwickelt ein beachtlicher Anteil aller NF2-Patienten eine axonale Schädigung der peripheren Nervenbahnen (periphere Neuropathie) (Hagel *et al.*, 2002). In klinischen Studien konnte gezeigt werden, dass 47% aller untersuchten NF2-Patienten neuropathische Beschwerden aufwiesen (Sperfeld *et al.*, 2002). Mithilfe elektrophysiologischer Untersuchungen konnte bei demselben Patientenkollektiv sogar eine Prävalenz von 67% festgestellt werden, sodass offensichtlich eine zusätzliche, subklinische Ausprägung der NF2-assoziierten Neuropathie bei einem Teil der Patienten vorliegt. Verschiedene Studien konnten weiterhin aufzeigen, dass die bei NF2-Patienten feststellbare Neuropathie sensomotorischer Natur ist – also sensible und motorische Faserqualitäten gleichermaßen betrifft – und vornehmlich symmetrisch auftritt (Sperfeld *et al.*, 2002; Bosch *et al.*, 1981; Overweg-Plandsoen *et al.*, 1996; Iwata *et al.*, 1998).

Als ursächlich für das gehäufte Auftreten von neuropathischen Beschwerden bei NF2-Patienten galt bislang, dass Schwann-Zell-Tumore (Schwannome) durch Kompression von umliegenden Nervenfasern die oben beschriebenen Symptome auslösen würden (Grazzi *et al.*, 1998). Schwannome

können nämlich im Rückenmark, entlang peripherer Nervenbahnen, an Spinalnervenzwurzeln und im Bereich von Hirnnerven auftreten. Die jeweilige Beschwerdesymptomatik, die durch ein Schwannom hervorgerufen wird, ist selbstverständlich abhängig von der Lokalisation des Tumors. Jedoch scheint die Ausprägung der peripheren Neuropathie bei NF2-Patienten unabhängig von der Tumorbeltung sein. So bewirkt beispielsweise die chirurgische Resektion von Schwannomen nur in seltenen Fällen eine Verbesserung der neuropathischen Symptome (Baumer *et al.*, 2013). Weiterhin gibt es Beobachtungen, wonach viele NF2-Patienten eine Areflexie aufweisen, ohne dass Tumore im Bereich der peripheren Beinnerven oder der entsprechenden Rückenmarksegmente zu finden sind (MacCollin and Mautner, 1998). Klinisch besteht mitunter also eine Diskrepanz zwischen neuropathischer Beschwerdesymptomatik der NF2-Patienten und dem Auftreten bzw. der Lokalisation der vermeintlich ursächlichen Schwann-Zell-Tumore.

Es wurde daher vermutet, dass andere Faktoren als die Tumorbeltung durch Schwannome die Entstehung von NF2-assoziiierter Neuropathie bewirken können (Hagel *et al.*, 2002; Hanemann *et al.*, 2007).

2.5. Das Tumorsuppressorprotein Merlin

Das *NF2* Gen, das im Falle seiner Mutation die Erkrankung NF2 hervorruft, umfasst 17 Exons, die für das 595 Aminosäuren lange Protein Merlin codiert. Es ist ein Aktin-bindendes Protein aus der Gruppe der ERM-Proteine, das Membranproteine mit dem kortikalen Zytoskelett verknüpfen (McClatchey and Fehon, 2009). ‚Merlin‘ ist hierbei ein Akronym aus der englischsprachigen Beschreibung „Moesin-Ezrin-Radixin like protein“ und ist außerdem als ‚Schwannomin‘ bekannt (McClatchey and Fehon, 2009).

Die tumorsuppressive Funktion Merlins wird durch die Einbeziehung diverser Signalkaskaden in verschiedenen Zellkompartimenten bewerkstelligt. Es wurde berichtet, dass Merlin im Zellkern agiert (Muranen *et al.*, 2005; Li *et al.*, 2010), an der Zellmembran (Morrison *et al.*, 2001; Mani *et al.*, 2011), in Endosomen (Scoles *et al.*, 2000) und sogar in Assoziation mit Mitosespindeln während der Zellteilung (Muranen *et al.*, 2007). Obgleich Merlin mit einer großen Zahl verschiedener Moleküle zu interagieren imstande ist (Scoles, 2008),

begründet sich seine tumorverhindernde Wirkung insbesondere auf der Regulierung kleiner G-Proteine wie dem klassischen Proto-Onkogen Ras (Morrison *et al.*, 2007). Die mit Merlin interagierenden kleinen GTPasen haben entscheidenden Anteil an der Regulation des Aktin-Zytoskeletts in diversen Zelltypen und wurden mit Vorgängen der Tumorprogression in Verbindung gebracht (Karnoub and Weinberg, 2008).

Da Mutationen des Proteins Merlin primär die Entstehung von Tumoren bewirken, die aus Schwann- sowie Ependymzellen hervorgehen, ist – aufgrund des daraus resultierenden wissenschaftlichen Interesses – die Expression und Funktion Merlins in glialen Zelltypen des PNS und ZNS gut charakterisiert (Ramesh, 2004). Das Expressionsmuster einschließlich der daraus folgenden funktionalen Konsequenzen von Merlin in Nervenzellen ist demgegenüber noch nicht vergleichbar gut verstanden. Inwieweit neuronal exprimierte Merlin beteiligt ist an der Entwicklung und Stabilität von peripheren myelinisierten Axonen ist unbekannt. Jedoch konnte in der eigenen Arbeitsgruppe gezeigt werden, dass Merlin in Nervenzellen des ZNS eine relevante Rolle bei der neuronalen Morphogenese spielt (Schulz *et al.*, 2010).

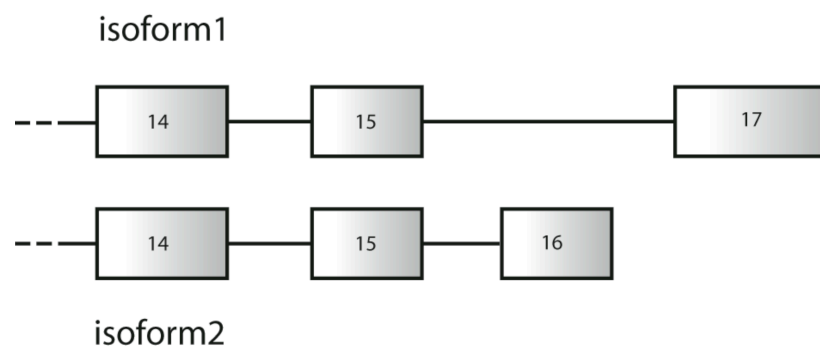


Abb. 4: Die C-terminale Exonkomposition der beiden hauptsächlich vorkommenden Merlin-Isoformen (eigene Abbildung).

Infolge alternativen Spleißens wird das Protein Merlin in einer noch nicht endgültig bekannten Zahl von Isoformen exprimiert. Obgleich hauptsächlich zwei Isoformen vorkommen (Merlin Isoform 1 und Merlin Isoform 2), wurden eine Reihe anderer ähnlicher Genprodukte beschrieben (Schmucker *et al.*, 1999; Pykett *et al.*, 1994). Hinsichtlich ihrer Sequenz gleichen sich die beiden Haupt-Isoformen von Merlin in den ersten 579 Aminosäuren und unterscheiden sich lediglich in den letzten 11 bzw. 16 Aminosäuren. Während bei Merlin Isoform 1 im C-terminalen Bereich

Exon 16 nicht transkribiert wird, enthält Merlin Isoform 2 dieses Exon, was durch die Anwesenheit eines Stop-Codons zu einem verkürzten Protein führt (Abbildung 4).

Obwohl bis heute kein wissenschaftlicher Konsens darüber besteht, vermutet man dass lediglich Merlin Isoform 1 eine tumorsuppressive Funktion besitzt. Merlin Isoform 2 konnte bislang keine eigenständige oder relevante Funktion zugeordnet werden (Sherman *et al.*, 1997; Bashour *et al.*, 2002). Jedoch mutmaßte eine frühe Expressionsstudie, dass Merlin Isoform 2 womöglich eine bedeutsame Funktion in Nervenzellen spielen könnte. Im Vergleich zu Isoform 1 wurde Merlin Isoform 2 auf mRNA-Ebene wesentlich häufiger in Nervengewebe des PNS und ZNS gefunden (Gutmann *et al.*, 1995).

3. Ziele der Arbeit

Das Ziel der vorliegenden Arbeit war die Überprüfung der Hypothese, dass es eine Neuronen-intrinsische Funktion des Tumorsuppressors Merlin gibt, die einen Einfluss auf die Struktur und Stabilität von axonalen Fortsätzen hat.

Diese Fragestellung basierte auf früheren Veröffentlichungen, in denen einerseits gezeigt werden konnte, dass Merlin nicht nur in Gliazellen, sondern auch in Nervenzellen exprimiert wird (Gronholm *et al.*, 2003; Yamauchi *et al.*, 2008; Schulz *et al.*, 2010). Andererseits gab es neuropathologische und klinische Studien, die darlegen konnten, dass NF2-Patienten an peripherer Neuropathie leiden können, ohne dass dafür eine krankheitsassoziierte, gesicherte Raumforderung mit entsprechender Lokalisation im Rückenmark oder entlang von Nervenbahnen verantwortlich ist (Sperfeld *et al.*, 2002; Hagel *et al.*, 2002; Kuo *et al.*, 2010; Overweg-Plandsoen *et al.*, 1996). Wir vermuteten daher, dass eine Merlin-assoziierten Pathogenese der Polyneuropathie bei NF2-Patienten existiert, die bei fehlender Druckschädigung peripherer Nerven durch Schwann-Zell-Tumore auftritt und so am ehesten intrinsisch in Axonen stattfinden sollte.

Ein derartig postulierter Signalweg von Merlin in Nervenzellen sollte zunächst *in vitro* mithilfe von Zelllinien und Kulturen primärer Nervenzellen verifiziert und charakterisiert werden. Die daraus gewonnenen Erkenntnisse sollten anschließend im Tiermodell überprüft werden. Hierzu sollte das motorische und sensible Verhalten von gentechnisch veränderten Mäusen erfasst und Nervengewebe dieser Tiere histologisch und ultrastrukturell analysiert werden. Außerdem sollte eine experimentelle Methodik etabliert werden, mit der man elektrophysiologische Nervenuntersuchungen an Mäusen durchführen kann.

Abschließend sollten die gewonnenen Befunde in Kollaboration mit Neuropathologen und Klinikern an Nerven-Biopsien von NF2-Patienten evaluiert werden.

4. Publierte Originalarbeiten

4.1. „The role of merlin isoform 2 in neurofibromatosis type 2-associated polyneuropathy”

Schulz A, Baader SL, Niwa-Kawakita M, Jung MJ, Bauer R, Garcia C, Zoch A, Schacke S, Hagel C, Mautner VF, Hanemann CO, Dun XP, Parkinson DB, Weis J, Schröder JM, Gutmann DH, Giovannini M, Morrison H. The role of merlin isoform 2 in neurofibromatosis type 2-associated polyneuropathy. Nature Neuroscience. 2013. 4:426-33.

Online-Link:

<http://www.nature.com/neuro/journal/v16/n4/full/nn.3348.html>

Anteil der beteiligten Autoren an der Veröffentlichung:

Dr. Alexander Schulz und Dr. Helen Morrison konzipierten die Studie.

Dr. Alexander Schulz führte die Mehrheit der Experimente durch und erstellte das Manuskript.

Prof. Dr. Stephan Baader erstellte die ultrastrukturelle Analyse und Auswertung aller verwendeten Nervenproben von Mäusen und menschlichen Biopsien.

Dr. Michiko Niwa-Kawakita und Prof. Dr. Marco Giovannini kreierten die in der Arbeit verwendeten Isoform-spezifischen Merlin-Knockout-Tiere.

Prof. Dr. Reinhard Bauer etablierte die elektrophysiologischen Experimente und nahm deren Auswertung vor.

Cynthia Garcia und Prof. Dr. David Gutmann synthetisierten die in der Arbeit verwendeten Isoform-spezifischen Merlin-Antikörper.

Ansgar Zoch und Marie Juliane Jung beteiligten sich an der Verhaltensanalyse der getesteten Tiere und halfen bei der Präparation von primären Nervenzellkulturen.

Stephan Schacke führte Bindungsexperimente und Nucleotid-Austausch-Versuche durch.

Dr. Xing-Pen und Dr. David Parkinson lieferten Gewebe von Schwann-Zell-spezifischen Merlin-Knockout-Tieren.

Prof. Dr. Christian Hagel und Prof. Dr. Victor-Felix Mautner steuerten N. suralis-Biopsien von NF2-Patienten für immunohistochemische Färbungen bei.

Prof. Dr. Oliver Hanemann lieferte Biopsien von NF2-Patienten für ultrastrukturelle Untersuchungen.

Prof. Dr. Joachim Weis und Prof. Dr. Michael Schröder beteiligten sich an der ultrastrukturellen Analyse von menschlichen Biopsien.

Dr. Helen Morrison überwachte das experimentelle Programm der Studie und erstellte das Manuskript.

Merlin isoform 2 in neurofibromatosis type 2–associated polyneuropathy

Alexander Schulz¹, Stephan L Baader^{2,12}, Michiko Niwa-Kawakita^{3,11,12}, Marie Juliane Jung¹, Reinhard Bauer⁴, Cynthia Garcia⁵, Ansgar Zoch¹, Stephan Schacke¹, Christian Hagel⁶, Victor-Felix Mautner⁷, C Oliver Hanemann⁸, Xin-Peng Dun⁸, David B Parkinson⁸, Joachim Weis⁹, J Michael Schröder⁹, David H Gutmann⁵, Marco Giovannini¹⁰ & Helen Morrison¹

The autosomal dominant disorder neurofibromatosis type 2 (NF2) is a hereditary tumor syndrome caused by inactivation of the *NF2* tumor suppressor gene, encoding merlin. Apart from tumors affecting the peripheral and central nervous systems, most NF2 patients develop peripheral neuropathies. This peripheral nerve disease can occur in the absence of nerve-damaging tumors, suggesting an etiology that is independent of gross tumor burden. We discovered that merlin isoform 2 (merlin-iso2) has a specific function in maintaining axonal integrity and propose that reduced axonal *NF2* gene dosage leads to NF2-associated polyneuropathy. We identified a merlin-iso2–dependent complex that promotes activation of the GTPase RhoA, enabling downstream Rho-associated kinase to promote neurofilament heavy chain phosphorylation. Merlin-iso2–deficient mice exhibited impaired locomotor capacities, delayed sensory reactions and electrophysiological signs of axonal neuropathy. Sciatic nerves from these mice and sural nerve biopsies from NF2 patients revealed reduced phosphorylation of the neurofilament H subunit, decreased interfibrillar spacings and irregularly shaped axons.

Neurons of both the peripheral nervous system (PNS) and central nervous system (CNS) are highly polarized complex cellular units. During development, several morphological steps are required for normal functioning and plasticity of the developing nervous system. New neurons migrate to their appropriate locations, extend axons and dendrites into the correct target regions, and form synapses with their partners. These distinct morphological processes depend on the spatiotemporal control of intrinsic neuronal signaling networks in which the Rho family of small GTPases are important regulatory components¹. The signaling mechanisms that establish these highly plastic neuronal processes are well characterized, but the manner in which these neurons achieve and maintain more stable structures, such as axon radial growth over far-reaching distances, throughout life is less well understood.

Neurofilaments are at least one component known to be required to promote and maintain radial growth also known as axonal caliber². Neurofilaments are neuron-specific intermediate filaments composed of NF-H (200 kDa), NF-M (150 kDa) and NF-L (68 kDa) subunits. To date, transcriptional upregulation³ and/or extensive side-arm phosphorylation of the NF-M or NF-H subunits⁴ are thought to determine structural integrity in axons², whereas the upstream signaling mechanisms that control and modify neurofilaments are

not well characterized. *Nefl* (which encodes NF-L) gene disruption in mice results in loss of neurofilaments and subsequent failure of axons to grow radially⁵. Neurofilament abnormalities in humans have been documented in a number of neurological diseases, including several inherited neuropathies². Inherited genetic mutations related to neurofilaments induce axonal alterations that result in nerve damage, leading to typical neuropathic symptoms, such as loss of sensation, pain or muscular weakness⁶.

NF2 is a hereditary tumor syndrome caused by inactivation of the *NF2* tumor suppressor gene encoding merlin. Apart from gliogenic tumors in the PNS and CNS, most NF2 patients develop peripheral neuropathies^{7,8}. NF2-related neuropathy mostly appears in a symmetric and distal manner and occurs in the absence of compressive spinal or peripheral tumors⁸, indicating a systemic, rather than focal, etiology. This suggests the involvement of factors other than gross tumor burden.

We identified a function for merlin in neurons of the developing CNS⁹. At least two alternatively spliced merlin variants are expressed: merlin isoform 1 (merlin-iso1), which lacks exon 16, and merlin-iso2, which contains exon 16 and encodes a C-terminally truncated protein. Merlin-iso1 has been established as a tumor suppressor, but little is known about merlin-iso2's function. We found that both merlin

¹Leibniz Institute for Age Research, Fritz Lipmann Institute, Jena, Germany. ²Institute of Anatomy, Anatomy and Cell Biology, University of Bonn, Bonn, Germany. ³Inserm U674, Université Paris, Paris, France. ⁴Institute of Molecular Cell Biology and Center for Sepsis Control and Care, Jena University Hospital, Friedrich Schiller University, Jena, Germany. ⁵Department of Neurology, Washington University School of Medicine, St. Louis, Missouri, USA. ⁶Department of Neuropathology, University Medical Center Hamburg-Eppendorf, Hamburg, Germany. ⁷Department of Neurology, University Medical Center Hamburg-Eppendorf, Hamburg, Germany. ⁸Plymouth University Peninsula Schools of Medicine and Dentistry, Plymouth, UK. ⁹Institute of Neuropathology, RWTH Aachen, University Hospital Aachen, Aachen, Germany. ¹⁰House Ear Institute, Center for Neural Tumor Research, Los Angeles, California, USA. ¹¹Present address: Inserm U944, CNRS U7212, Université Paris, Institut Universitaire d'Hématologie, Paris, France. ¹²These authors contributed equally to this work. Correspondence should be addressed to H.M. (helen@fli-leibniz.de).

Received 10 September 2012; accepted 30 January 2013; published online 3 March 2013; doi:10.1038/nn.3348

Figure 1 Merlin-iso2 expressed in axons, mediates neurofilament phosphorylation and axonal radial growth. (a,b) Merlin-iso1 (a) and merlin-iso2 (b) immunolabeling in the cerebellar cortex at postnatal day 15. Merlin-iso2 was expressed in Purkinje cell axons (Ax arrow). Arrowheads indicate Purkinje cell somata. Molecular layer (ML) is mainly composed of Purkinje cell dendrites. Scale bars represent 75 μ m and 15 μ m (magnified images). White boxes indicate areas shown at higher magnification. We quantified merlin-iso2 expression in Purkinje cell axons during postnatal development (P3–15) and in adults (P3, 0%; P5, 0%; P9, 5.15%; P15, 45.53%; adult, 96.92%; $n = 50$ axons from 2 mice for each investigated age). (c,d) Merlin isoform-specific immunolabeling (green) in primary DRG neurons. Co-staining with phosphorylated neurofilaments (pNF-H, red) indicates expression in axons. Merlin-iso1 was present in axonal growth cones (arrows) and merlin-iso2 was detected along the whole axon. Scale bars represent 20 μ m. (e,f) Quantification of axon diameters following specific knockdown (duplexes) in primary cerebellar neurons (** $P < 0.01$, $t = 4.119$, degrees of freedom (df) = 20; *** $P < 0.001$, $t = 5.809$, df = 20; $n = 393$ cells from 3 mice; mean \pm s.e.m.; n.s., not significant, $P = 0.16$). Scrambled control (scrambled *Nf2*), both isoforms (siRNA *Nf2*), merlin-iso1 (siRNA *Nf2-iso1*), merlin-iso2 (siRNA *Nf2-iso2*) or following overexpression in differentiated P19 cells are shown in e. Empty vector control (vc), merlin-iso1 (iso1), merlin-iso2 (iso2) are shown in f (** $P < 0.01$, $t = -8.201$, df = 19; $n = 460$ cells; mean \pm s.e.m.; n.s., not significant, $P = 0.07$). Immunoblots for actin (loading control), merlin-iso1 and merlin-iso2 or merlin were used to confirm knockdown and overexpression. Merlin overexpression migrated as a doublet; the upper band representing phosphorylated merlin and the lower band represented dephosphorylated merlin. For full-length blots and quantitations, see **Supplementary Figure 3**.

isoforms were able to restrict dendritic morphogenesis through inhibition of the small GTPase Rac1 (ref. 9). Our finding suggest that merlin, a known tumor suppressor, is involved in controlling highly plastic neuronal processes such as dendrites in the developing brain. We hypothesize that merlin may also function in the development and maintenance of more stable structures such as axons, and suggest that the specific loss or reduction of merlin in neurons may contribute to NF2-related polyneuropathy.

RESULTS

Merlin-iso2 mediates neurofilament phosphorylation

Using isoform-specific antibodies, we detected both merlin isoforms in cerebellar Purkinje cell somata (Fig. 1a,b) and dendrites in the molecular layer. Only isoform 2 was localized to axonal processes running from Purkinje cells toward the white cerebellar matter (Fig. 1a,b and **Supplementary Fig. 1**).

Merlin-iso2-positive signals in Purkinje cells began to appear between postnatal days 9 and 15 (P9 and P15) in Purkinje cell axons (Fig. 1 and Online Methods), coinciding with a period of Purkinje cell axonal maturation characterized by extensive neurofilament phosphorylation and diameter adjustment¹⁰. In addition, we detected predominant merlin-iso2 expression in cells belonging to the PNS, including sciatic nerve axons (**Supplementary Fig. 2**) and axons of primary dorsal root ganglion (DRG) cells (Fig. 1c,d).

We used primary neuronal monocultures independent of the associated influence of glial cells and the murine embryonic carcinoma P19 cell line, which are known to differentiate into neuronal cells¹¹, to investigate whether merlin-iso2 affects axon-intrinsic morphogenesis. Specific knockdown of merlin-iso2 or of both isoforms in isolated primary cerebellar neurons decreased axonal diameter, whereas merlin-iso1-specific knockdown had no detectable influence (Fig. 1e and **Supplementary Fig. 3a**). Concordantly, overexpression of merlin-iso2 elicited a substantial increase in axonal diameter compared with overexpression of merlin-iso1

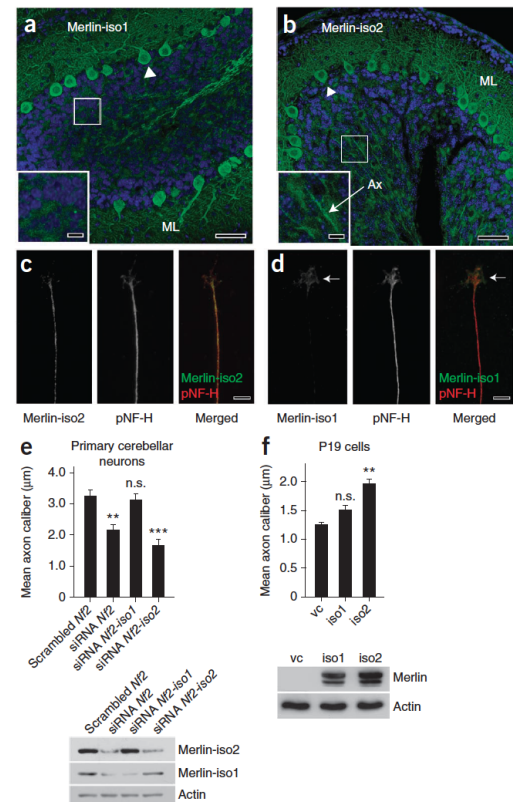


(Fig. 1f). The decrease in axonal diameter resulting from merlin-iso2 protein reduction could be rescued by the expression of human merlin-iso2 in mouse P19 cells (Fig. 2).

We investigated whether the merlin-iso2 effect on axonal caliber is mediated through neurofilament regulation. Although the total amount of neurofilaments remained unaffected (data not shown), the phosphorylation status of NF-H in primary cerebellar neurons was decreased by merlin-iso2 knockdown, but merlin-iso1 knockdown (Fig. 2a). Accordingly, merlin-iso2 overexpression led to a robust neurofilament phosphorylation in P19 cells, whereas merlin-iso1 overexpression had only minor effects (Fig. 2b). Taken together, these findings establish a specific intrinsic neuronal role of merlin-iso2 in the regulation of neurofilament phosphorylation that leads to radial axonal growth.

Axonal merlin-iso2 involves RhoA signaling

Neurofilaments are phosphorylated by several serine/threonine kinases². Because merlin lacks any endogenous kinase activity, we screened for serine/threonine kinases that were involved in merlin and/or neurofilament signaling (**Supplementary Table 1**). We monitored whether the knockdown of each tested kinase could prevent or decrease neurofilament phosphorylation following merlin-iso2 overexpression *in vitro*. One of the kinases that we identified, Rho-associated kinase (ROCK), has been reported to directly phosphorylate neurofilaments *in vitro*¹². Overexpression of merlin-iso2

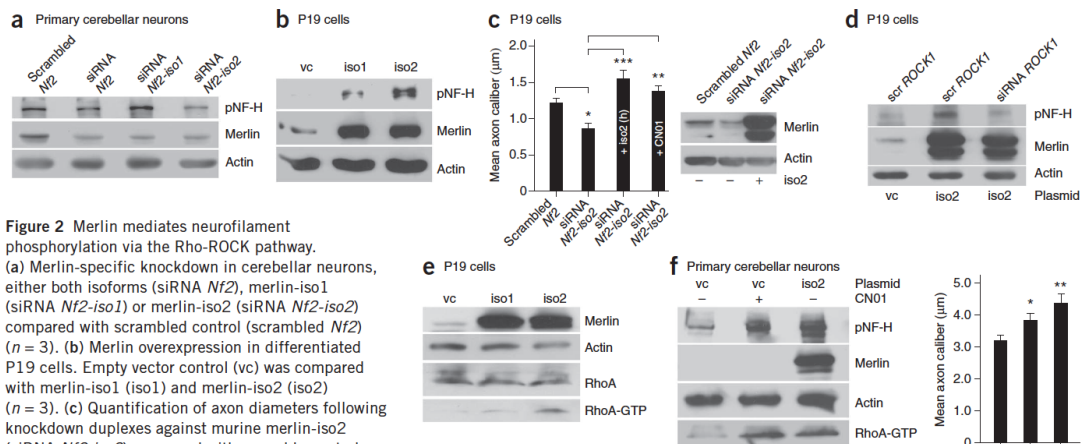


Figure 2 Merlin mediates neurofilament phosphorylation via the Rho-ROCK pathway. (a) Merlin-specific knockdown in cerebellar neurons, either both isoforms (siRNA *Nf2*), merlin-iso1 (siRNA *Nf2-iso1*) or merlin-iso2 (siRNA *Nf2-iso2*) compared with scrambled control (scrambled *Nf2*) ($n = 3$). (b) Merlin overexpression in differentiated P19 cells. Empty vector control (vc) was compared with merlin-iso1 (iso1) and merlin-iso2 (iso2) ($n = 3$). (c) Quantification of axon diameters following knockdown duplexes against murine merlin-iso2 (siRNA *Nf2-iso2*) compared with scramble control (scrambled *Nf2*) ($*P < 0.01$, $t = 3.738$, $df = 26$, $n = 102$ cells, mean \pm s.e.m.), co-transfection with human merlin-iso2 (+iso2) or treatment with Rho activator (+CN01) ($**P < 0.01$, $t = -4.782$, $df = 27$; $***P < 0.001$, $t = -5.596$, $df = 24$; $n = 112$ cells, mean \pm s.e.m.). Right, immunoblot for merlin and actin confirmed effective knockdown and transfection levels ($n = 3$). (d) ROCK knockdown prevented merlin-iso2-induced neurofilament phosphorylation. P19 cells were treated with scrambled control duplexes (scr) and empty vector control, scr and merlin-iso2 overexpression (iso2), siRNA ROCK and merlin-iso2 overexpression (*ROCK1/iso2*) ($n = 3$). (e) P19 cells were measured for RhoA-GTP level after merlin-iso2 (iso2) and merlin-iso1 (iso1) overexpression compared with empty vector control (vc) ($n = 3$). (f) RhoA-GTP level was measured in cerebellar neurons after treatment with Rho activator (CN01) or overexpression with merlin-iso2 (iso2) compared with vector control (vc) ($n = 3$). Right, radial axonal growth ($*P < 0.05$, $t = -2.381$, $df = 23$, $n = 98$ cells from 3 mice; $**P < 0.01$, $t = -3.804$, $df = 22$, $n = 116$ cells from 3 mice; mean \pm s.e.m.). For full-length blots and quantitations, see **Supplementary Figures 3 and 4**.

and simultaneous silencing of ROCK using siRNA prevented merlin-iso2-specific NF-H phosphorylation (Fig. 2d), suggesting that merlin-iso2 acts upstream of ROCK.

To elucidate how merlin-iso2 regulates ROCK, we examined the activity of the GTPase RhoA, an upstream regulator of ROCK. Merlin-iso2, but not merlin-iso1, overexpression activated RhoA in P19 cells (Fig. 2e). In primary neurons, merlin-iso2 overexpression was mimicked by the application of a Rho activator (CN01), as indicated by increased RhoA activity, NF-H phosphorylation and an increase in axonal caliber (Fig. 2f). Furthermore, application of the same Rho activator alone could rescue the axonal caliber decrease following merlin-iso2 repression in P19 cells (Fig. 2c).

In addition to the CNS, we found that merlin-iso2 function is important in PNS neurons. We isolated glia-free primary DRG cells whose axons (known as afferents) relay sensory information into the CNS. A merlin-iso2-specific knockdown in these cells resulted in a decrease in neurofilament phosphorylation (Fig. 3a). We also examined the effect of merlin loss using genetically engineered mice bearing complete isoform-specific knockouts of merlin, designated *Nf2-iso1^{-/-}* and *Nf2-iso2^{-/-}*. We confirmed merlin isoform-specific knockout at the protein level in forebrain and hindbrain lysates (Supplementary Fig. 4c). As expected, neurofilament phosphorylation was predominantly reduced in *Nf2-iso2^{-/-}* brains (Supplementary Fig. 4c). Similar to CNS nerve cells, *in vitro* DRG neurons isolated from *Nf2-iso2^{-/-}* mice had smaller axonal diameters than wild-type control and *Nf2-iso1^{-/-}* mice (Fig. 3b). Moreover, *Nf2-iso2^{-/-}* DRG neurons could be rescued by expression of merlin-iso2, with a substantial RhoA activation accompanied by neurofilament phosphorylation and subsequent radial axonal growth (Fig. 3c and Supplementary Fig. 4d). Transfection of a constitutively active form of RhoA (RhoA 63L) into DRG cells¹³ resulted in an increase in neurofilament phosphorylation and axonal caliber growth (Fig. 3d).

These data indicate that RhoA activity contributes to axonal diameter adjustment in both the CNS and PNS. Our data imply that part of merlin-iso2's mechanism of action involves activation of RhoA, enabling downstream ROCK to promote neurofilament phosphorylation.

Merlin assembles a multi-protein complex

Guanine nucleotide exchange factors (GEFs), GTPase-activating proteins (GAPs) and GDP dissociation inhibitors (GDIs) are considered to be the primary determinants in neuronal Rho regulation. Our data indicate that merlin is involved in controlling Rho activity, specifically axonal caliber growth in neurons *in vitro*. We therefore explored how merlin-iso2 might operate in the axon to promote Rho signaling.

Because merlin has been suggested to interact with the guanine nucleotide dissociation inhibitor RhoGDI¹⁴, as well as with p190RhoGAP (unpublished observations), in other cell types, we hypothesized the existence of a neurofilament-associated multi-protein complex in which merlin-iso2 regulates RhoA activity in neurons. Both RhoGDI and p190RhoGAP were expressed in DRG cell axons (Supplementary Fig. 4f and 5a). The reduction of either RhoGDI or p190RhoGAP in neuronal cells led to an increase in Rho activity, neurofilament phosphorylation and radial axonal growth (Fig. 3e and Supplementary Fig. 5c,d), establishing the importance of these regulatory components *per se* in axonal Rho activity control.

In wild-type mouse sciatic nerves, the levels of the two major merlin isoforms, RhoA and RhoGDI remained unchanged during development (Supplementary Fig. 5e–g). The level of p190RhoGAP appeared to be higher at birth (P0) and was reduced around P20, coinciding with axonal maturation characterized by extensive neurofilament phosphorylation (Supplementary Fig. 5g).

Notably, the sciatic nerves of adult *Nf2-iso2^{-/-}* mice (P60) showed reduced levels of active RhoA (RhoA-GTP) and reduced

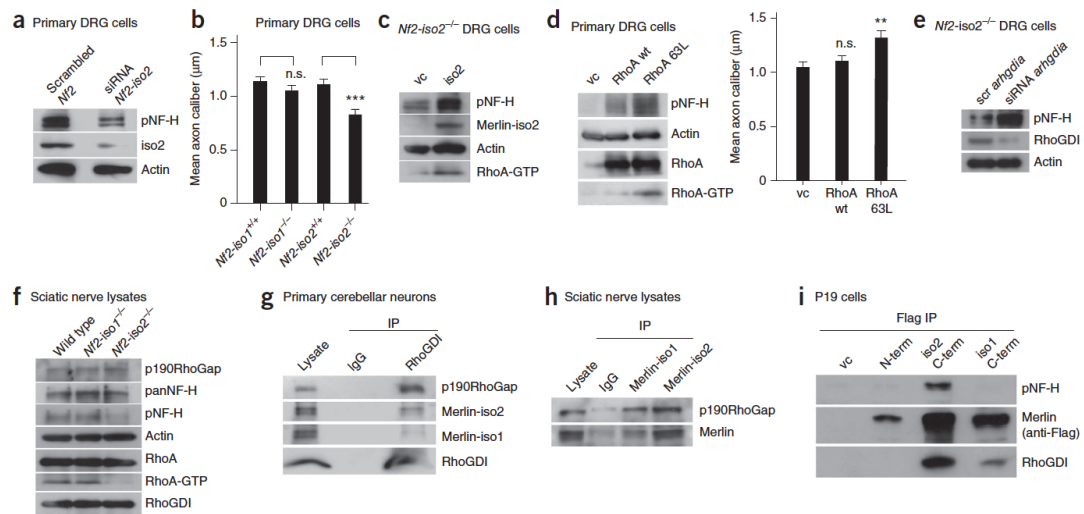


Figure 3 Merlin assembles a multi-protein complex relevant for Rho activation. (a) Merlin-iso2-specific knockdown (siRNA *Nf2-iso2*) in primary DRG neurons compared with scrambled duplex control (scr *Nf2*) ($n = 3$). (b) DRG neurons were isolated from isoform-specific knockout mice and axonal calibers were measured. *Nf2-iso2*^{-/-} mice compared with *Nf2-iso1*^{-/-} and wild-type controls (*Nf2-iso2*^{+/+} and *Nf2-iso1*^{+/+}) ($***P < 0.001$, $t = -2.687$, $df = 28$, $n = 365$ cells from 3 mice, mean \pm s.e.m.; n.s., not significant, $P = 0.11$). (c) DRG neurons prepared from *Nf2-iso2*^{-/-} transfected with merlin-iso2 (iso2) compared with empty vector control (vc) ($n = 3$). (d) Wild-type DRG cells transfected with constitutively active RhoA mutant (RhoA 63L) compared with wild-type RhoA (RhoA wt) and empty vector control (vc) ($n = 3$). Right, radial axon growth *in vitro* ($**P < 0.01$, $t = -3.045$, $df = 65$, $n = 361$ cells from 3 mice, mean \pm s.e.m.; n.s., not significant). (e) Knockdown of RhoGDI (siRNA *arhgdia*) compared with scrambled control duplexes (scr *arhgdia*) in *Nf2-iso2*^{-/-} DRGs ($n = 3$). (f) Sciatic nerve lysates from *Nf2-iso2*^{-/-} mice compared with *Nf2-iso1*^{-/-} mice and wild-type mice ($n = 4$). (g) Immunoprecipitation (IP) of endogenous RhoGDI from primary neurons compared with IgG control ($n = 3$). (h) Immunoprecipitation from sciatic nerve lysates using merlin-specific antibodies (merlin-iso1 and merlin-iso2) compared with IgG control ($n = 3$). (i) Flag-tagged merlin N-terminal fragments (N-term), C-terminal (iso2 C-term and iso1 C-term) and empty vector control (vc) were transfected into P19 cells and immunoprecipitated with antibody to Flag ($n = 4$). For full-length blots and quantifications, see **Supplementary Figures 4–6**.

phosphorylated neurofilaments (Fig. 3f). However, the total protein amounts of p190RhoGAP, RhoA and RhoGDI remained unchanged, indicating that the reduction of merlin-iso2 has no effect on the expression and/or stability of these components in adult mice.

Using immunoprecipitation, we confirmed the existence of a multi-protein complex and examined its composition. Antibodies to RhoGDI co-precipitated both merlin isoforms, as well as p190RhoGAP from primary granule cell lysates (Fig. 3g). Antibodies to merlin-iso2 and merlin-iso1 both co-precipitated p190RhoGAP from sciatic nerve lysates (Fig. 3h). The fact that merlin-iso2 differs from merlin-iso1 in the C terminus, a precise function distinct from the C-terminal merlin-iso1 is suggested. We tested whether a C-terminal fragment of merlin-iso2 was sufficient to associate with neurofilaments. Indeed, only the C-terminal merlin-iso2 co-immunoprecipitated with phosphorylated neurofilaments (Fig. 3i and **Supplementary Fig. 6**), indicating that, although both full-length isoforms can form a complex with RhoGDI and p190RhoGAP, merlin-iso2 likely acts locally in axons.

We examined the interaction between merlin and RhoGDI *in vitro* (**Supplementary Fig. 7**). No interaction was detected *in vitro* using purified merlin full-length proteins (**Supplementary Fig. 7a,b**). An interaction could only be shown with the FERM domain of merlin (N terminus, shared by the two isoforms) using both purified GST- and His-tagged RhoGDI. We next tested whether merlin acts as a RhoGDI displacement factor (that is, releases inactive RhoA-GDP from RhoGDI to result in RhoA activation). In an *in vitro* Rho

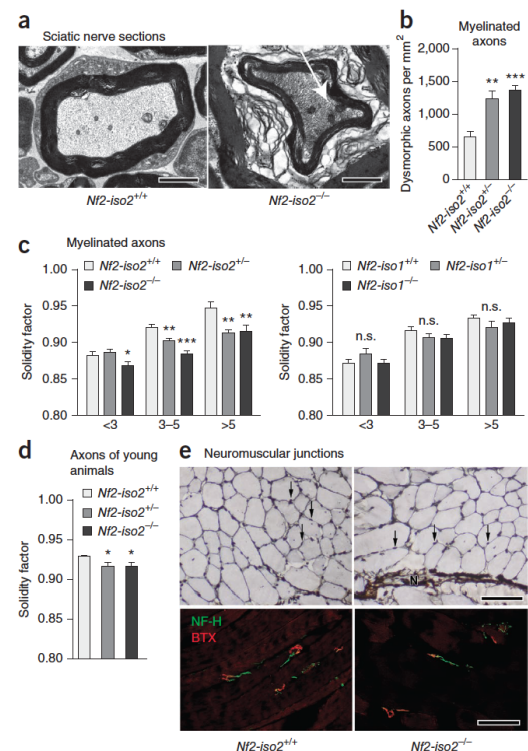
activity assay¹⁵, addition of a Rho GEF induced a rapid nucleotide exchange. Addition of RhoGDI sufficiently inhibited this exchange by maintaining RhoA in its inactive form. Inclusion of N-terminal merlin (FERM domain) did not affect the intrinsic RhoA GTP loading or the activity of Rho GEF toward RhoA (**Supplementary Fig. 7c**) and was unable to induce release of RhoGDI from RhoA (**Supplementary Fig. 7c**). Taken together, at least in this *in vitro* assay, we could not detect merlin-dependent inhibition of RhoGDI. Other partners might be required for a complete merlin-dependent RhoGDI displacement from RhoA *in vivo*. In addition, *in vivo* full-length merlin has distinct molecular conformations¹⁶ that may be required to bind and control RhoGDI activity coordinating RhoA signal activation.

Analysis of merlin isoform-specific knockout mice

The availability of isoform-specific *Nf2* knockout mice enabled us to test merlin-iso2-specific functions in an intact nervous system and to determine whether merlin-iso2 loss contributes to an axonal pathogenesis of NF2-associated polyneuropathy. On the basis of our *in vitro* data, we expected these mice to display axonal structure alterations resulting from irregular neurofilament phosphorylation. Because aberrant axonal signals can induce secondary Schwann cell changes in older mice¹⁷, we studied young mice (2 months old), which allowed us to concentrate on specific axonal changes. Our initial studies revealed that both mouse lines appeared to be devoid of NF2-typical tumors, suggesting a compensatory potential for the two major merlin isoforms (unpublished data).

Figure 4 Axon structure abnormalities in *Nf2-iso2*^{-/-} mice. (a) Electron micrographs of sciatic nerve axons from *Nf2-iso2*^{-/-} mice compared with *Nf2-iso2*^{+/+} mice. Arrow indicates densely packed neurofilaments and mitochondria. Scale bars represent 1 μ m. (b) More dysmorphic sciatic nerve axons were found in *Nf2-iso2*^{+/+} and *Nf2-iso2*^{-/-} than in *Nf2-iso2*^{+/+} mice (** P < 0.01, t = -3.401, df = 29; *** P < 0.001, t = -5.578, df = 34; n = 542 axons from 3 mice, mean + s.e.m.). (c) The mean solidity factor was decreased in myelinated axons in sciatic nerve cross sections from *Nf2-iso2*^{+/+} and *Nf2-iso2*^{-/-} mice compared with *Nf2-iso2*^{+/+} mice, whereas loss of merlin-iso1 (*Nf2-iso1*^{-/-}, *Nf2-iso1*^{+/+} and *Nf2-iso1*^{+/+} mice) had no significant effect (* P < 0.05, t = -5.196, df = 165; ** P < 0.01, t = -7.135, df = 183; *** P < 0.001, t = -5.871, df = 169; n.s., not significant; n = 1,488 axons from 3 mice, mean + s.e.m.). Axons were categorized according to their diameter (x axis represents axon calibers in μ m). (d) Sciatic nerve axons of young P7 *Nf2-iso2*^{+/+} and *Nf2-iso2*^{-/-} mice showed comparable solidity factors (* P < 0.05, t = -5.677, df = 1,039, n = 1,512 axons from 3 mice, mean + s.e.m.). (e) Gastrocnemius muscle fibers of *Nf2-iso2*^{+/+} and *Nf2-iso2*^{-/-} mice were stained with silver impregnation (top) and immunohistochemically for acetylcholine receptor and myelinated nerve fibers (bottom). Muscle fibers are equal in size, without signs of dying muscle cells or accumulation of fat cells or connective tissue. Muscle fibers appear straight and not wrinkled and the cell bodies (arrows) are arranged along the border of the muscle fiber, not centrally. We detected equal amounts of myelinated nerve fibers by NF-H staining and normal amounts and sizes of endplates by bungarotoxin (BTX) staining (n = 2 mice per genotype). Scale bars represent 100 μ m.

Sciatic nerve axons of *Nf2-iso2*^{-/-} mice exhibited morphological abnormalities, such as misshaped and dysmorphic axons and accumulations of densely packed neurofilaments and mitochondria (Fig. 4a,b). Axonal shrinkage resulting from an irregular bending of the axonal surface led to a strong reduction in the solidity factor in both heterozygous (*Nf2-iso2*^{+/+}) and homozygous (*Nf2-iso2*^{-/-}) mice (Fig. 4c). Loss of merlin-iso1 had no effect on the roundness of axons. Even young merlin-iso2-deficient mice (P7) displayed a significant reduction in the solidity factor (P < 0.05; Fig. 4d), indicating that the observed phenotype originates in the early period of axonal structure maintenance. This abnormal phenotype, including axonal atrophy with shrunken and collapsed axons of peripheral nerves, resembles that described in mice with a neurofilament mutation¹⁸. Although we detected a high number of shrunken axons in *Nf2-iso2*^{-/-} mice,



the total number of axons and the overall axon caliber in sciatic nerve sections appeared to be unaffected (Supplementary Fig. 8a). Immunohistochemical analysis of longitudinal sciatic nerve sections from *Nf2-iso2*^{-/-} mice, including *Nf2-iso2*^{-/-} DRG cells cultured for 14 d (data not shown), revealed no obvious signs of degeneration,

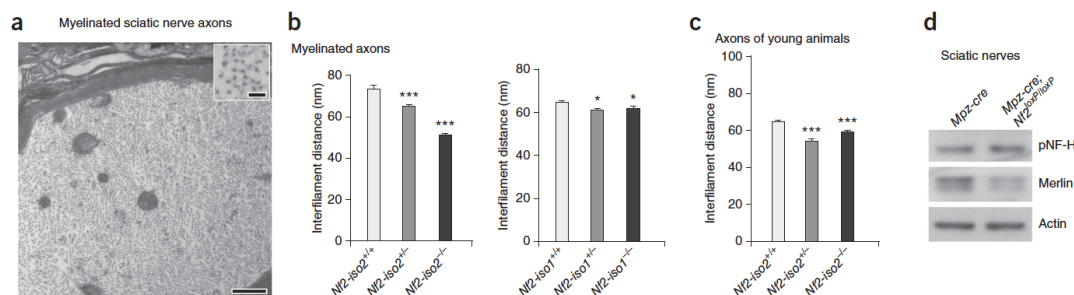


Figure 5 Reduced interfibril distances in *Nf2-iso2*^{-/-} mice. (a) Representative electron micrograph of a myelinated sciatic nerve axon. Upper right, 20,000 \times magnification. Scale bars represent 500 nm and 100 nm (inset). Single neurofilament molecules can be identified as black dots in the axoplasm. (b) Distances between single neurofilaments were quantified in sciatic nerve axons of adult *Nf2-iso2*^{+/+} and *Nf2-iso2*^{-/-} mice compared with *Nf2-iso2*^{+/+} mice, and adult *Nf2-iso1*^{+/+} and *Nf2-iso1*^{-/-} mice compared with *Nf2-iso1*^{+/+} mice (* P < 0.05, t = -4.396, df = 2,968; *** P < 0.001, t = -6.346, df = 3,021; n = 3,298 distances from 3 mice, mean + s.e.m.). (c) Young *Nf2-iso2*^{+/+} and *Nf2-iso2*^{-/-} mice compared with *Nf2-iso2*^{+/+} mice (*** P < 0.001, t = -6.117, df = 1,066, n = 1,454 distances from 3 mice, mean + s.e.m.). (d) Sciatic nerve lysates from *Mpz-cre*; *Nf2*^{loxP/loxP} mice showed slightly elevated levels of neurofilament phosphorylation compared with control littermates (*Mpz-cre*) (n = 4). For full-length blots and quantifications, see Supplementary Figure 8.

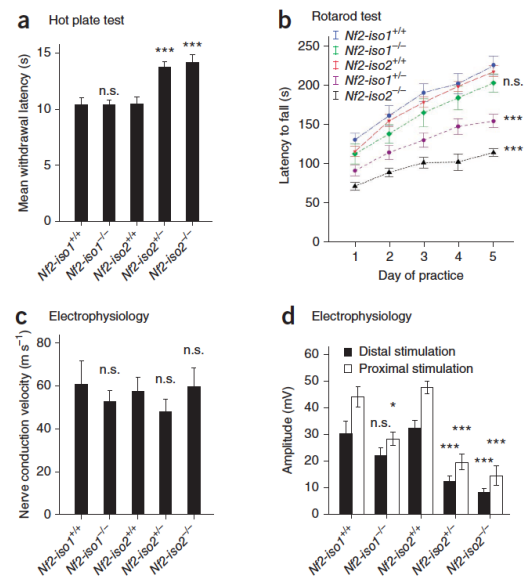
Figure 6 Behavioral abnormalities in *Nf2-iso2*^{-/-} mice. (a) Hot plate test measuring response to thermal stimuli revealed greater withdrawal latencies for *Nf2-iso2*^{+/-} and *Nf2-iso2*^{-/-} mice than for *Nf2-iso2*^{+/+} mice ($***P < 0.001$, $t = -4.557$, $df = 39$; n.s., not significant, $t = 0.007$, $df = 15$; $n = 8$ mice per group, mean \pm s.e.m.). (b) Rotarod performance of mice trained for 5 consecutive days. *Nf2-iso2*^{+/-} and *Nf2-iso2*^{-/-} mice showed weakened performances compared with *Nf2-iso2*^{+/+}, *Nf2-iso1*^{+/+} and *Nf2-iso1*^{-/-} mice ($***P < 0.001$, $t = 6.417$, $df = 32$; n.s., not significant; $n = 8$ mice per group, mean \pm s.e.m.). (c) Nerve conduction velocities ($n = 6$ mice per group; n.s., not significant) in *Nf2-iso2*^{+/-}, *Nf2-iso2*^{-/-} and *Nf2-iso1*^{-/-} mice compared with *Nf2-iso2*^{+/+} and *Nf2-iso1*^{+/+} mice (mean \pm s.e.m.). (d) Compound muscle action potential amplitudes recorded after proximal and distal sciatic nerve stimulation. Amplitudes in both *Nf2-iso2*^{+/-} and *Nf2-iso2*^{-/-} mice were markedly reduced, suggesting axonal-type neuropathy, compared with *Nf2-iso2*^{-/-}, *Nf2-iso2*^{+/+} and *Nf2-iso1*^{+/+} mice ($*P < 0.05$, $t = 6.912$, $df = 12$, $t = 7.280$, $df = 10$; $***P < 0.001$; n.s., not significant, $t = 3.377$, $df = 10$; $n = 6$ per group, mean \pm s.e.m.).

such as spheroid formations or amyloid precursor protein (APP) accumulations, along axons (Supplementary Fig. 8b). As no classical signs of axonal degeneration were detected, we propose that the number of normal functional axons was decreased. However, because axonal integrity is thought to be essential for myelin maintenance, it is possible that an active neurodegeneration may occur in older *Nf2-iso2*^{-/-} mice. Axonal targeting also appeared to be normal in merlin isoform-specific knockout mice, despite the morphological axonal alterations. Silver impregnation and immunohistochemical staining for acetylcholine receptors and myelinated nerve fibers of gastrocnemius muscles did not show relevant alterations concerning muscular structure or nerve targeting (Fig. 4e), indicating proper muscle innervation in *Nf2-iso2*^{-/-} mice.

Given that phosphorylation events equate to addition of repulsive negative charges, neurofilament phosphorylation results in a larger distance between single neurofilament molecules⁴. Accordingly, axons of both heterozygous and homozygous *Nf2-iso2*^{-/-} mice showed decreased interfilament distances as a result of reduced neurofilament phosphorylation (Fig. 5a,b). In contrast, *Nf2-iso1*^{-/-} axons showed only a slight reduction in interfilament spacing. Again, comparable effects of merlin-iso2 loss could be detected in young mice at P7 (Fig. 5c).

As merlin has important tumor suppressive functions in Schwann cells of the PNS¹⁹, axonal structure and shape alterations in *Nf2-iso2*^{-/-} mice could be indirectly determined by modified Schwann cell signals. In an established NF2 mouse model in which both merlin isoforms are conditionally deleted in Schwann cells (*Mpz-cre; Nf2^{loxP/loxP}* mice)²⁰, neurofilament phosphorylation was slightly increased, as was the distance between single neurofilaments (Fig. 5d and Supplementary Fig. 8c). These findings indicate that the described axonal changes in *Nf2-iso2*^{-/-} sciatic nerves are of axonal origin and are not a product of merlin loss in Schwann cells.

We next tested whether the described morphological alterations are causative for neuropathic symptoms *in vivo*. Hot plate testing measuring pain sensitivity revealed that both heterozygous and homozygous *Nf2-iso2*^{-/-} mice had prolonged withdrawal latencies to thermal stimuli compared with wild-type littermates and *Nf2-iso1*^{-/-} mice (Fig. 6a), indicating thermal hypoalgesia and impaired responses to noxious thermal stimuli. Rotarod testing revealed that *Nf2-iso2*^{-/-} mice also displayed deficits in motor function. After 5 d of training, they had a mean latency to fall of 115 s compared with 217 s for wild-type littermates (Fig. 6b). Even *Nf2-iso2*^{+/-} mice showed a relevant phenotype (155 s).



Electrophysiological measurements on sciatic nerves *in vivo* revealed similar nerve conduction velocities (mainly determined by myelination and reduced in demyelinating neuropathies) in *Nf2-iso1*^{-/-} and *Nf2-iso2*^{-/-} mice (Fig. 6c). In contrast, compound muscle action potential amplitudes (reflecting axonal functionality) were greatly reduced in *Nf2-iso2*^{-/-} mice, indicative of axonal neuropathy (Fig. 6d). Apart from minor effects following proximal stimulation (possibly because of additional alterations in other tissues as a result of complete isoform-specific knockout of merlin), merlin-iso1 loss had no relevant influence (Fig. 6d). These results clearly correlate both homozygous and heterozygous merlin-iso2 inactivation with axonal neuropathy development. These findings are consistent with clinical findings suggesting that polyneuropathy in NF2 patients occurs in the absence of associated tumors (schwannomas)^{8,21} and that germline NF2 mutations cause merlin haploinsufficiency and polyneuropathy in patients²².

NF2 patient-derived mutations and specimens

We analyzed sural nerve biopsy sections from NF2 patients carrying germline NF2 mutations who presented clinically with severe neuropathy²¹. Immunohistochemical analysis revealed reduced phospho-neurofilament staining per vital axon compared with healthy control biopsies (Fig. 7a and Supplementary Fig. 9a). Ultrastructural analysis revealed intrinsic axonal structure abnormalities that closely resembled those of *Nf2-iso2*^{-/-} mice *in vivo* and neurons *in vitro*. Sural nerve axons of the same patients exhibited reduced interfilament distances compared with healthy control samples (Supplementary Fig. 9b). In addition, non-myelinated fibers frequently displayed irregularly shaped axons containing accumulations of condensed mitochondria and neurofilaments (Fig. 7b), as well as aggregations of pleomorphic vesicles and dense bodies (Fig. 7c) that could not be found in biopsies of healthy control individuals (Fig. 7d).

In vitro, the C-terminal nonsense NF2 mutation C784T, which was previously reported to provoke axonal type neuropathy determined by electrophysiological means⁸, could not induce neurofilament

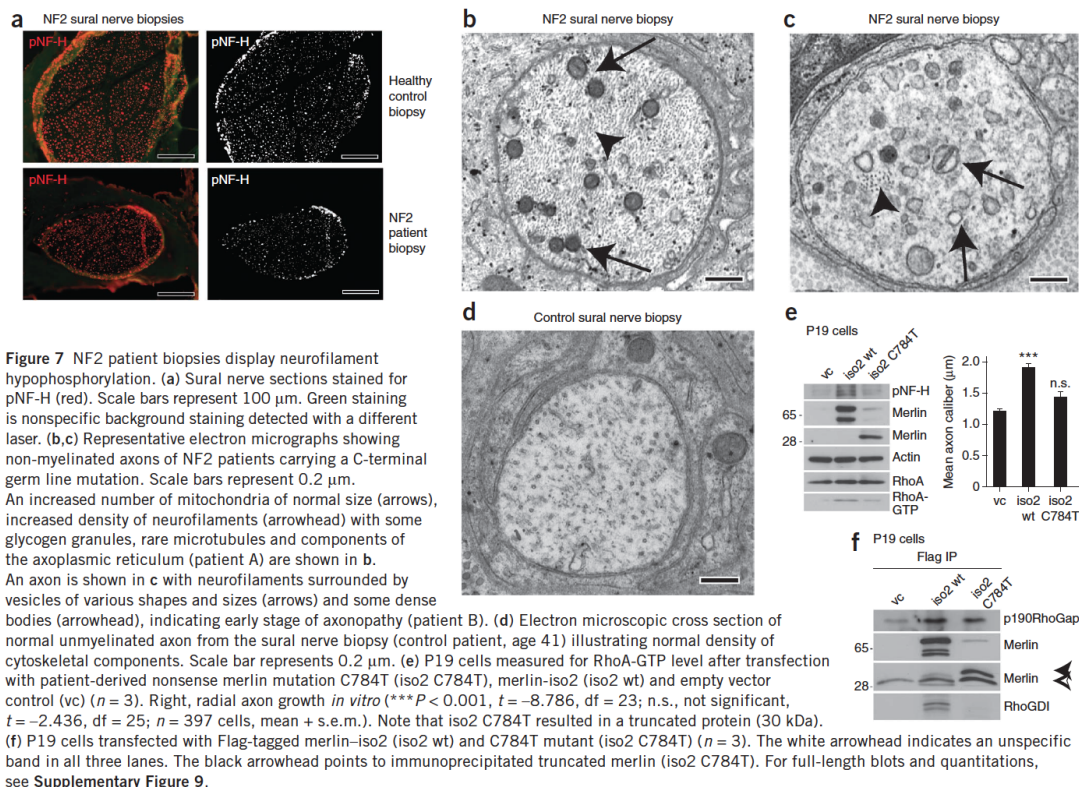


Figure 7 NF2 patient biopsies display neurofilament hypophosphorylation. **(a)** Sural nerve sections stained for pNF-H (red). Scale bars represent 100 μm. Green staining is nonspecific background staining detected with a different laser. **(b,c)** Representative electron micrographs showing non-myelinated axons of NF2 patients carrying a C-terminal germ line mutation. Scale bars represent 0.2 μm. An increased number of mitochondria of normal size (arrows), increased density of neurofilaments (arrowhead) with some glycogen granules, rare microtubules and components of the axoplasmic reticulum (patient A) are shown in **b**. An axon is shown in **c** with neurofilaments surrounded by vesicles of various shapes and sizes (arrows) and some dense bodies (arrowhead), indicating early stage of axonopathy (patient B). **(d)** Electron microscopic cross section of normal unmyelinated axon from the sural nerve biopsy (control patient, age 41) illustrating normal density of cytoskeletal components. Scale bar represents 0.2 μm. **(e)** P19 cells measured for RhoA-GTP level after transfection with patient-derived nonsense merlin mutation C784T (iso2 C784T), merlin-iso2 (iso2 wt) and empty vector control (vc) ($n = 3$). Right, radial axon growth *in vitro* ($***P < 0.001$, $t = -8.786$, $df = 23$; n.s., not significant, $t = -2.436$, $df = 25$; $n = 397$ cells, mean + s.e.m.). Note that iso2 C784T resulted in a truncated protein (30 kDa). **(f)** P19 cells transfected with Flag-tagged merlin-iso2 (iso2 wt) and C784T mutant (iso2 C784T) ($n = 3$). The white arrowhead indicates an unspecific band in all three lanes. The black arrowhead points to immunoprecipitated truncated merlin (iso2 C784T). For full-length blots and quantitations, see Supplementary Figure 9.

phosphorylation or axonal diameter growth in P19 cells (Fig. 7e). This mutation was still able to form a complex with p190RhoGAP, but could not bind RhoGDI (Fig. 7f), demonstrating the importance of the merlin-RhoGDI complex at least in intact cells. Furthermore, these findings were associated with a loss of RhoA activation (Fig. 7e) and indicate that NF2 patients lacking the intact C terminus of one NF2 allele in neurons fail to regulate Rho-ROCK-dependent neurofilament phosphorylation, leading to insufficient axonal structure maintenance.

DISCUSSION

We found that the ubiquitously expressed tumor suppressor protein merlin (specifically merlin-iso2) functions intrinsically in neurons to regulate axonal integrity and propose that reduced NF2 gene dosage in axons is relevant in NF2-related polyneuropathy. Specifically, we found that merlin-iso2 regulates RhoA, leading to downstream ROCK activity, which promotes neurofilament phosphorylation and ultimately controls the growth of axonal diameter *in vitro* and axon structure maintenance *in vivo*. Consequently, merlin-iso2 reduction resulted in inhibition of RhoA and neurofilament hypophosphorylation.

Irregular neurofilament phosphorylation has been previously reported to coincide with axonal dysfunction²³ and increased axon vulnerability²⁴. Several neuropathic disorders display altered neurofilament phosphorylation levels². Our results highlight importance of neurofilament modulation and provide, to the best of our knowledge, the first *in vivo* evidence that Rho-ROCK signals are

important for neurofilament phosphorylation and the consequent maintenance of axonal structure.

While exploring how merlin-iso2 operates in the axon, we identified a merlin-dependent multi-protein complex. Both RhoGDI and p190RhoGAP, important determinants for Rho activity control, were found to associate with neuronal merlin. Our data suggest that axonally expressed merlin-iso2, coupled to neurofilaments, acts as a tethering system, fine-tuning local RhoA signals in the axon. A NF2 patient-derived mutation causing severe polyneuropathy (C784T)²¹, which maintains p190RhoGAP interaction, but results in deficient RhoGDI binding, was unable to promote Rho activity and radial axon growth *in vitro*, illustrating the importance of the merlin-RhoGDI complex in intact cells. This scaffold-mediated assembly provides a versatile tool for the spatiotemporal organization of signal transduction. Specific merlin signaling hubs defined to cellular substructures such as axons enable Rho-ROCK signals to promote phosphorylation of neurofilaments, which is important for axon structure.

Our data contribute to the mechanistic understanding of why NF2 patients suffer from polyneuropathy even in the absence of nerve damaging tumors. Merlin was originally identified as a tumor suppressor protein and is known to be involved in gliogenic tumor development. It is assumed, but not proven, that the cause of nerve damaging processes associated with NF2 disease is a result of secondary problems, such as compressive glial cell tumors (schwannomas)^{8,22,25} or hyperproliferative Schwann cells (tumorlets)⁸. We found that NF2 patients have axon-intrinsic ultrastructural irregularities and

ARTICLES

reduced phosphorylated neurofilaments relative to normal healthy controls, indicating that the nerve damage in NF2 patients develops from an inner axonal process resulting from reduced merlin protein levels. This neuron-intrinsic impairment was verified in our mouse model, in which the specific loss of merlin-iso2, or even a reduction in the merlin-iso2 dosage, resulted in nerve damage and neuropathic symptoms without the appearance of Schwann cell-derived tumors. Despite the described axonal abnormalities, we could not detect classical signs of axon degeneration in *Nf2-iso2*^{-/-} mice. We observed a phenotype resembling 'axonal atrophy', with shrunken and collapsed axons of peripheral nerves as have described previously in the context of neurofilament mutations¹⁸. We detected neuropathy of axonal origin in mutant mice and propose that the loss of merlin-iso2 leads to a reduction of functional axons.

Our findings are unexpected for this tumor suppressor and relevant for a complete understanding of the spectrum of nervous system abnormalities in the human NF2 disease. It is reasonable to assume that the signaling pathway downstream of merlin that we describe has a broader implication for other hereditary neuropathies whose mechanisms remain elusive. Elucidation of the signaling pathways of radial axonal growth and maintenance is will be necessary to fully understand nerve regeneration and protection from axonal degeneration.

METHODS

Methods and any associated references are available in the [online version of the paper](#).

Note: Supplementary information is available in the [online version of the paper](#).

ACKNOWLEDGMENTS

The authors would like to thank U. Petz, C. Poser and S. Ramrath for their expert technical assistance, H. Rosemann, F. Kaufmann and D. Galendo for their skilled breeding and husbandry of animals, and R.E. Ferner for discussions and support. *Mpz-cre* mice were kindly provided M.L. Feltri (Hunter James Kelly Research Institute). This work was supported by Sonderforschungsbereich 604, Deutsche Forschungsgemeinschaft MO 1421/2-1 and Krebshilfe 107089. A.S. is recipient of a Young Investigator Award from the Children's Tumor Foundation.

AUTHOR CONTRIBUTIONS

A.S. and H.M. conceived and designed the study. H.M. supervised the experimental program and prepared the manuscript. A.S. performed and analyzed the majority of the experiments and prepared the manuscript. S.L.B. performed the nerve section analysis of both knockout mice and patient biopsies, as well as their analysis. M.N.-K. and M.G. generated the *Nf2-iso1*^{-/-} and *Nf2-iso2*^{-/-} mice. R.B. designed the electrophysiological experiments and participated in data acquisition. C.G. and D.H.G. synthesized isoform-specific merlin antibodies. A.Z. and M.J.J. participated in the behavioral analysis of merlin knockout mice and the preparation of primary cell cultures. S.S. conducted nucleotide exchange and binding assays. X.-P.D. and D.B.P. provided tissue samples of *Mpz-cre*; *Nf2^{loxP/loxP}* mice. C.H. and V.-F.M. provided NF2 patient biopsy sections for immunohistochemistry. C.O.H. provided NF2 patient biopsy sections for ultrastructural analysis. J.W. and J.M.S. performed the ultrastructural analysis of human NF2 patient biopsies.

COMPETING FINANCIAL INTERESTS

The authors declare no competing financial interests.

Reprints and permissions information is available online at <http://www.nature.com/reprints/index.html>.

- Luo, L. Rho GTPases in neuronal morphogenesis. *Nat. Rev. Neurosci.* **1**, 173–180 (2000).
- Perrot, R., Berges, R., Bocquet, A. & Eyer, J. Review of the multiple aspects of neurofilament functions, and their possible contribution to neurodegeneration. *Mol. Neurobiol.* **38**, 27–65 (2008).
- Zhu, Q., Couillard-Despres, S. & Julien, J.P. Delayed maturation of regenerating myelinated axons in mice lacking neurofilaments. *Exp. Neurol.* **148**, 299–316 (1997).
- de Waegh, S.M., Lee, V.M. & Brady, S.T. Local modulation of neurofilament phosphorylation, axonal caliber and slow axonal transport by myelinating Schwann cells. *Cell* **68**, 451–463 (1992).
- Dubois, M., Strazielle, C., Julien, J.P. & Lalonde, R. Mice with the deleted neurofilament of low molecular weight (*Nefl*) gene. 2. Effects on motor functions and spatial orientation. *J. Neurosci. Res.* **80**, 751–758 (2005).
- England, J.D. & Asbury, A.K. Peripheral neuropathy. *Lancet* **363**, 2151–2161 (2004).
- Astthagiri, A.R. *et al.* Neurofibromatosis type 2. *Lancet* **373**, 1974–1986 (2009).
- Sperfeld, A.D., Hein, C., Schroder, J.M., Ludolph, A.C. & Hanemann, C.O. Occurrence and characterization of peripheral nerve involvement in neurofibromatosis type 2. *Brain* **125**, 996–1004 (2002).
- Schulz, A. *et al.* Merlin inhibits neurite outgrowth in the CNS. *J. Neurosci.* **30**, 10177–10186 (2010).
- Gianola, S. & Rossi, F. Evolution of the Purkinje cell response to injury and regenerative potential during postnatal development of the rat cerebellum. *J. Comp. Neurol.* **430**, 101–117 (2001).
- Jones-Villeneuve, E.M., McBurney, M.W., Rogers, K.A. & Kalnins, V.I. Retinoic acid induces embryonal carcinoma cells to differentiate into neurons and glial cells. *J. Cell Biol.* **94**, 253–262 (1982).
- Hashimoto, R. *et al.* Domain- and site-specific phosphorylation of bovine NF-L by Rho-associated kinase. *Biochem. Biophys. Res. Commun.* **245**, 407–411 (1998).
- Moorman, J.P., Luu, D., Wickham, J., Bobak, D.A. & Hahn, C.S. A balance of signaling by Rho family small GTPases RhoA, Rac1 and Cdc42 coordinates cytoskeletal morphology, but not cell survival. *Oncogene* **18**, 47–57 (1999).
- Maeda, M., Matsui, T., Imamura, M. & Tsukita, S. Expression level, subcellular distribution and rho-GDI binding affinity of merlin in comparison with Ezrin/Radixin/Moesin proteins. *Oncogene* **18**, 4788–4797 (1999).
- Yamashita, T. & Tohyama, M. The p75 receptor acts as a displacement factor that releases Rho from Rho-GDI. *Nat. Neurosci.* **6**, 461–467 (2003).
- Sherman, L. *et al.* Interdomain binding mediates tumor growth suppression by the NF2 gene product. *Oncogene* **15**, 2505–2509 (1997).
- Bremer, J. *et al.* Axonal prion protein is required for peripheral myelin maintenance. *Nat. Neurosci.* **13**, 310–318 (2010).
- Elder, G.A., Friedrich, V.L. Jr., Margita, A. & Lazzarini, R.A. Age-related atrophy of motor axons in mice deficient in the mid-sized neurofilament subunit. *J. Cell Biol.* **146**, 181–192 (1999).
- Giovannini, M. *et al.* Conditional biallelic Nf2 mutation in the mouse promotes manifestations of human neurofibromatosis type 2. *Genes Dev.* **14**, 1617–1630 (2000).
- Feltri, M.L. *et al.* Conditional disruption of beta 1 integrin in Schwann cells impedes interactions with axons. *J. Cell Biol.* **156**, 199–209 (2002).
- Hagel, C. *et al.* Polyneuropathy in neurofibromatosis 2: clinical findings, molecular genetics and neuropathological alterations in sural nerve biopsy specimens. *Acta Neuropathol.* **104**, 179–187 (2002).
- Hanemann, C.O., Diebold, R. & Kaufmann, D. Role of NF2 haploinsufficiency in NF2-associated polyneuropathy. *Brain Pathol.* **17**, 371–376 (2007).
- Jackson, S.J., Pryce, G., Diemel, L.T., Cuzner, M.L. & Baker, D. Cannabinoid-receptor 1 null mice are susceptible to neurofilament damage and caspase 3 activation. *Neuroscience* **134**, 261–268 (2005).
- Morrison, J.H. *et al.* A monoclonal antibody to non-phosphorylated neurofilament protein marks the vulnerable cortical neurons in Alzheimer's disease. *Brain Res.* **416**, 331–336 (1987).
- Iseki, C. *et al.* *Rinsho Shinkeigaku* [A case of neurofibromatosis type 2 (NF2) presenting with late-onset axonal polyneuropathy] **49**, 419–423 (2009).

ONLINE METHODS

Experimental animals. All mice handled in strict adherence to local governmental and institutional animal care regulations (Thüringer Landesamt für Lebensmittelsicherheit und Verbraucherschutz). *Nf2-iso1*^{-/-} and *Nf2-iso2*^{-/-} mice were generated by M.N.-K. and M.G. (unpublished data) and purchased from Riken BioResource (C57BL/6 background). Average day of birth, on the 19th day of pregnancy, was defined as P0 and adult was defined as P60. Behavior and electrophysiology tests, immunohistochemistry and electron microscopy were carried out on mice or tissue taken from 8-week-old mice unless otherwise stated. All of the mice used for this study were age and gender matched, as well as derived from group housing. Genotyping was performed by PCR of tail biopsies. For *Nf2-iso1*^{-/-} mice, the primers Nf2 insert (5'-CCT CAA GCC CAA GGC AGA AGA-3') and Nf2 insert2a (5'-CCT CAG AGT GAG GCA GTC TTC TAG G-3') were used, yielding 267 bp or 391 bp products for wild-type or knockout alleles, respectively. For *Nf2-iso2*^{-/-} mice, primers Nf2 (5'-CAG TAC ACC TGA GGT CAC TGT CTC-3') and Nf2 insert2a were used to generate 235 bp and 378 bp products for knockout and wild-type alleles, respectively.

Immunohistochemistry. Mice were perfused transcardially using phosphate-buffered saline (PBS), followed by 4% paraformaldehyde (vol/vol) in PBS. Following dissection, brains were post-fixed in the same fixative overnight at 20 °C. Floating sections were cut to 50 µm thicknesses or to 8 µm thickness for paraffin-embedded sections. Floating sections were heated in 10 mM sodium citrate buffer (pH 9) at 80 °C for 30 min and, after cooling, incubated in 2% non-fat dry milk (vol/vol) for 30 min. Sections were treated with 0.5% Triton X-100 (vol/vol) for 30 min and incubated in 0.2% gelatine and 2% goat serum (vol/vol) diluted in PBS for 2 h. Sections were submersed in primary antibody solution overnight at 4 °C. For primary antibodies, we used antibodies to calbindinD-28k (rabbit polyclonal, 1:2,000, Swant, clone CB38), MBP (mouse monoclonal, 1:500, clone MAB384, Millipore Bioscience Research Reagents) phospho-neurofilament (SMI31, 1:500, Hiss Diagnostics), merlin (A-19, 1:200, Santa Cruz Biotechnology), and merlin-iso1 (WA27, 1:100) and merlin-iso2 (WA28, 1:100) (D.H.G.)²⁶. The rabbit polyclonal merlin antibodies were raised after repeated immunizations and peptide purification (WA27, C-PQAQGRRPICL; WA28, C-LTLQSAKARVAFFEL). After vigorous washings, sections were incubated with the secondary antibody solution (Alexa488- and Alexa546-conjugated goat antibodies to mouse or rabbit, 1:500 in PBS, A-11034 and A-11030, Invitrogen) at 20 °C for 2 h. Sections were counterstained using Hoechst 34580 (1 µg ml⁻¹ PBS, 5 min), washed for at least 1 h and embedded in Mowiol. Merlin-specific staining was confirmed previously⁹ and we tested the antibody to merlin-iso2 antibody on tissues from *Nf2-iso2*^{-/-} mice (Supplementary Fig. 2).

Paraffin-embedded sections were rehydrated, boiled in 10 mM sodium citrate buffer (pH 9) for 30 min in a microwave and subsequently treated with 0.5% Triton X-100 for 10 min. Sections were incubated in 0.2% gelatine and 2% goat serum diluted in PBS for at least 2 h. Sections were submersed in the primary antibody solution overnight at 4 °C. For primary antibodies, we used antibodies to phospho-neurofilament (SMI31, 1:500, Hiss Diagnostics), merlin-iso1 (WA-27, 1:100), merlin-iso2 (WA-28, 1:100) and APP (rabbit polyclonal antibody, Calbiochem, 1:500, 171610). After vigorous washings, sections incubated with secondary antibody solution (Alexa488- and Alexa546-conjugated goat antibodies to mouse or rabbit, 1:500 in PBS, Invitrogen) at 20 °C for 2 h. Finally, specimens were washed in PBS, counterstained using Hoechst 34580 (1 µg ml⁻¹ PBS, 5 min), dehydrated and embedded.

Immunocytochemistry. P19 cells, primary cerebellar neurons or DRG cells were grown on coverslips and fixed with 4% paraformaldehyde in PBS for 20 min. After washing in PBS, cells were permeabilized with 0.3% Triton X-100 for 1 min and incubated for 2 h in 1% bovine serum albumin (vol/vol). Cells incubated with primary antibodies at 20 °C for 1 h. For primary antibodies, we used antibody to phospho-neurofilament (SMI31, 1:200, Hiss Diagnostics), RhoGDI (A-20, 1:100, Santa Cruz Biotechnology), growth-associated protein (GAP-43, clone H-100, 1:400, Santa Cruz Biotechnology), APP (rabbit polyclonal antibody, Calbiochem, 1:100), merlin-iso1 (WA-27, 1:50), merlin-iso2 (WA-28, 1:50) and p190RhoGAP (mouse monoclonal antibody, Sigma, clone D2D6, 1:100). After extensive rinsing in PBS, cells were incubated with secondary antibodies (Alexa488-conjugated antibody to rabbit, 1:500; Alexa546-conjugated antibody to mouse, 1:500) for 1 h. Cells were washed in PBS and

counterstained with Hoechst 34580 (1:1,000 in PBS) for 5 min. Cells were mounted on cover plates with a Mowiol-based mounting medium.

Developmental appearance of merlin in Purkinje cell axons. Axonal expression of merlin-iso2 determined by colocalization of merlin (iso2) with the Purkinje cell-specific marker calbindin. Continuous calbindin-positive signals in the granular layer of the mouse cerebellum with lengths of more than 20 µm were analyzed for additional merlin staining. Note the methodical difference with apparent discrepant results in a previous study⁹. There, the appearance of merlin in the proximal axon initial segment was monitored.

Immunoblotting. Immunoblotting was performed as described previously²⁷. For primary antibodies, we used antibodies to merlin (clone A-19, 1:500), actin (clone I-19, 1:1,500, Santa Cruz Biotechnology), RhoA (1:500, Upstate), phospho-neurofilament (SMI31, 1:500, Hiss Diagnostics), pan-axonal neurofilament (SMI312, 1:500, Hiss Diagnostics), Flag (clone M2, 1:1,000, Sigma-Aldrich), RhoGDI (A-20, 1:500, Santa Cruz Biotechnology), merlin-iso1 (WA-27, 1:500), merlin-iso2 (WA-28, 1:500) and p190RhoGAP (mouse monoclonal antibody, Sigma, clone D2D6, 1:1,000). Western blot results were quantified using gel analysis software by ImageJ. Density values were normalized to actin and appropriate controls of transfection or wild-type tissue.

Pulldowns to detect active RhoA. A detection kit was used (Active Rho Pull-Down and Detection Kit, Pierce Biotechnology) according to manufacturer instructions. Precipitates and total lysates were resolved on a 10% SDS-PAGE gel and immunoblotted using antibody to RhoA (1:500, Upstate). Total lysates were used as loading controls. Pulldown assays were repeated at least three times in each case.

P19 cell culture. P19 cells¹¹ purchased from ATCC (CRL-1825) maintained in Dulbecco's modified Eagle's medium supplemented with 10% fetal calf serum (vol/vol). Induction of neuronal phenotype, aggregates were generated on bacterial-grade dishes and treated with 5 × 10⁻⁷ M all-trans retinoic acid (Sigma) for 4 d. Cells were re-plated on cell culture dishes in the absence of retinoic acid.

Primary dissociated cerebellar cultures. Primary dissociated cerebellar cultures (referred to as cerebellar granular cells) were established from cerebellar tissue of 8-d-old pups (C57BL/6 mice) as described previously²⁸. Cells were grown at a density of 200,000 cells cm⁻² in defined neurobasal medium with B27 supplement (Invitrogen).

DRG culture. Cells were prepared from 4–6-d-old mice (P4–6) as described²⁹. Arabinofuranosyl cytidine (Sigma, C1768, working concentration of 10 µM) was used to assure glial-free conditions.

Transfection procedures. P19 cells were transfected 3–4 d after plating using Lipofectamine 2000 (Invitrogen) according to the manufacturer's protocol. Transfection efficiency averaged around 45 to 50%. For siRNA knockdown experiments, primary cells were transfected using Dharmafect 3 according to the manufacturer's instructions (Dharmacon, Thermo Scientific). Using siGLO RNA, a transfection rate of 75% was obtained. For overexpression studies, primary neurons were transfected according to a method described previously³⁰.

For inhibition of merlin expression, the following oligonucleotides were used: si-nf2 5'-UAC CGA GCU UCG ACA UUA UUG-3' (knockdown of both major merlin isoforms), si-iso1 5'-AAA GAA GGC CAC UCG GGA CUU-3', si-iso2 5'-UAG GUC UUC UGC CUU GGG CUU-3' and scr-nf2 5'-AAU CCG GUU GCA UAG UUC AUG-3' (untargeted control). For RhoGDI knockdown, siRNA was purchased from Santa Cruz Biotechnology (sc-36416). For overexpression of merlin, pcDNA3-based *Nf2* full-length sequences for isoform 1 and 2 was used. Backbone vector pcDNA3 used as control. Merlin fragment constructs used: N-terminus amino acids (aa) 1–299; C-terminus merlin-iso1 aa 300–595; C-terminus of merlin-iso2 aa 300–590. QuikChange Site-Directed Mutagenesis Kit (Stratagene) was used according to the manufacturer's instructions.

For knockdown of p190RhoGAP, we used the pGIPZ plasmid containing shRNA against the *ARHGAP35* gene according to manufacturers recommendation (Open Biosystems, Oligo ID: V3LHS_349456, GeneID: 2909; antisense

sequence: TCCAGGTAGACATAGTCCT). The shRNA was directed against the human gene, but is homologous to rat and mouse. In brief, shRNA was co-transfected with pMD.G-VSVG and pCMVdelR8.91 packaging plasmids into HEK293T cells using Lipofectamine 2000. After 48 h, the supernatant containing viral particles was harvested, sterile filtered and used for transduction of DRG cells. Thus, DRG cells were incubated with viral particles in DMEM/5% fetal bovine serum for 16 h and subsequently grown in DMEM/10% fetal bovine serum.

Quantification of axonal diameter *in vitro*. Diameters of axonal processes of differentiated P19 cells, primary cerebellar neurons and DRG cells were measured 3 d after transfection. To identify axonal processes, cells were co-stained with the axonal markers GAP-43 and phospho-neurofilaments p(NF-H) (Supplementary Fig. 3a). Using the ImageJ plugin NeuronJ, axons longer than a cell soma were measured and scaled in micrometers. Processes that could be clearly distinguished from processes of neighboring cells were evaluated. Changes of axon calibers *in vitro* are also referred to as changes in radial axon growth.

Microscopy and image acquisition. Confocal images were obtained with a Leica TCS SP5 laser-scanning microscope. Images were acquired with a 40× objective (HCK APO 40.0X 0.75 DRY, NA = 0.75) at a pinhole size of three airy discs and a resolution of $0.73 \times 0.73 \times 0.50 \mu\text{m}^3$. Images were taken from a single optical planes (voxel size = 189 nm). Epifluorescent images of dissociated neurons were obtained with a Leica DMIRE2 microscope equipped with a Leica DFC350FX camera. All digital processing was performed using Adobe Photoshop 6.0. For all images, only linear adjustments of the brightness and contrast were performed.

RhoA activation. Rho activator #CN01 (Cytoskeleton) was used according to the manufacturer's recommendations.

Analysis of axonal caliber and myelination in merlin knockout mice. Analysis was carried out on semi-thin and thin sections of the sciatic nerve obtained from transcardially perfused *Nf2-iso1*^{-/-}, *Nf2-iso2*^{-/-}, *Nf2-iso1*^{+/-}, *Nf2-iso2*^{+/-} and wild-type mice. Mice were perfused with a solution containing 3% paraformaldehyde and 3% glutaraldehyde (vol/vol) in 0.1 M phosphate buffer (pH 7.4). Sections were post-fixed for 1 h and kept in fixative that included 3% sucrose (vol/vol). Sections were obtained from the mid part of the sciatic nerve reaching from gluteal to the popliteal regions. Sectioning and staining was performed as described³¹. Images of toluidine blue were stained semithin sections taken using an Axioskop 2 MOT (Carl Zeiss) equipped with a 100× immersion oil objective and an Olympus XC50 digital camera (Olympus). Standardized settings for camera sensitivity, resolution ($2,576 \times 1,932$ pixels) and brightness of illumination were used for all micrographs. Thin sections were analyzed with an electron microscope (EM910, Carl Zeiss) equipped with an integrated TRS 1K digital camera (Carl Zeiss). Image analysis was carried out using ImageJ version 1.43u. RGB color images obtained from semi-thin sections were split into single channels, and the green channel was chosen for measurements. The picture was contrasted using the auto function. Using the freehand selection tool, the axon and the myelin was grossly circumscribed and the area was adapted using the ABSnake PlugIn (gradient threshold varied between 20 and 30, 10–20 iterations per image). Low-contrasted myelin sheaths were surrounded manually. Based on measured areas, we calculated the thicknesses of the axons and myelin sheaths. Providing a measure for bending of the transversely cut axonal surface, the axon was surrounded as described above and solidity factor was measured using the implemented ImageJ software tools (shape descriptor). Solidity factor describes the area covered by a given structure in relation to the smallest convex area, which covers this structure, that is, the solidity factor of a round circle or ellipse would be 1, while whereas circle with an invagination would give a factor smaller than 1. This solidity factor is superior to the circularity factor often used for measuring changes in surface structures, as it provides a factor to measure changes in surface curvatures independent of the plane of section. Changes of axon structure *in vivo* are also referred to as axon structure maintenance or integrity. Three pairs of mice from the same litter were used for experiments. Electron microscopical images were taken from 50-nm-thick sections. Neurofilaments are easily identified by size and compact structure. The positions of all neurofilaments in a defined area covering only tangentially cut neurofilaments were measured and distances to their neighbors evaluated. The nearest neighbor of a neurofilament

was defined as the average distance of the three nearest neighbors of a neurofilament. The values provided in Figure 5b–d are derived from 300 to 800 distances measured per genotype. At least two mice were taken per genotype. Axon calibers were classified as described previously³².

Muscle preparations and immunostainings. Preparations were carried out as described before³³. BTX (Invitrogen, conjugated to Texas Red) was used at a concentration of $1 \mu\text{g ml}^{-1}$, and antibody to N52 (Sigma) was used at a dilution of 1:500. Silver staining was done as described³⁴. Images were taken with standard bright-field upright microscopes. Images of fluorescent stains were taken using the Leica laser-scanning microscope LSM TCS SP2. Pictures shown are maximum projections of ten images taken at a distance of $1 \mu\text{m}$.

Co-immunoprecipitation. Co-immunoprecipitation studies were performed as described previously²⁷.

Kinase screening assay. We selected 23 serine/threonine kinases on the basis of reports of their association with merlin and/or neurofilament signaling (Supplementary Table 1). Appropriate siGENOME SMARTpool duplexes (Thermo Fisher) targeting kinases were transfected into neuronally differentiated P19 cells. Medium was replaced after 24 h, following plasmid transfection of either an empty vector control or merlin-iso2. After 2 additional days, cells were lysed, and subjected to SDS-PAGE and immunoblotting to determine the phosphorylation state of heavy subunit neurofilaments (pNF-H). Consistent results were obtained in three consecutive experiments in 24-well plate format.

Sural nerve biopsies of NF2 patients. Biopsy sections for immunohistochemistry were provided by C.H. For phospho-neurofilament analysis, specimens of two healthy control males (57 and 52 years of age) were compared with nerve tissue from two NF2 patients (both 36 years of age), referred to as patients 718 and 21.3 in ref. 21. Sections were stained for phosphorylated neurofilament epitopes using antibody to SMI31 (Fig. 7a). Monochrome single-channel images were excised from fluorescent background staining by threshold setting to a range of 95 to 255 (Fig. 7a). By means of ImageJ plugin Analyze Particles, total area covered by phospho-neurofilament staining was determined as pixel² per μm^2 and subsequently divided by the number of vital axons. Taking the total axon number into account, the decrease was not simply a result of loss of fibers. Quantifications of interfibril distances (Supplementary Fig. 9b) was performed as described above.

NF2 sural nerve biopsies for ultrastructural analysis of non-myelinated fibers (mutation in patient A: A1447-2G, age 37; mutation in patient B: 1594 ins3 del59, age 27) were kindly provided by C.O.H. Nerve specimens were fixed in 3.9% phosphate-buffered glutaraldehyde, embedded in epoxy resin and processed for electron microscopy as described previously²³.

The immunohistochemical and ultrastructural studies were performed on archival tissue that was processed and diagnosed in the Institutes of Neuropathology in Hamburg and Aachen. According to the law for hospitals in Hamburg (Germany) and North Rhine–Westphalia (Germany), samples of closed cases that were processed and investigated in a medical institution may be used for research purposes by the same institution without need for a separate written informed consent from the patients.

GST-pulldown assays. GST-RhoGDI (in pGEX2T vector backbone). For pull-down assays from bacteria lysates, frozen pellets of bacteria induced for protein expression were resuspended and lysed in buffer containing 50 mM Tris pH 7.5, 100 mM NaCl, 0.5% CHAPS (vol/vol) and protease inhibitor cocktail. Samples were sonicated on ice for 5–10 min and cell debris was collected for 15 min at 12,000g and 4 °C. Cleared lysates were diluted in 1 ml of pull-down buffer and incubated with GST alone or GST-tagged proteins bound to glutathione beads for 1.5–2 h rotating at 4 °C. Four washing steps were performed with 1 ml of pull-down buffer. Simultaneously, beads were spun down at 5,000g for 30 s and boiled in 2× SDS sample buffer and analyzed by subsequent SDS-PAGE and western blotting.

Protein interactions *in vitro*. We applied 1.5 μg of purified His-RhoGDI α (aa 24–204, Fitzgerald) or 3 μg bovine serum albumin (BSA) point-wise on dry nitrocellulose membrane. Membrane was blocked in 5% skimmed-milk (vol/vol)



in TBS-Tween for 1 h followed by 2.5-h incubation with 5 $\mu\text{g ml}^{-1}$ purified Merlin FERM domain or BSA in 0.5% CHAPS, 50 mM Tris (pH 7.5) and 100 mM NaCl at 20 °C, respectively. After three washes with TBS-Tween, membranes were treated with antibody to merlin (A-19, 1:750) for 1 h at 20 °C, followed by incubation with horseradish peroxidase-coupled antibody to rabbit (1:2,000) for 1 h.

Nucleotide exchange assay. Assay was performed on the basis of a Rho GEF exchange assay kit (Cytoskeleton BK100) according to manufacturers recommendation. In brief, 2 \times exchange reaction buffer contained 1.5 μM mant-GTP in 40 mM Tris (pH 7.5), 100 mM NaCl and 20 mM MgCl_2 . Samples containing a final concentration of 2 μM RhoA, 3 μM His-RhoGDI (aa 24–204, Fitzgerald) and 4 μM merlin FERM domain (aa 1–313, 50 mM Tris (pH 7.5), 300 mM NaCl) were pre-incubated on ice for 30 min in a black 384 round bottom well plate (Corning). The 2 \times exchange buffer was added to a final concentration of 0.75 μM of mant-GTP. Samples immediately analyzed with a Mithras LB 940 Multimode Microplate Reader (Berthold Technologies) at 20 °C. Fluorescence emission was recorded at 460 nm after excitation with lamp energy of 5,000 (5.72 W) at 355 nm every 20 s. The hDbs GEF (human Dbl Big Sister) fragment was added to a final concentration of 0.5 μM and a total reaction volume of 15 μl . Measurement measured for 6 h. Control protein samples components replaced by BSA.

Rotarod test. Measures motor coordination and proprioception. Determines time that mice can stay on a rotating rod, referred to as latency to fall. To increase test sensitivity, we used a program accelerating the rod from 1 to 50 rpm in 4.2 min (accelerates at 1 rpm per 5 s). Each mouse underwent the same 5-d procedure passing two sessions per d including two trials each session. Mice still on the apparatus at 252 s were scored as 252 s. Rotating on the rod for two consecutive rotations without running equaled falling event. Day 5 performances were used for statistical analysis using Bonferroni correction.

Hot plate test. The hot plate test measures response to thermal stimuli. Mice were placed on a horizontal surface that was heated to 55 °C. Subsequently, the latency for hind paw withdrawal was measured, with a 60-s cut-off time to prevent severe tissue damage.

Electrophysiology. An investigation of the sciatic nerve conduction characteristics in 8-week-old mice was performed as described previously³⁵ in a blinded way. Statistical analysis, results of six gender-matched mice per genotype were quantified.

Statistical evaluation. Differences between *Nf2-iso1*^{−/−} and *Nf2-iso2*^{−/−} mice and their appropriate wild-type littermates were determined. For all quantitative analyses, we compared two independent groups of experiments. To demonstrate their comparable distribution, we performed Levene's test for equal variances. Comparisons between groups were made with unpaired *t* tests unless stated otherwise (SPSS software, Statistical Package for the Social Sciences). For each experiment we calculated the *P* value, the *t* value and the degrees of freedom. Differences were considered to be significant when *P* < 0.05. All values are presented as means and their s.e.

26. Scherer, S.S. & Gutmann, D.H. Expression of the neurofibromatosis 2 tumor suppressor gene product, merlin, in Schwann cells. *J. Neurosci. Res.* **46**, 595–605 (1996).
27. Morrison, H. *et al.* The NF2 tumor suppressor gene product, merlin, mediates contact inhibition of growth through interactions with CD44. *Genes Dev.* **15**, 968–980 (2001).
28. Baader, S.L. & Schilling, K. Glutamate receptors mediate dynamic regulation of nitric oxide synthase expression in cerebellar granule cells. *J. Neurosci.* **16**, 1440–1449 (1996).
29. Malin, S.A., Davis, B.M. & Moliver, D.C. Production of dissociated sensory neuron cultures and considerations for their use in studying neuronal function and plasticity. *Nat. Protoc.* **2**, 152–160 (2007).
30. Watanabe, S.Y. *et al.* Calcium phosphate-mediated transfection of primary cultured brain neurons using GFP expression as a marker: application for single neuron electrophysiology. *Neurosci. Res.* **33**, 71–78 (1999).
31. Jankowski, J., Miething, A., Schilling, K. & Baader, S.L. Physiological purkinje cell death is spatiotemporally organized in the developing mouse cerebellum. *Cerebellum* **8**, 277–290 (2009).
32. Michailov, G.V. *et al.* Axonal neuregulin-1 regulates myelin sheath thickness. *Science* **304**, 700–703 (2004).
33. Mundegar, R.R., Franke, E., Schafer, R., Zwyer, M. & Wernig, A. Reduction of high background staining by heating unfixed mouse skeletal muscle tissue sections allows for detection of thermostable antigens with murine monoclonal antibodies. *J. Histochem. Cytochem.* **56**, 969–975 (2008).
34. Mulisch, M.W.U. *Romeis-Mikroskopische Technik* (Spektrum Akademischer Verlag, 2010).
35. Xia, R.H., Yosef, N. & Ubogu, E.E. Dorsal caudal tail and sciatic motor nerve conduction studies in adult mice: technical aspects and normative data. *Muscle Nerve* **41**, 850–856 (2010).

4.2. „In vivo Electrophysiological Measurements on Mouse Sciatic Nerves“

Schulz A, Walther C, Morrison H, Bauer R. *In vivo* Electrophysiological Measurements on Mouse Sciatic Nerves. *J. Vis. Exp* (86). 2014. e51181.

Online-Link:

<http://www.jove.com/video/51181/in-vivo-electrophysiological-measurements-on-mouse-sciatic-nerves>

Anteil der beteiligten Autoren an der Veröffentlichung:

Dr. Alexander Schulz führte die Experimente durch und half bei Etablierung der gezeigten Methodik. Außerdem hat Dr. Schulz Anteil an der filmischen Umsetzung und schriftlichen Ausarbeitung des Manuskriptes.

Christian Walther half bei den Filmaufnahmen zum angefertigten Video.

Dr. Helen Morrison hat Anteil an der Erstellung des Manuskriptes.

Prof. Dr. Reinhard Bauer etablierte die elektrophysiologischen Experimente, nahm deren Auswertung vor und schrieb das Manuskript.

Video Article

In Vivo Electrophysiological Measurements on Mouse Sciatic Nerves

Alexander Schulz¹, Christian Walther², Helen Morrison¹, Reinhard Bauer³

¹Leibniz Institute for Age Research, Fritz Lipmann Institute

²Friedrich Schiller University Jena

³Institute of Molecular Cell Biology & Center for Sepsis Control and Care (CSCC) Jena University Hospital, Friedrich Schiller University Jena

Correspondence to: Reinhard Bauer at reinhard.bauer@med.uni-jena.de

URL: <http://www.jove.com/video/51181>

DOI: [doi:10.3791/51181](https://doi.org/10.3791/51181)

Keywords: Neuroscience, Issue 86, Demyelinating Diseases, Neurodegenerative Diseases, electrophysiology, sciatic nerve, mouse, nerve conduction velocity, neuromuscular diseases

Date Published: 4/13/2014

Citation: Schulz, A., Walther, C., Morrison, H., Bauer, R. *In Vivo* Electrophysiological Measurements on Mouse Sciatic Nerves. *J. Vis. Exp.* (86), e51181, doi:10.3791/51181 (2014).

Abstract

Electrophysiological studies allow a rational classification of various neuromuscular diseases and are of help, together with neuropathological techniques, in the understanding of the underlying pathophysiology¹. Here we describe a method to perform electrophysiological studies on mouse sciatic nerves *in vivo*.

The animals are anesthetized with isoflurane in order to ensure analgesia for the tested mice and undisturbed working environment during the measurements that take about 30 min/animal. A constant body temperature of 37 °C is maintained by a heating plate and continuously measured by a rectal thermo probe². Additionally, an electrocardiogram (ECG) is routinely recorded during the measurements in order to continuously monitor the physiological state of the investigated animals.

Electrophysiological recordings are performed on the sciatic nerve, the largest nerve of the peripheral nervous system (PNS), supplying the mouse hind limb with both motoric and sensory fiber tracts. In our protocol, sciatic nerves remain *in situ* and therefore do not have to be extracted or exposed, allowing measurements without any adverse nerve irritations along with actual recordings. Using appropriate needle electrodes³ we perform both proximal and distal nerve stimulations, registering the transmitted potentials with sensing electrodes at gastrocnemius muscles. After data processing, reliable and highly consistent values for the nerve conduction velocity (NCV) and the compound motor action potential (CMAP), the key parameters for quantification of gross peripheral nerve functioning, can be achieved.

Video Link

The video component of this article can be found at <http://www.jove.com/video/51181/>

Introduction

Electrophysiological measurements are an indispensable tool for investigating the functional integrity of peripheral nerves in both clinical and laboratory environments. In humans, a large number of neuromuscular disorders and neuropathies diagnostically rely on electrophysiological measurements. By measuring nerve properties as conduction velocity or potential amplitudes of the signal, it is possible to characterize the rough origin of peripheral nerve diseases.

The nerve conduction velocity is highly dependent on rapid signal propagation enabled by myelination. Therefore, demyelinating processes generally show decreased conduction velocities⁴. The compound motor action potential (CMAP) - correlating with the number of functional axons - is an indicator for axonal damage when significantly reduced⁵.

Thus, by means of electrophysiological methods the etiology of peripheral nerve damage can be discriminated, such as for hereditary neuropathies^{6,7}, diabetic neuropathy^{8,9}, chronic inflammatory demyelinating polyneuropathies (CIPD)¹⁰, or metabolic neuropathies¹¹.

Normally, in the human application noninvasive recordings on the sural or ulnar nerve are preferred. In mice, it is straightforward to analyze nerve properties of sciatic nerves, the largest nerve of the peripheral nervous system (PNS) containing both large - and small-caliber axons of the motoric and sensory system.

The procedure as demonstrated here is a quick, easy and reliable method to measure all standard values relevant for electrophysiology on peripheral nerves in the intact mouse. By taking recordings from a preserved organism, physiological conditions of the nerve environment are guaranteed.

Protocol

The present study was performed according to the Protection of Animals Act of the Federal Republic of Germany (Tierschutzgesetz der Bundesrepublik Deutschland) and was approved by the Thuringian State Office for Food Safety and Consumer Protection (Thüringer Landesamt für Lebensmittelsicherheit und Verbraucherschutz).

1. Setting Up the Measurements

1. Anesthetize the mice by isoflurane/O₂ inhalation - for initiation of anesthesia 3%, for maintenance 2% isoflurane in 100% oxygen (**Figure 1**). Confirm sufficient anesthesia by testing simple reflexes such as movement reflexes and testing of sensitivity for low-grade pain. Use of ointment on the eyes to prevent dryness during anesthesia is recommended but not indispensable because the procedure typically takes just 30 min/animal in total. In case of survival experiments, administer timely longer acting analgesics for managing postoperative pain.
2. Shave the fur covering the hind limbs with an electric razor and perform depilation with a commercially available hair-removal cream while animals are already under analgesia. In order to maintain pathogen-free status throughout the procedure, wear aseptic gloves and always use instruments carefully cleaned with 70% ethanol.
3. Control body temperature stability by a feedback controlled heating plate and rectal thermo probe (**Figure 2**). If necessary, please use a sterile drape to cover the heating plate between the animals in order to keep a sterile experimental environment. Furthermore, it is recommended to use a heating plate, which is electronically controlled via an integrated sensor to limit the heating temperature to ≤ 40 °C in order to avoid tissue damage.

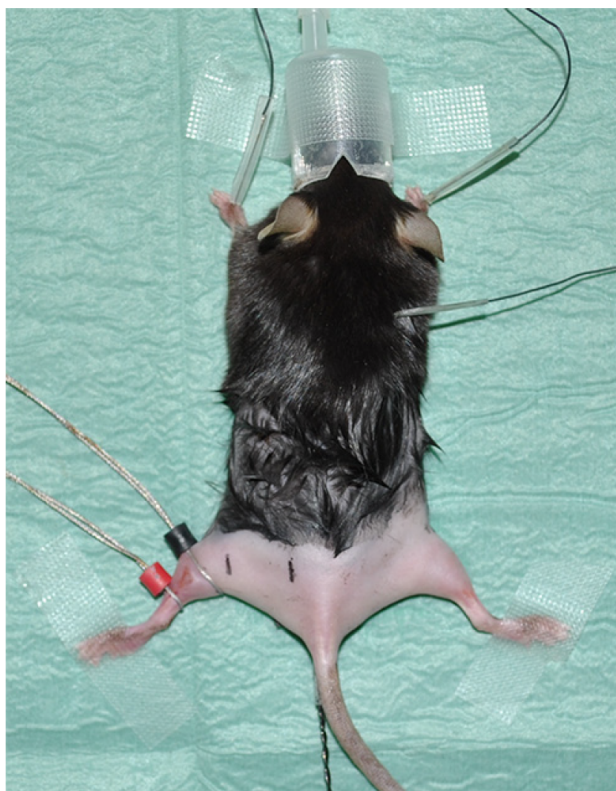


Figure 1. Experimental setup showing an anesthetized mouse with shaved hind limbs.

4. Take electrocardiography (ECG) recordings to monitor the heart rate as a vital parameter. Install three electrodes for ECG recordings as follows: one electrode under the skin of each forelimb and one electrode under the skin in the neck area.
5. Place ring electrodes using contact gel for optimal conductivity / transfer resistance. The sensing electrode (labeled in black) is placed at the position where the gastrocnemius muscle has its maximum diameter. The reference electrode (indicated in red) is placed just beneath the sensing electrode.

Note: Please see 'Material table' for equipment details.

6. Mark the correct positions of measurement with predetermined but consistent distances between the proximal and distal sciatic nerve stimulation and the lead electrode. Experimental proposal: At a distance of 4 mm from the sensing electrode, the distal stimulation will take place. In a distance of 16 mm to the sensing electrode, the proximal stimulation will be carried out (Figure 2).

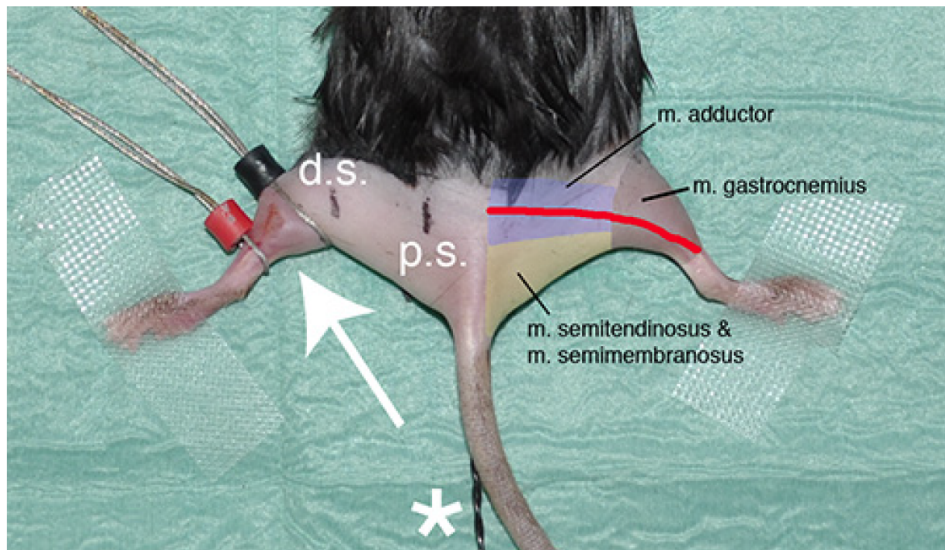
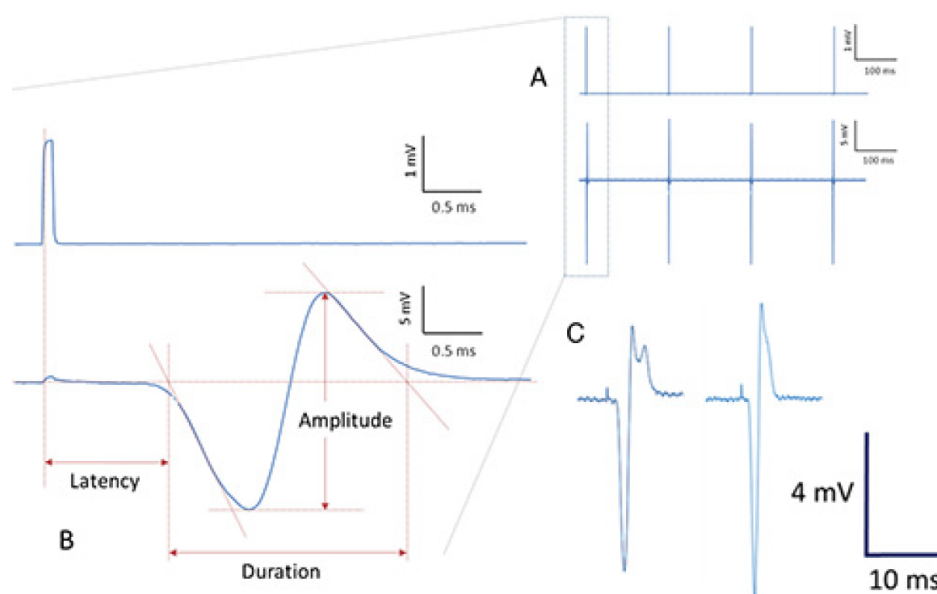


Figure 2. Representative picture showing the experimental situation just prior to the beginning of the measurements. The white arrow indicates the position of the sensing (black) and reference (red) electrode at the gastrocnemius muscle of the left hind limb. The stimulation by needle electrodes will be performed at defined positions in relation to the black sensing electrode. The point of distal stimulation (black mark with "d.s." at the left hind limb) has a distance of 4 mm from the sensing electrode; the place of proximal stimulation (black mark with "p.s.") is 16 mm away. The red line on the right hind limb shows the approximate anatomical course of the sciatic nerve. Furthermore, the rough positions of relevant hind limb muscles are shown as landmarks. The asterisk indicates the rectal thermal probe.

2. Measurement

1. Principle: Perform a series of nerve stimulations with repetitively generated single square-wave pulses of 0.1 msec duration by monopolar disposable 28 G needle electrodes (repetition rate 200 msec; see Figure 3A). For off-line data analysis, it is recommended to simultaneously acquire stimulation signals together with the neuromuscular function response curve (Figure 3B) due to nerve stimulation. Average a series of maximal responses ("representative neuromuscular function response") for subsequent data analysis. In order to produce reliable data, record and later average at least 3 independent, optimal response curves per stimulation site and animal.



- Figure 3. Procedure for data acquisition and analysis (schematic presentation).** Repetitively generated pulses are applied to the sciatic nerve via needle electrodes (upper row in **Figure 3A**). Simultaneously, several corresponding neuromuscular response curves due to stimulation pulses are recorded (lower row in **Figure 3A**). When averaged and magnified, neuromuscular response curves due to stimulation pulses (upper row in **Figure 3B**) show the following characteristic properties (lower row in **Figure 3B**): Latency of the signal response as well as duration and amplitude of the signal are indicated and can be obtained for subsequent calculations and statistics. Irregular signal conduction and / or suboptimal recordings usually result in various signal deformations with more than just one positive and one negative deflection or signal deformation (bimodal shape) with reduced amplitude (**Figure 3C**).
2. Perform proximal stimulation with a needle electrode at determined position ("p.s." in **Figure 2**).
 1. In order to achieve best recording conditions with maximum amplitudes, visualize the actual response curves simultaneous to the stimulation process. By doing so, the experimenter is able to immediately assess the shape of the response curves as well as the size of the amplitude.
 2. If necessary, slightly and carefully manipulate the position and / or the angle of the stimulation needle with respect to the sciatic nerve. This gentle optimization of stimulation conditions allows reaching constant amplitudes with the largest possible value and a response curve of typical biphasic shape (**Figure 4**).
 3. Perform distal stimulation with a needle electrode at determined position ("d.s." in **Figure 2**).
 4. After completion of measurement, transfer the tested mouse to a separate cage until it has regained sufficient consciousness to maintain sternal recumbency. Do not leave an animal unattended and in the company of other animals until it has fully recovered from anesthesia. Administer timely longer acting analgesics for managing postoperative pain. Systemic administration of nonsteroidal anti-inflammatory drugs (NSAIDs) and opioids are recommended for 1-3 days.
 5. Alternatively, sacrifice the still anesthetized mouse in a quick and humane fashion without any further pain for the animal, e.g. by neck dislocation.

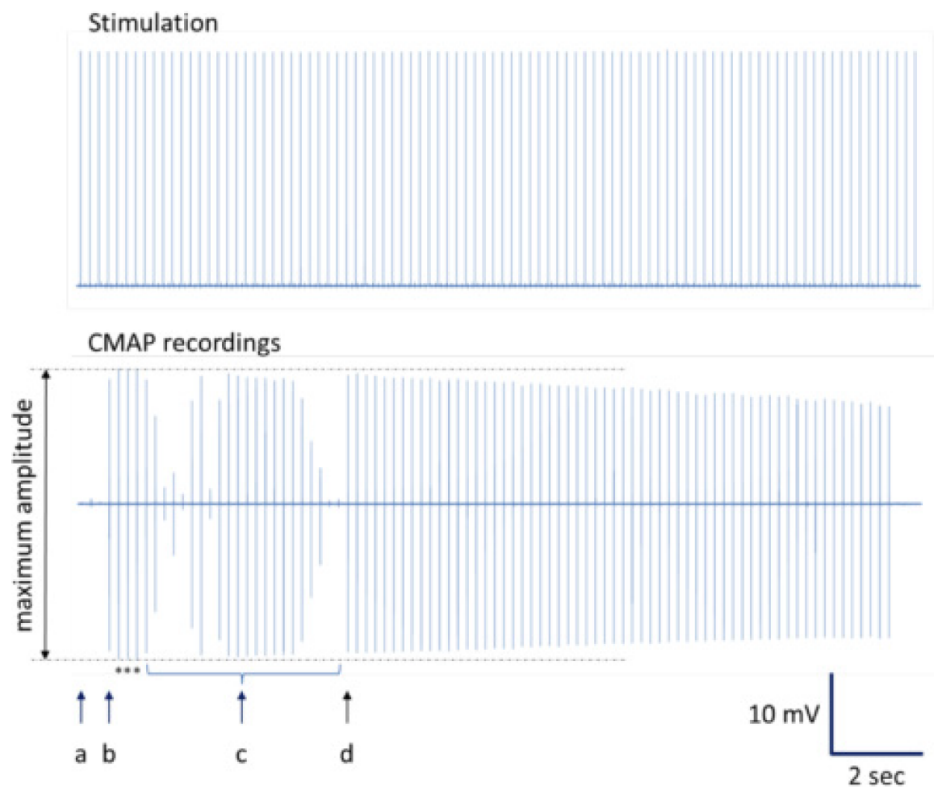


Figure 4. Illustration to determine the CMAP recordings with maximum amplitudes. A complete registration series is presented. (a) Insertion point with minimal CMAP response. (b) Slight stimulation needle movement results in CMAP recordings with maximum amplitudes. (c) Additional changes in needle placement produce CMAP recordings with different amplitudes including near-maximum amplitudes. (d) Stimulation needle replacement with serial CMAP recordings of near-maximum amplitudes. Note: Typical decrement in CMAP amplitudes can occur during repetitive stimulation at optimal stimulation site^{12,13}. Asterisks indicate CMAP recordings with maximum amplitudes depicted for averaging.

3. Analysis

1. Extract nerve conduction parameters based on the representative neuromuscular function response data set using an appropriate software package (e.g. AtisaPro).

Note: Please handle time-related data determination with special care because inflection point determination of compound motor action potential (CMAP) onset and termination can be difficult. A procedure with verified reproducibility is given in **Figure 3B**, where tangents on signal deflections after onset and before termination are used.

2. Calculate 'signal latency' and 'CMAP' values.
 1. Latency' represents the time delay between stimulation and CMAP onset, whereas the time span between CMAP onset of initial negative deflection to initial return to baseline is called 'CMAP duration'. Use the difference between distal and proximal latencies to calculate conduction velocity together with the distance between distal and proximal stimulation sites.

$$\text{conduction velocity} = \text{latency} / \text{distance between stimulation sites}$$

2. CMAP' (compound motor action potential) amplitude represents the magnitude between maximum positive and negative turnaround point of the CMAP signal (given in mV).

$$\text{CMAP} = \text{value 'positive turnaround point'} - \text{value 'negative turnaround point'}$$

Representative Results

We conducted a series of *in vivo* electrophysiological measurements on sciatic nerves of 12 mice in total for this study: 6 animals of each gender. The measurements were performed with the presented protocol and delivered the following results:

Both male and female mice display a mean sciatic nerve conduction velocity of approximately 20 m/sec (**Figure 5**). This is consistent with other measurements in the literature. Furthermore, it shows that there are no relevant differences in nerve conduction speed between males and females according to our data.

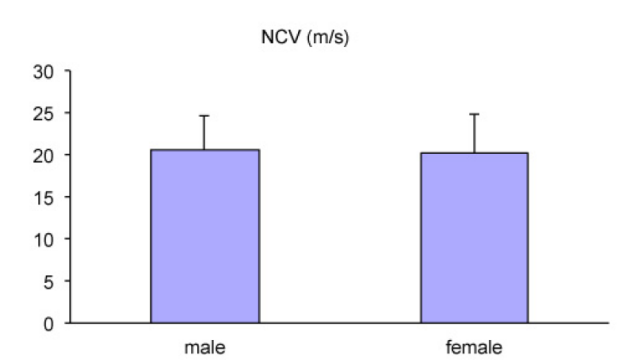


Figure 5. Nerve conduction velocities of the sciatic nerve measured for male and female mice *in vivo*.

Furthermore, we determined the amplitude of compound motor action potentials (CMAP) after proximal and distal stimulation of the sciatic nerve (**Figure 6**). Again, we did not find any apparent variances between genders. However, the CMAP amplitudes in response to proximal stimulation tend to be larger compared to the potential following distal stimulation. This is an expected finding since proximal sciatic nerve stimulation leads typically to an enhanced motor unit recruitment compared to distal stimulation.

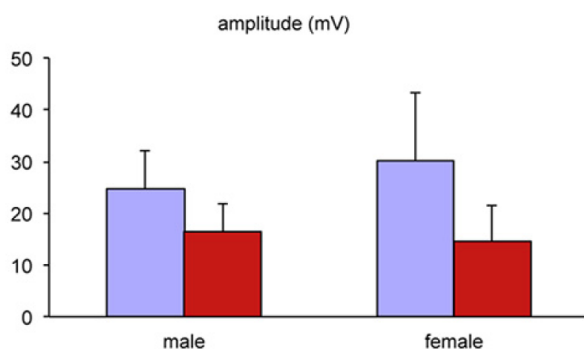


Figure 6. CMAP amplitudes after proximal (purple) and distal (red) stimulation of the sciatic nerve *in vivo*.

Discussion

The described protocol provides an easy and reliable method to determine sciatic nerve conduction properties on anesthetized mice without the need to expose the nerve of interest. Nevertheless, this experimental procedure causes tissue injury by needle puncture. It is therefore a reasonable option to sacrifice the animals after finishing the recordings. However, compared to other more invasive procedures, which require the exposure of the nerve prior to recordings, tissue damage is comparably small^{3,14}. Therefore, repeated measurements are possible and depend on the design of the respective study. However, certain points have to be considered in order to assure consistent results.

In order to perform optimal recording conditions, it is important to reduce skin resistance by complete hair removal, extensive skin cleaning and by using contact gel, all of which permits an appropriately low noise level/contamination during measurements.

Furthermore, it is important to look for optimal, biphasic curve shapes of the detected signals as shown in **Figure 3B**. Occasionally, we also detect curves that are obviously a product of irregular signal conduction through antidrome signal spreading or by some nerve branches. This

scenario results in different signal deformations with more than just one positive and one negative deflection or with a split signal shape, reduced amplitude, and/or broadened signal (Figure 3C). In order to assure the classical orthodrome signal propagation from the point of stimulation to the muscle, only those recordings should be used for quantifications that display a clear shape as shown in Figure 3B.

It must be taken into account that anesthesia may influence electrophysiological recordings on peripheral nerves. Previous reports indicated that the use of isoflurane for anesthesia reduces CMAP values markedly, compared to CMAP measurement under nonanesthetized conditions¹⁴. Nevertheless, the herein used procedure has minimal impact on NCV, delivers reproducible data throughout the experimental performance and is the safest, most effective method of anaesthesia in order to assess peripheral nerve functions in mice¹⁵.

Finally, one has to consider that the sciatic nerve contains both motoric and sensory fiber tracts. A separate analysis of either motor or sensory components is impossible because of the herein used external supra-maximal nerve stimulation and induced orthodrome signal propagation. In order to address this issue, we also performed electrophysiological recordings from sural nerve¹⁶, a pure sensory nerve that can be stimulated at the lateral ankle of the mouse's hind limb. However, the small size of the sural nerve leads to the following problems: First, typically a rather small potential size during recordings can be obtained which required sophisticated data analysis. Second, a certain number of accidental injuries of the sural nerve under study due to puncturing cannot be avoided while trying to accomplish recordings.

In contrast to other protocols¹⁷, it is not necessary to extract the nerve of interest – in our case the sciatic nerve – prior to the measurements. By taking recordings from a preserved organism, physiological conditions of the intact nerve environment are preserved. Furthermore, tissue damage to the mice is small compared to more invasive procedures.

On the other hand, the lack of nerve exposure using this technique makes consistent reproduction of stimulations more difficult since visible confirmation of proper electrode placement with respect to the sciatic nerve is not possible. However, simultaneous monitoring of the response curves during recordings is an easy way to reliably define proper stimulation needle positioning.

Using this method, various existing and new mouse models of neuromuscular diseases could be properly characterized in terms of nerve conduction properties: Demyelinating phenotypes can be clearly distinguished from animal models of primarily muscular or axonal diseases, e.g. as shown in a previous work where the described method has been performed⁷.

Disclosures

The authors have nothing to disclose.

Acknowledgements

This work was supported by SFB 604, DFG MO 1421/2-1 and Krebshilfe 107089 (to H.M.). A.S. is recipient of a Young Investigator Award from the Children's Tumor Foundation (New York, USA).

References

- Kimura, J. *Electrodiagnosis in Diseases of Nerve and Muscle*. 3rd ed. Oxford University Press (2001).
- Rutkove, S. B. Effects of temperature on neuromuscular electrophysiology. *Muscle Nerve*. **24**, 867-882 (2001).
- Xia, R. H., Yosef, N., & Ubogu, E. E. Dorsal caudal tail and sciatic motor nerve conduction studies in adult mice: technical aspects and normative data. *Muscle Nerve*. **41**, 850-856, doi:10.1002/mus.21588 (2010).
- Zielasek, J., Martini, R., & Toyka, K. V. Functional abnormalities in P0-deficient mice resemble human hereditary neuropathies linked to P0 gene mutations. *Muscle Nerve*. **19**, 946-952, doi:10.1002/(SICI)1097-4598(199608)19:8<946::AID-MUS2>3.0.CO;2-8 (1996).
- Raynor, E. M., Ross, M. H., Shefner, J. M., & Preston, D. C. Differentiation between axonal and demyelinating neuropathies: identical segments recorded from proximal and distal muscles. *Muscle Nerve*. **18**, 402-408, doi:10.1002/mus.880180406 (1995).
- Pareyson, D., Scafoli, V., & Laura, M. Clinical and electrophysiological aspects of Charcot-Marie-Tooth disease. *Neuromol. Med.* **8**, 3-22, doi:10.1385/NMM:8:1:123 (2006).
- Schulz, A. et al. Merlin isoform 2 in neurofibromatosis type 2-associated polyneuropathy. *Nat. Neurosci.* **16**, 426-433, doi:10.1038/nn.3348 (2013).
- Lamontagne, A., & Buchthal, F. Electrophysiological studies in diabetic neuropathy. *J. Neurol. Neurosurg. Psychiatry*. **33**, 442-452 (1970).
- Andersen, H., Nielsen, J. F., & Nielsen, V. K. Inability of insulin to maintain normal nerve function during high-frequency stimulation in diabetic rat tail nerves. *Muscle Nerve*. **17**, 80-84, doi:10.1002/mus.880170111 (1994).
- Magda, P. et al. Comparison of electrodiagnostic abnormalities and criteria in a cohort of patients with chronic inflammatory demyelinating polyneuropathy. *Arch. Neurol.* **60**, 1755-1759, doi:10.1001/archneur.60.12.1755 (2003).
- Lindberg, R. L. et al. Motor neuropathy in porphobilinogen deaminase-deficient mice imitates the peripheral neuropathy of human acute porphyria. *J. Clin. Invest.* **103**, 1127-1134, doi:10.1172/JCI5986 (1999).
- Massey, J. M. Electromyography in disorders of neuromuscular transmission. *Sem. Neurol.* **10**, 6-11, doi:10.1055/s-2008-1041247 (1990).
- Stalberg, E., & Falck, B. The role of electromyography in neurology. *Electroencephalogr. Clin. Neurophysiol.* **103**, 579-598 (1997).
- Osuchowski, M. F., Teener, J., & Remick, D. Noninvasive model of sciatic nerve conduction in healthy and septic mice: reliability and normative data. *Muscle Nerve*. **40**, 610-616, doi:10.1002/mus.21284 (2009).
- Oh, S. S., Hayes, J. M., Sims-Robinson, C., Sullivan, K. A., & Feldman, E. L. The effects of anesthesia on measures of nerve conduction velocity in male C57Bl6/J mice. *Neurosci. Lett.* **483**, 127-131, doi:S0304-3940(10)01013-X [pii]10.1016/j.neulet.2010.07.076 (2010).
- Dilley, A., Lynn, B., & Pang, S. J. Pressure and stretch mechanosensitivity of peripheral nerve fibres following local inflammation of the nerve trunk. *Pain*. **117**, 462-472, doi:10.1016/j.pain.2005.08.018 (2005).

17. Vleggeert-Lankamp, C. L. *et al.* Electrophysiology and morphometry of the alpha- and beta-fiber populations in the normal and regenerating rat sciatic nerve. *Exp. Neurol.* **187**, 337-349, doi:10.1016/j.expneurol.2004.01.019 (2004).

5. Zur Veröffentlichung eingereichte Übersichtsarbeit

5.1. „A neuronal function of the tumor suppressor protein merlin”
(Frontiers in Cellular Neuroscience, under review)

Anteil der beteiligten Autoren an der Veröffentlichung:

Dr. Alexander Schulz sichtete die Quellen und schrieb das Manuskript.

Ansgar Zoch half bei der Erstellung der Kapitel zu den Isoformen und Signalwegen Merlins und gab konstruktive Hinweise zur Verbesserung des Manuskripts.

Dr. Helen Morrison erstellte die Endversion des Manuskripts.

A neuronal function of the tumour suppressor protein merlin

Schulz Alexander¹, Ansgar Zoch¹ and Morrison Helen^{1,2}

¹ Leibniz Institute for Age Research, Fritz Lipmann Institute, Jena, Germany

² Corresponding author: Dr. Helen Morrison

Leibniz Institute for Age Research, Fritz Lipmann Institute, Beutenbergstraße 11,
D-07745 Jena, Germany; Fax +49 3641 656133; helen@fli-leibniz.de

Key words: Neurofibromatosis type 2; merlin isoforms; peripheral neuropathy; axon-Schwann cell interaction; tumour development; intelligence

Abstract

Mutagenic loss of the *NF2* tumour suppressor gene encoded protein merlin is known to provoke the hereditary neoplasia syndrome Neurofibromatosis type 2 (NF2). In addition to glial cell-derived tumours in the PNS and CNS, disease-related lesions also affect the skin and the eyes. Furthermore, 60% of NF2 patients suffer from peripheral nerve damage, clinically referred to as peripheral neuropathy. Strikingly, NF2-associated neuropathy often occurs in the absence of nerve damaging tumours, suggesting tumour-independent events. Recent findings indicate an important role of merlin in neuronal cell types concerning neuromorphogenesis, axon structure maintenance and communication between axons and Schwann cells. In this review, we compile clinical and experimental evidences for the underestimated role of the tumour suppressor merlin in the neuronal compartment.

The hereditary disease Neurofibromatosis type 2

Mutations in the *NF2* gene are causative for the autosomal-dominant disease Neurofibromatosis Type 2 (NF2). This rare multiple neoplasia syndrome affects about 1 in 25.000 live births (Baser *et al.* , 2003). However, recent population studies suggest that up to 1 in 300 people will develop a tumour with an underlying sporadic *nf2* mutation in their lifetime (Evans *et al.* , 2009). The heritable NF2 disease is mainly characterized by the development of benign Schwann cell-derived tumours, called schwannomas, due to the mutagenic loss of the tumour suppressor merlin. The hallmark feature of NF2 is the bilateral occurrence of schwannomas at the eighth cranial nerve (vestibular schwannoma). These tumours regularly develop in close vicinity to the 'Obersteiner-Redlich zone' (Roosli *et al.* , 2012) – the boundary between CNS and PNS – where the transition between Schwann cell and oligodendrocyte myelination takes place. Compressive effects of the schwannoma onto the vestibulo-cochlear nerve may subsequently result in loss of hearing and balance. In addition to vestibular schwannomas and schwannomas occurring within the spinal cord and along peripheral nerves, mutations in the *NF2* gene are responsible for virtually all non-hereditary, sporadically occurring schwannomas and 50% of sporadic meningioma cases (Lee *et al.* , 1997).

However, NF2 is a clinical syndrome that presents with a variety of other clinical manifestations. In addition to tumours of various entities, NF2 patients suffer from disease-related lesions that affect the skin and the eyes (for detailed review see (Asthagiri *et al.* , 2009)). Most affected individuals will develop damage to peripheral nerves (peripheral neuropathy) in their lifetime, another common clinical feature in NF2. To date, the pathogenesis of NF2-related neuropathy is not completely understood. Taken together, due to a variety of organ systems being affected by NF2 disease, affected individuals may suffer from severe morbidity in addition to their tumour burden.

Open questions

The tumour suppressor protein merlin, responsible for NF2, is ubiquitously expressed in all tissues during all periods of development (Gutmann *et al.* , 1995). Homozygous deletion of merlin in mice leads to embryonic failure, even before gastrulation (McClatchey *et al.* , 1997). Moreover, conditional ablation of merlin

during embryogenesis results in a global tissue fusion defect (McLaughlin *et al.* , 2007), indicating the importance of merlin from the earliest stage of development. While the role of merlin in glial cell types has been extensively characterized during both development and adulthood, the expression and function in non-tumour related tissues has only occasionally been subjected to mainstream NF2 research.

Microenvironment considerations have become a large field of interest in life science. In fact, any given cell type cannot be comprehensively considered without the context of its environment. Cells in direct or close vicinity influence their neighbouring cells effecting tissue homeostasis. Since Schwann cells – the origin for NF2-related tumours – are in tight and direct contact with axons, which results in extensive inter-cellular crosstalk; one could hypothesize that axons and/or axon-derived signals, respectively, contribute to tumourigenic activity of Schwann cells. We propose that an exclusive focus on Schwann cell biology in NF2 research risks neglecting not only other high-prevalence symptoms, which occur in NF2 disease but also potential microenvironmental issues that could contribute to NF2 tumourigenesis. For instance, peripheral neuropathy has been found to appear in individuals who bear mutations in just one merlin allele and lack a significant load of potentially compressive Schwann cell tumours (Hanemann *et al.* , 2007). This led us to the idea that merlin expressed in neurons might have functions unrelated to its tumour suppressor role in glial cells (Ramesh, 2004).

The tumour suppressor protein merlin

The human *NF2* gene on Chromosome 22q12.2 comprises 17 exons that encode for the 595 amino acid protein merlin; also known as schwannomin (Rouleau *et al.* , 1993, Trofatter *et al.* , 1993). This actin-binding protein belongs to the ezrin–radixin–moesin (ERM) family of proteins that organizes and links membrane proteins to the cortical cytoskeleton (McClatchey and Fehon, 2009). Merlin mediates contact inhibition of proliferation in multiple cell types including Schwann cells (Morrison *et al.* , 2001) and is reported to target many signalling components to restrict proliferation (Morrison *et al.* , 2007). For an extensive review of merlin effected pathways please see (Li *et al.* , 2012). Moreover the tumour suppressor merlin activity is suggested to take place in various cellular compartments, including the cell nucleus (Muranen *et al.* , 2005, Li *et al.* , 2010),

at the plasma membrane (Morrison *et al.* , 2001, Mani *et al.* , 2011), in endosomes (Scoles *et al.* , 2000) and even in association with mitotic spindles during mitosis (Muranen *et al.* , 2007). Although merlin interacts with a high number of different molecules (for detailed review see (Scoles, 2008)) in different locations of the cell, we still conclude that part of merlins tumour suppressor activity is at the plasma membrane mediating contact inhibition of proliferation by regulating several small GTPases like Ras or the Rho GTPase family (see Box 2), as well as the Hippo pathway (Yin *et al.* , 2013).

The appearance of merlin isoforms

The human gene *NF2* and its close homologue the murine gene *Nf2* are subject to alternative splicing (Golovnina *et al.* , 2005). By far the most abundant isoforms are isoform 1 (595 aa) and isoform 2 (590 aa), which differ in their last 11 and 16 amino acids, respectively (Gutmann *et al.* , 1995). While merlin isoform 1 contains exon 17 instead of exon 16, merlin isoform 2 contains the stop codon bearing exon 16, which results in a C-terminal truncated protein (Gutmann *et al.* , 1995).

The altered C-terminus of isoform 2 is hydrophilic and positively charged, while the isoform 1 C-terminus is much less hydrophilic and has no net charge. As a consequence isoform 1 C-terminus binds strongly to the N-terminal FERM domain, while the isoform 2 C-terminus shows only weak binding (Scoles *et al.* , 1998). Apparently, both C-termini can interact with each other, proposing the formation of isoform hetero-dimers (Meng *et al.* , 2000). Due to the structural and charge differences in their very C-terminus, the two main merlin isoforms are likely to have different binding partners. So far, only syntenin, an adaptor protein involved in the subcellular trafficking of receptors, has been shown to specifically interact with the C-terminus of isoform 1 (Jannatipour *et al.* , 2001). However, although merlin has been implicated in receptor trafficking (Lallemant *et al.* , 2009), the functional consequence of a specific merlin isoform 1 interaction, has not been described.

To date, it still remains controversial as to whether both major merlin isoforms exert a tumour suppressive function. No pathogenic mutation that specifically hits one isoform of *NF2* has been described; tumourigenic mutations always inactivate both isoforms (Jacoby *et al.* , 1996, Baser *et al.* , 2005). The only data on functional differences of the two Merlin isoforms comes from *in vitro*

studies: Of the two major merlin isoforms, only isoform 1 was originally thought to have proliferation suppressive potential (Sherman *et al.* , 1997, Gutmann *et al.* , 1999). However, more recent studies suggest that both isoforms have equal proliferation inhibiting potential and so far act similarly in most analysed assays (James *et al.* , 2009, Laulajainen *et al.* , 2012, Zhan *et al.* , 2011). It is reasonable to assume that generally both isoforms perform similar functions. However in an intact cellular system differences between the two major merlin isoforms may be due to their potential sites of activity that could be determined by specific isoform binding partners targeting them to distinct cellular and subcellular localizations (Gavilan *et al.* , 2014). Clearly, a greater focus and effort is required on identifying and cataloguing merlin isoforms and their functions. Early studies investigating the spatiotemporal expression pattern of *NF2/Nf2* isoforms suggest that merlin plays a pivotal role in neuronal tissue, especially during development. High *NF2* expression was found in brains of humans (Bianchi *et al.* , 1994, Schmucker *et al.* , 1999) as well as rodents (Gutmann *et al.* , 1995, Huynh *et al.* , 1996). Interestingly, Gutmann *et al.* reported an increase in isoform 2 expression during neuronal maturation in the cerebral cortex and cerebellum. Additionally, compared to embryonic tissue, neuronal tissue was one of the few organs to retain high expression levels of *Nf2* in adult rats (Gutmann *et al.* , 1995). However, a relevant function of merlin isoform 2, in neurons or other cell types, remained elusive. Only recently have we been able to decipher a unique function for merlin isoform 2, where this specific isoform and not isoform 1 is located and operates in the axonal compartment of neurons (Schulz *et al.* , 2013).

Expression pattern of merlin in neuronal cells

Although merlin has been primarily studied in glial cells, due to loss of merlin primarily attracting attention by causing benign tumours, several lines of evidence now support additional and functional roles of merlin in neurons. Up until now, several studies have reported protein expression of merlin in different types of neuronal cells of both the PNS and CNS.

Through different imaging techniques such as immunohistochemistry and in-situ-hybridization, merlin has been detected in sciatic nerve axons (Schulz *et al.* , 2013), in neurons that belong to autonomic ganglia in the intestinal tract (den Bakker *et al.* , 1999) and dorsal root ganglion cells of the PNS (Schulz *et al.* ,

2013).

In the CNS, merlin appears in motor neurons of the spinal cord (Claudio *et al.* , 1995), cortical neurons (Huynh *et al.* , 1996, Claudio *et al.* , 1995, Schulz *et al.* , 2010), hippocampal neurons (Schulz *et al.* , 2010, Wang *et al.* , 2006), neurons of cranial nerve ganglia (Claudio *et al.* , 1995) and in cerebellar Purkinje cells (den Bakker *et al.* , 1999, Claudio *et al.* , 1995, Schulz *et al.* , 2010, Chen *et al.* , 2001). Particularly in Purkinje cells of the cerebellum, merlin could be functionally associated with neuromorphogenesis and dendritic arborization through the regulation of the small GTPase Rac1 (Schulz *et al.* , 2010). Furthermore, embryonic expression of merlin in neural stem cells could be demonstrated in neuroepithelial cells of the neural tube, as well as in ventricular and subventricular zone of the developing brain (McLaughlin *et al.* , 2007, Lavado *et al.* , 2013). Consistently, the analysis of brain tissue and neuronal progenitor cell (NPC) cultures showed that merlin is predominantly present in neurons (Gronholm *et al.* , 2005).

On the subcellular level, neuronal merlin was found to be expressed in dendrites (Schulz *et al.* , 2010), in axons (Schulz *et al.* , 2013, Seo *et al.* , 2009), in the cytoplasm (Claudio *et al.* , 1995, Stemmer-Rachamimov *et al.* , 1997) and in neuronal synaptic junctions (Gronholm *et al.* , 2005). Conclusively, multiple studies provide evidence for a broad merlin expression in neuronal cell types in both rodent and human tissue.

Polyneuropathy in NF2 patients

Besides the development of multiple gliogenic tumours affecting both the PNS and CNS, many NF2 patients will develop peripheral neuropathy during their lifetime. Affected individuals can suffer from stocking-like hypoalgesia (reduced sensitivity to pain) and hypesthesia (decreased tactile sensibility) as well as loss of vibration sense (pallhypesthesia). Patients may also present with a distal reflex loss that can be followed by a slow but progressive distal muscle atrophy and paresis in later stages of the disease (England and Asbury, 2004). In general, peripheral neuropathy can occur as rather local phenomenon (mononeuropathy simplex or multiplex) or more generalized (polyneuropathy).

Indeed, the exact proportion of NF2 sufferers who develop peripheral nerve damage remains obscure as prevalence numbers vary largely. In a huge clinical

study, peripheral nerve lesions unrelated to tumour masses were observed in 6% of patients suffering from NF2 (Evans *et al.* , 1992). Another investigation with primary focus on NF2-related neuropathy found that clinical signs manifesting as peripheral neuropathy occurred in 47% of investigated patients (Sperfeld *et al.* , 2002). Further electrophysiological examination even revealed evidence of neuropathy in 67% of those individuals (see Box 1).

The general observation that many NF2 patients present with areflexia, which cannot be completely explained by the actual tumour load, suggests that subclinical or masked neuropathy is potentially underdiagnosed in NF2 disease (MacCollin, 1999).

Originally, schwannomas were held to primarily account for observable neuropathic symptoms developing in the course of NF2 (Grazzi *et al.* , 1998). Schwannomas can occur within the spinal cord, on spinal nerve roots, along peripheral nerves and around cranial nerves – with the vestibular nerve being the most frequently involved cranial nerve. The localization of a given tumour naturally determines the presenting features and symptoms of an individual, e.g. affections of a spinal nerve root by a tumour may cause motoric and sensory problems that are clearly related to its innervation area. However, clinical signs of neuropathy mostly appear independently from the site of peripheral nerve schwannomas. In single NF2 patients, polyneuropathy even developed years before other NF2-related symptoms like tumours became evident (Sperfeld *et al.* , 2002).

Although benign in nature, schwannomas are thought to produce pain and other symptoms by compressive effects, thereby impairing axonal integrity in a given nerve. However, the clinical appearance of neuropathy can hardly be explained by the tumour burden alone. Concretely, in some NF2 patients suffering from polyneuropathy, muscle weakness occurs without significant spinal or peripheral nerve tumour burden, suggesting that factors other than gross tumour growth might be responsible for this disorder (Hagel *et al.* , 2002). Besides, surgical resection of gross tumour load along peripheral nerves often lacks a beneficial outcome for affected individuals in terms of neuropathic symptoms (Baumer *et al.* , 2013). Furthermore, NF2-associated polyneuropathy typically involves more than two peripheral nerves and predominantly affects extremities in a distal and symmetric fashion (Sperfeld *et al.* , 2002, Iwata *et al.* , 1998, Iseki *et al.* , 2009), suggesting a systemic rather than local issue. Thus, tumourlets -

hyperproliferative Schwann cells – are also unlikely to explain the complete aetiology of peripheral neuropathy in these patients (Hanemann *et al.* , 2007). However, a high-resolution MRI study – aiming to link tumour load with severity of polyneuropathy in NF2 patients – indicated that non-compressive fascicular microlesions along peripheral nerves correlated with severity of clinical symptoms of NF2-related neuropathy. Apart from that, compressive tumour macrolesions were absent in most neuropathy-affected extremities (Baumer *et al.* , 2013).

Both neuropathological and electrophysiological investigations initially suggested that NF2-related polyneuropathy might develop independently of large solitary schwannomas (Kuo *et al.* , 2010). Hagel *et al.* (Hagel *et al.* , 2002) provided evidence for an axon-intrinsic pathogenesis of neuropathy in sural nerve biopsies, referred to as axonopathy. By determining nerve conduction properties, it was shown that NF2-related peripheral neuropathy is commonly of axonal origin (Sperfeld *et al.* , 2002, Baumer *et al.* , 2013). It was previously hypothesized that NF2 and axonal neuropathies would exist as independent diseases (Bosch *et al.* , 1981, Overweg-Plandsoen *et al.* , 1996). Our group recently deciphered a promising pathomechanism indicating how the loss of merlin could contribute to the development of NF2-related neuropathy in an axon-intrinsic manner (Schulz *et al.* , 2013). Specifically merlin's splice variant isoform 2 promotes, via the GTPase Rho/RhoKinase signalling network, phosphorylation of neurofilaments that are neuron-specific intermediate filaments essential for axon structure and calibre (Perrot *et al.* , 2008). Using a mouse model bearing loss of merlin isoform 2, as well as sural nerve biopsies of NF2 patients, we could show that proper merlin signalling in axons (see Figure 2) is essential for axon structure maintenance. Strikingly, heterozygous deletion of *Nf2* isoform 2 caused haploinsufficiency *in vivo*. This is consistent with clinical findings that *NF2* germline mutations are sufficient to cause polyneuropathy; the loss of the second allele is not required in humans (Hanemann *et al.* , 2007).

Merlin in axon-Schwann cell interactions

The implication of merlin in prevention of Schwann cell tumourigenesis has been extensively studied (Ramesh, 2004, Bretscher *et al.* , 2002). NF2-related schwannomas are encapsulated tumours composed almost entirely of Schwann cells perched on, but not commingled with, normal nerve bundles (Corfas *et al.* ,

2004). However, the benign dignity of NF2-associated Schwann cell-derived tumours is accompanied by sparse response to classical chemotherapy (Hanemann, 2008).

Importantly, the role of merlin in Schwann cells is not just restricted to its tumour suppressive function. It has been reported to play a critical role in the control of Schwann cell numbers and is necessary for the correct organization and regulation of axo-glial heterotypic contacts (Denisenko *et al.* , 2008). Consistently, merlin in Schwann cells has been reported to promote their alignment along axons and ultimately influences myelin segment length (Thaxton *et al.* , 2011).

Generally, the behaviour of Schwann cells is strictly under the control of axonal signals, both during development and in adulthood (Jessen and Mirsky, 2005). As such, Schwann cell actions should not be assessed solely by endogenous Schwann cell signalling pathways, but rather with respect to the influence of axons and vice versa. Signals from axons regulate the intimate communication of Schwann cells with axons of the PNS, provide proliferative and survival signals, and determine the polarization and differentiation programs to either non-myelinating or myelinating phenotypes (Michailov *et al.* , 2004, Taveggia *et al.* , 2005). Moreover, axonal damage triggers rapid Schwann cell de-differentiation, which is accompanied by myelin breakdown, Schwann cell detachment from axons and subsequent proliferation (Scherer, 2001). Consistently, patients with NF2 typically present with different types of benign Schwann cell tumours, in which most Schwann cells lose contact with axons (Corfas *et al.* , 2004, Gijtenbeek *et al.* , 2001). Focusing on the pathogenesis of polyneuropathy affecting NF2 patients, Sperfeld and colleagues (Sperfeld *et al.* , 2002) also suggested that the nerve damaging disease could possibly occur because Schwann cells can no longer adhere properly to the axons. This underlines the importance of the microenvironment of peripheral nerves, where damage to one cell type invariably leads to pathophysiological changes in the other (Fricker and Bennett, 2011).

The literature contains several reported observations suggesting that neuronally expressed merlin could also be involved in the tightly regulated crosstalk between axonal processes and Schwann cells. For instance, N-terminal merlin can be associated with Caspr/paranodin, an axonal transmembrane glycoprotein enriched at paranodal junctions and important for the reciprocal axo-

glial signalling (Denisenko-Nehrbass *et al.* , 2003). Merlin also interacts with β II-spectrin, another molecule supporting the axonal cytoskeleton at paranodes (see Table 1), essential for myelinated axon domain organization (Scoles *et al.* , 1998, Chen *et al.* , 2001, Zhang *et al.* , 2013). Paranodal junctions, in general, are specialized molecular domains of myelinated axons that are thought to promote adhesion between Schwann cells and axons (for detailed review see (Salzer *et al.* , 2008)). This data implies that neuronally expressed merlin could be directly involved in the mechanism determining proper axon-Schwann cell contact formation.

Table 1: Binding or interaction partners of neuronal merlin

Protein	Cell type; species	Reference
Neurofilaments	DRG, sciatic nerve lysates (mouse)	(Schulz <i>et al.</i> , 2013)
Ri β (PKA subunit)	brain lysates (rat)	(Gronholm <i>et al.</i> , 2003)
β II-spectrin	Purkinje cells	(Scoles <i>et al.</i> , 1998, Chen <i>et al.</i> , 2001)
Caspr/paranodin	brain extracts (rat)	(Denisenko-Nehrbass <i>et al.</i> , 2003)
Paxillin	neuroblastoma cells (mouse)	(Yamauchi <i>et al.</i> , 2008)
RhoGDI	Cell lysate from primary neurons (mouse)	(Schulz <i>et al.</i> , 2013, Maeda <i>et al.</i> , 1999)
p190RhoGap	Sciatic nerve lysates (mouse)	(Schulz <i>et al.</i> , 2013)

Recently, we analysed the impact of neuronally expressed merlin on the best-characterized signalling cascade between axon and Schwann cells, namely the Neuregulin1 - ErbB2/3 pathway (Schulz *et al.* , 2013). We were intrigued to find that the Neuregulin splice variant Nrg1 type III, expressed on axonal membranes as a juxtacrine growth factor molecule for Schwann cells, shows reduced expression following loss of merlin *in vitro* and *in vivo* (see Figure 2). In contrast to merlin isoform 2, which is specifically implicated in axon structure maintenance, both major merlin isoforms appear to have equal potency on affecting Nrg1 type III.

In accordance, human sural nerve biopsies taken from NF2 patients suffering from polyneuropathy show a strong and consistent reduction of Nrg1 type III. This is accompanied by a compensatory up-regulation of ErbB2 expression on Schwann cells, as analysed in mice bearing neuron-specific merlin knockout as well as NF2 patient samples. Strikingly, the expression abnormalities of both Nrg1 type III and ErbB2 receptor appear to be very specific to NF2 disease and much more pronounced than in other axonal types of neuropathies (Schulz *et al.* , 2013).

ErbB2/ErbB3 heterodimers are neuregulin receptors which are required for SC development (Citri *et al.* , 2003). In mature peripheral nerves, Nrg1 participates in the regeneration and re-myelination of injured myelinated fibers, processes that involve SC de-differentiation, proliferation and re-differentiation to a myelinating phenotype (Zanazzi *et al.* , 2001).

Interestingly, the loss of merlin activity in Schwann cells is also associated with elevated levels of ErbB receptors in primary SCs (Lallemant *et al.* , 2009). Furthermore, merlin in Schwann cells interacts with CD44 (Morrison *et al.* , 2001), a membrane glycoprotein that enhances neuregulin-induced erbB2 phosphorylation (Sherman *et al.* , 2000). Concerning the regulation of ErbB2/3 receptor expression, merlin obviously has synergistic functions in neurons and Schwann cells, arguing for a holistic function of merlin in both cellular compartments of peripheral nerves. Consequently, ErbB2/3 receptor overexpression has been identified as a potential target for NF2 therapy (Thaxton *et al.* , 2008) using the monoclonal antibodies Trastuzumab (Clark *et al.* , 2008) or Lapatinib (Ammoun *et al.* , 2010).

In adulthood, axons are thought to maintain Schwann cells in a differentiated state to ensure the correct functioning of the nerve (Michailov *et al.* , 2004, Taveggia *et al.* , 2005). It is therefore reasonable to assume that misregulation of axon surface proteins – essential for Schwann cell alignment and differentiation – could contribute to the initial events in tumour development. Notably, a comparable pathogenesis is likely to occur in the related tumour syndrome Neurofibromatosis Type 1 (NF1); possibly the most common inherited disorder caused by a single gene, which is characterized by the development of multiple neurofibromas. Since heterotypic cell–cell contacts control cell proliferation and suppress tumourigenesis (Parrinello *et al.* , 2008), the loss of Schwann cell contact to axons is a frequent and important early event in tumour

development for these highly heterotypic benign tumours of the peripheral nerve sheath. Joseph *et al.* (Joseph *et al.* , 2008) could additionally show that NF1-related tumours arise from differentiated glial cells instead of undifferentiated neural crest cells. These results further support the hypothesis that Schwann cell detachment from axons is an important early event in tumour development – a mechanism neuronally expressed merlin could be also involved in concerning NF2 disease. Taken together, new findings on merlin in the neuronal compartment suggest pathogenesis of NF2 disease, wherein the *NF2* gene encoded protein has cell type-dependent functions in order to prevent tumour formation.

Concluding remarks

In a recent study (Schulz *et al.* , 2013) the impressive number of proteins merlin can interact with was again expanded (for detailed review see (Scoles, 2008)). More precisely, merlin has now been reported to associate with all three classes of cytoskeletal elements; namely actin filaments (James *et al.* , 2001), microtubules (Muranen *et al.* , 2007, Xu and Gutmann, 1998) and intermediate filaments (Schulz *et al.* , 2013). This connection underlines merlin's fascinating role as a versatile cytoskeleton associated molecule involved in a vast variety of signalling events. This makes merlin a highly enigmatic and extraordinary tumour suppressor. However, the contribution of merlin splice variants may play an additional role for the interaction with multiple proteins in a large variety of different cell types.

According to Knudson's two-hit-hypothesis, merlin acts as a classical tumour suppressor. Interestingly, inactivating mutations of merlin seem to have tissue-dependent diverse effects. Loss of heterozygosity, the functional loss of one gene allele in which the other allele was already inactivated, is known to be crucial for merlin owed tumour formation in Schwann cells (Hadfield *et al.* , 2010, Stemmer-Rachamimov *et al.* , 1998). However, deficient effects due to loss of merlin can already be detected in neurons where only one mutation is verifiable (Hanemann *et al.* , 2007); thus explaining why polyneuropathy in NF2 patients is frequently found in the absence of compressive tumours and may even appear chronologically earlier. In line with this notion, axons of mice heterozygous for merlin isoform 2 mutations show functional and morphological abnormalities

(Schulz *et al.* , 2013). However, despite the clear relevance of merlin in neuronal cells of the PNS, a functional role for merlin in CNS neurons still remains elusive.

Grönholm *et al.* (Gronholm *et al.* , 2003) provided a first functional hint for neuronally expressed merlin in the CNS. It was shown to be the first known binding partner of R β , a regulatory subunit of protein kinase A (PKA), which is evidently implicated in learning-related functions (Huang *et al.* , 1995). Consistently, Wassink and colleagues (Wassink *et al.* , 2004) reported that merlin is candidate gene for the development of autism spectrum disorder (ASD), which has been shown to be associated with dendritic spine abnormalities (Penzes *et al.* , 2011). Because dendritic spine morphology in turn is highly susceptible to the activation state of small GTPases (Murakoshi *et al.* , 2011), an impact of merlin on spine morphology and/or plasticity is very likely but has yet to be characterized. In line with this hypothesis, the loss of merlin in neural progenitor cells results in severe reduction in hippocampus size (Lavado *et al.* , 2013); the implications of which in learning and memory acquisition are indisputable.

Despite merlin's possible implication in learning and memory acquisition, no study has ever suggested changes in NF2 patients' intelligence or cognitive performance. Nevertheless, the lack of reports on the mental abilities of persons suffering from NF2 does not equate to the non-existence of such effects. The potential effects of merlin germline mutations could be rather subtle, hidden by the vast environmental noise surrounding human intelligence. Therefore, future studies should address the question which physiological functions of merlin are preserved following *NF2* germline mutations.

Info Boxes

Box 1. Electrophysiological methods as a diagnostic tool for neuromuscular diseases

Electrophysiological measurements are an indispensable tool for investigating the functional integrity of peripheral nerves in both the clinical and laboratory environment (Kimura, 2001). In humans, a large number of neuromuscular disorders and neuropathies diagnostically rely on electrophysiological measurements. By measuring nerve properties as conduction velocity or potential amplitudes of the signal, it is possible to characterize the origin of peripheral nerve diseases. The nerve conduction velocity is highly dependent on rapid signal propagation enabled by myelination. Therefore, demyelinating processes generally show decreased conduction velocities. When significantly reduced, the compound motor action potential (CMAP) – correlating with the number of functional axons – is an indicator for axonal damage. Hence, by means of electrophysiological methods the aetiology of peripheral nerve damage can be discriminated, such as for hereditary neuropathies, diabetic neuropathy, chronic inflammatory demyelinating polyneuropathies (CIDP) or metabolic neuropathies.

Box 2. Rho GTPases in neuronal cell types

GTPase proteins are molecular switches that regulate many important processes in the cell, including the organization of the actin cytoskeleton (Hall, 1998). By provoking local actin rearrangements, the protein family of Rho GTPases is essential for the development of highly polarized cells like neurons (Luo, 2000). Regulators of these small GTPases are therefore of special interest in the broad field of neuromorphogenesis. Merlin has been often shown to exert its various functions through Rho GTPases by determining their activation state (Morrison *et al.*, 2007, Schulz *et al.*, 2010, Flaiz *et al.*, 2007). While GDP-bound molecules are considered to be inactive, GTP-bound proteins actively act on their downstream targets. Considering the significant importance of small GTPases in neuromorphogenesis, merlin, as well as other regulators of small GTPase activity, are plausible candidates for involvement in the vastly complex process of neuronal shape determination. Significantly, mutations in regulators and effectors of Rho GTPases have been associated with diseases of the nervous system,

including mental retardation and motor neuron diseases (Nadif Kasri and Van Aelst, 2008).

Outstanding questions

- How can future disease models and considerations regarding NF2 pathogenesis better emphasize the importance of the nerve microenvironment?
- Does the loss of neuronal merlin and its influence on Schwann cells behaviour impair peripheral nerve regeneration following injury?
- Does merlin deficiency in neurons contribute to NF2-related schwannoma formation?
- Is the downstream signalling of axonal merlin isoform 2 – involving RhoA and ROCK – relevant for other hereditary neuropathies whose mechanisms have yet to be deciphered?
- Are there alterations in cognitive performances in merlin-deficient animals and patients suffering from the NF2 disease?
- What are the specific functions of the two major merlin isoforms? Is there a cell type-specific expression? Which merlin isoforms can compensate for each other with regard to the variety of different merlin functions?

Figure Legends

Fig. 1: Potential role for merlin isoform 2 in NF2-related neuropathy.

Merlin isoform 2 in axons assembles a multi-protein complex with RhoGDI (Maeda *et al.* , 1999) and RhoGAP that leads to the local activation of the small GTPase RhoA by GTP loading (Schulz *et al.* , 2013). This results in subsequent neurofilament phosphorylation through Rho-associated kinase (ROCK). The specific loss of merlin isoform 2 can therefore provoke irregular neurofilament phosphorylation and impaired axon structure maintenance.

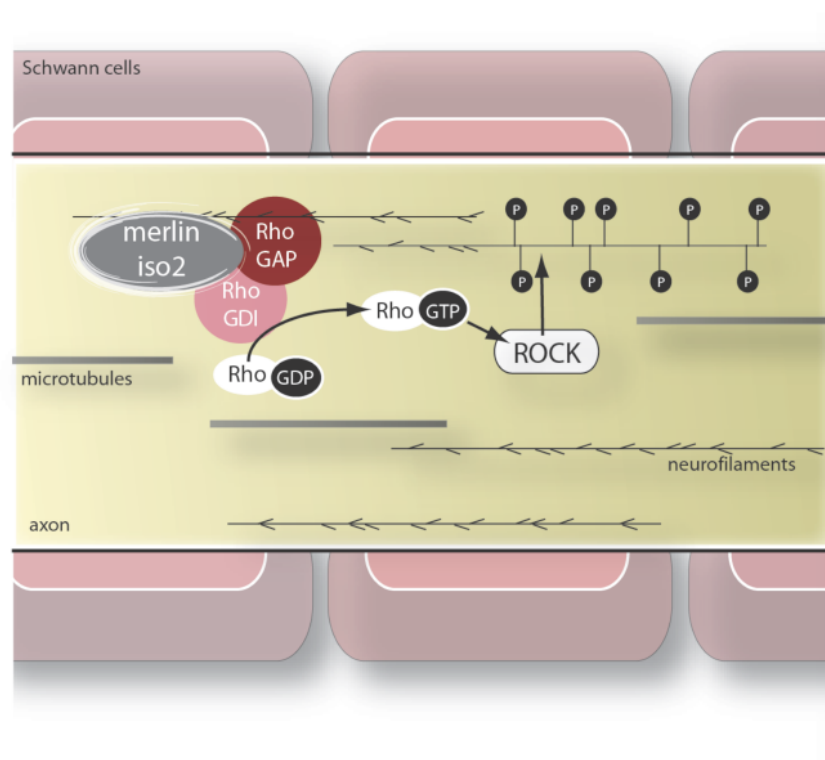
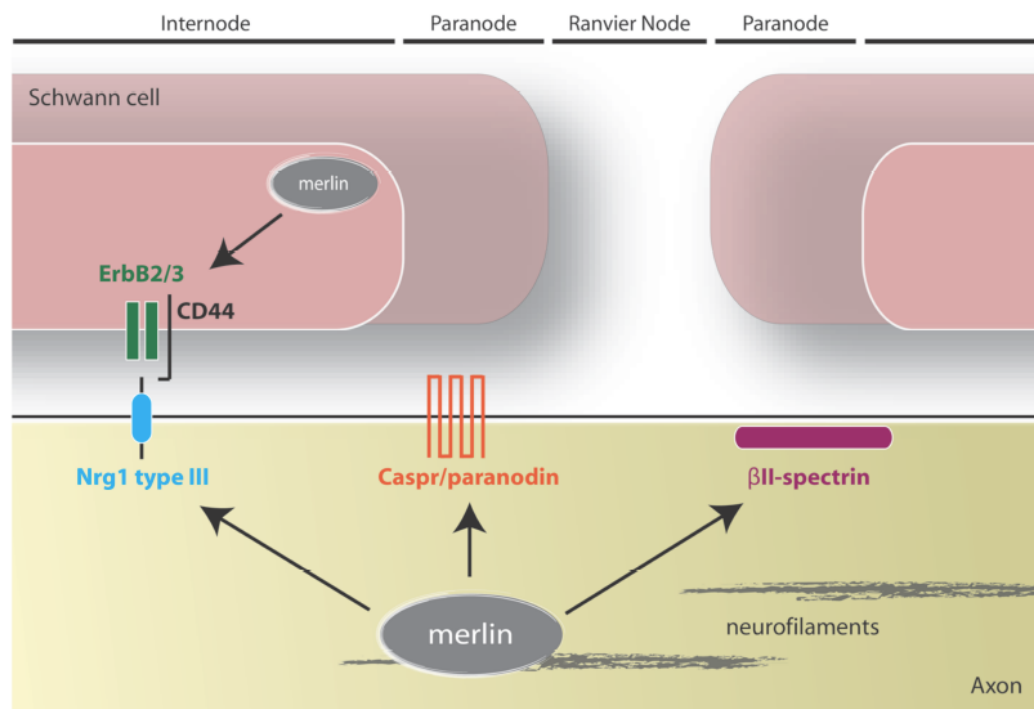


Fig. 2: Interaction of neuronally expressed merlin with axonal proteins essential for axon-Schwann cell signalling.

Merlin in neurons has been shown to interact with two axonal proteins in the paranode region of myelinated axons: Caspr/paranodin (Denisenko-Nehrbass *et al.* , 2003) and β II-spectrin (Scoles *et al.* , 1998). Furthermore, merlin regulates the expression of Nrg1 type III (Schulz *et al.* , 2013), an axon surface molecule with growth factor-like impact on Schwann cell behaviour. Interestingly, the receptor of Nrg1 type III on Schwann cells, ErBB2/3 (Lallemand *et al.* , 2009) as well as its co-

receptor CD44 (Morrison *et al.* , 2001) is regulated by merlin expressed in Schwann cells.



Acknowledgements

The authors would like thank to Prof. Stephan Baader for critical reading of the manuscript and valuable suggestions. This work was supported by SFB 604, DFG MO 1421/2-1 and Krebshilfe 107089. A.S. is a recipient of a Young Investigator Award from the Children's Tumour Foundation.

References

- Baser ME, DG RE, Gutmann DH. Neurofibromatosis 2. Current opinion in neurology. 2003 Feb;16(1):27-33.
- Evans DG, Kalamarides M, Hunter-Schaedle K, Blakeley J, Allen J, Babovic-Vuskanovic D, et al. Consensus recommendations to accelerate clinical trials for neurofibromatosis type 2. Clinical cancer research : an official journal of the American Association for Cancer Research. 2009 Aug 15;15(16):5032-9.
- Roosli C, Linthicum FH, Jr., Cureoglu S, Merchant SN. What is the site of origin of cochleovestibular schwannomas? Audiology & neuro-otology. 2012;17(2):121-5.
- Lee JH, Sundaram V, Stein DJ, Kinney SE, Stacey DW, Golubic M. Reduced expression of schwannomin/merlin in human sporadic meningiomas. Neurosurgery. 1997 Mar;40(3):578-87.
- Astthagiri AR, Parry DM, Butman JA, Kim HJ, Tsilou ET, Zhuang Z, et al. Neurofibromatosis type 2. Lancet. 2009 Jun 6;373(9679):1974-86.
- Gutmann DH, Wright DE, Geist RT, Snider WD. Expression of the neurofibromatosis 2 (NF2) gene isoforms during rat embryonic development. Hum Mol Genet. 1995 Mar;4(3):471-8.
- McClatchey AI, Saotome I, Ramesh V, Gusella JF, Jacks T. The Nf2 tumor suppressor gene product is essential for extraembryonic development immediately prior to gastrulation. Genes Dev. 1997 May 15;11(10):1253-65.
- McLaughlin ME, Kruger GM, Slocum KL, Crowley D, Michaud NA, Huang J, et al. The Nf2 tumor suppressor regulates cell-cell adhesion during tissue fusion. Proc Natl Acad Sci U S A. 2007 Feb 27;104(9):3261-6.
- Hanemann CO, Diebold R, Kaufmann D. Role of NF2 haploinsufficiency in NF2-associated polyneuropathy. Brain Pathol. 2007 Oct;17(4):371-6.
- Ramesh V. Merlin and the ERM proteins in Schwann cells, neurons and growth cones. Nat Rev Neurosci. 2004 Jun;5(6):462-70.
- Rouleau GA, Merel P, Lutchman M, Sanson M, Zucman J, Marineau C, et al. Alteration in a new gene encoding a putative membrane-organizing protein causes neurofibromatosis type 2. Nature. 1993 Jun 10;363(6429):515-21.
- Trofatter JA, MacCollin MM, Rutter JL, Murrell JR, Duyao MP, Parry DM, et al. A novel moesin-, ezrin-, radixin-like gene is a candidate for the neurofibromatosis 2 tumor suppressor. Cell. 1993 Mar 12;72(5):791-800.
- McClatchey AI, Fehon RG. Merlin and the ERM proteins--regulators of receptor distribution and signaling at the cell cortex. Trends in cell biology. 2009 May;19(5):198-206.
- Morrison H, Sherman LS, Legg J, Banine F, Isacke C, Haipiek CA, et al. The NF2 tumor suppressor gene product, merlin, mediates contact inhibition of growth through interactions with CD44. Genes Dev. 2001 Apr 15;15(8):968-80.
- Morrison H, Sperka T, Manent J, Giovannini M, Ponta H, Herrlich P. Merlin/neurofibromatosis type 2 suppresses growth by inhibiting the activation of Ras and Rac. Cancer Res. 2007 Jan 15;67(2):520-7.
- Li W, Cooper J, Karajannis MA, Giancotti FG. Merlin: a tumour suppressor with functions at the cell cortex and in the nucleus. EMBO reports. 2012 Mar;13(3):204-15.
- Muranen T, Gronholm M, Renkema GH, Carpen O. Cell cycle-dependent nucleocytoplasmic shuttling of the neurofibromatosis 2 tumour suppressor merlin. Oncogene. 2005 Feb 10;24(7):1150-8.
- Li W, You L, Cooper J, Schiavon G, Pepe-Caprio A, Zhou L, et al. Merlin/NF2 suppresses tumorigenesis by inhibiting the E3 ubiquitin ligase CRL4(DCAF1) in the nucleus. Cell. 2010 Feb 19;140(4):477-90.

Mani T, Hennigan RF, Foster LA, Conrady DG, Herr AB, Ip W. FERM domain phosphoinositide binding targets merlin to the membrane and is essential for its growth-suppressive function. *Mol Cell Biol*. 2011 May;31(10):1983-96.

Scoles DR, Huynh DP, Chen MS, Burke SP, Gutmann DH, Pulst SM. The neurofibromatosis 2 tumor suppressor protein interacts with hepatocyte growth factor-regulated tyrosine kinase substrate. *Hum Mol Genet*. 2000 Jul 1;9(11):1567-74.

Muranen T, Gronholm M, Lampin A, Lallemand D, Zhao F, Giovannini M, et al. The tumor suppressor merlin interacts with microtubules and modulates Schwann cell microtubule cytoskeleton. *Hum Mol Genet*. 2007 Jul 15;16(14):1742-51.

Scoles DR. The merlin interacting proteins reveal multiple targets for NF2 therapy. *Biochimica et biophysica acta*. 2008 Jan;1785(1):32-54.

Yin F, Yu J, Zheng Y, Chen Q, Zhang N, Pan D. Spatial organization of Hippo signaling at the plasma membrane mediated by the tumor suppressor Merlin/NF2. *Cell*. 2013 Sep 12;154(6):1342-55.

Golovkina K, Blinov A, Akhmametyeva EM, Omelyanchuk LV, Chang LS. Evolution and origin of merlin, the product of the Neurofibromatosis type 2 (NF2) tumor-suppressor gene. *BMC evolutionary biology*. 2005;5:69.

Scoles DR, Huynh DP, Morcos PA, Coulsell ER, Robinson NG, Tamanoi F, et al. Neurofibromatosis 2 tumour suppressor schwannomin interacts with betaII-spectrin. *Nature genetics*. 1998 Apr;18(4):354-9.

Meng JJ, Lowrie DJ, Sun H, Dorsey E, Pelton PD, Bashour AM, et al. Interaction between two isoforms of the NF2 tumor suppressor protein, merlin, and between merlin and ezrin, suggests modulation of ERM proteins by merlin. *J Neurosci Res*. 2000 Nov 15;62(4):491-502.

Jannatipour M, Dion P, Khan S, Jindal H, Fan X, Laganier J, et al. Schwannomin isoform-1 interacts with syntrophin via PDZ domains. *J Biol Chem*. 2001 Aug 31;276(35):33093-100.

Lallemand D, Manent J, Couvelard A, Watilliaux A, Siena M, Chareyre F, et al. Merlin regulates transmembrane receptor accumulation and signaling at the plasma membrane in primary mouse Schwann cells and in human schwannomas. *Oncogene*. 2009 Feb 12;28(6):854-65.

Jacoby LB, MacCollin M, Barone R, Ramesh V, Gusella JF. Frequency and distribution of NF2 mutations in schwannomas. *Genes, chromosomes & cancer*. 1996 Sep;17(1):45-55.

Baser ME, Kuramoto L, Woods R, Joe H, Friedman JM, Wallace AJ, et al. The location of constitutional neurofibromatosis 2 (NF2) splice site mutations is associated with the severity of NF2. *J Med Genet*. 2005 Jul;42(7):540-6.

Sherman L, Xu HM, Geist RT, Saporito-Irwin S, Howells N, Ponta H, et al. Interdomain binding mediates tumor growth suppression by the NF2 gene product. *Oncogene*. 1997 Nov 13;15(20):2505-9.

Gutmann DH, Sherman L, Seftor L, Haipak C, Hoang Lu K, Hendrix M. Increased expression of the NF2 tumor suppressor gene product, merlin, impairs cell motility, adhesion and spreading. *Hum Mol Genet*. 1999 Feb;8(2):267-75.

James MF, Han S, Polizzano C, Plotkin SR, Manning BD, Stemmer-Rachamimov AO, et al. NF2/merlin is a novel negative regulator of mTOR complex 1, and activation of mTORC1 is associated with meningioma and schwannoma growth. *Mol Cell Biol*. 2009 Aug;29(15):4250-61.

Laulajainen M, Melikova M, Muranen T, Carpen O, Gronholm M. Distinct overlapping sequences at the carboxy-terminus of merlin regulate its tumour suppressor and

morphogenic activity. *Journal of cellular and molecular medicine*. 2012 Sep;16(9):2161-75.

Zhan Y, Modi N, Stewart AM, Hieronimus RI, Liu J, Gutmann DH, et al. Regulation of mixed lineage kinase 3 is required for Neurofibromatosis-2-mediated growth suppression in human cancer. *Oncogene*. 2011 Feb 17;30(7):781-9.

Gavilan HS, Kulikaukas RM, Gutmann DH, Fehon RG. In Vivo Functional Analysis of the Human NF2 Tumor Suppressor Gene in *Drosophila*. *PloS one*. 2014;9(3):e90853.

Bianchi AB, Hara T, Ramesh V, Gao J, Klein-Szanto AJ, Morin F, et al. Mutations in transcript isoforms of the neurofibromatosis 2 gene in multiple human tumour types. *Nature genetics*. 1994 Feb;6(2):185-92.

Schmucker B, Tang Y, Kressel M. Novel alternatively spliced isoforms of the neurofibromatosis type 2 tumor suppressor are targeted to the nucleus and cytoplasmic granules. *Hum Mol Genet*. 1999 Aug;8(8):1561-70.

Huynh DP, Tran TM, Nechiporuk T, Pulst SM. Expression of neurofibromatosis 2 transcript and gene product during mouse fetal development. *Cell growth & differentiation : the molecular biology journal of the American Association for Cancer Research*. 1996 Nov;7(11):1551-61.

Schulz A, Baader SL, Niwa-Kawakita M, Jung MJ, Bauer R, Garcia C, et al. Merlin isoform 2 in neurofibromatosis type 2-associated polyneuropathy. *Nat Neurosci*. 2013 Apr;16(4):426-33.

den Bakker MA, Vissers KJ, Molijn AC, Kros JM, Zwarthoff EC, van der Kwast TH. Expression of the neurofibromatosis type 2 gene in human tissues. *The journal of histochemistry and cytochemistry : official journal of the Histochemistry Society*. 1999 Nov;47(11):1471-80.

Claudio JO, Lutchman M, Rouleau GA. Widespread but cell type-specific expression of the mouse neurofibromatosis type 2 gene. *Neuroreport*. 1995 Oct 2;6(14):1942-6.

Schulz A, Geissler KJ, Kumar S, Leichsenring G, Morrison H, Baader SL. Merlin inhibits neurite outgrowth in the CNS. *J Neurosci*. 2010 Jul 28;30(30):10177-86.

Wang Q, Zhou D, Yan B, Lin X, Zhang SF. [Expression of Merlin in cortex of temporal lobe and in hippocampal CA1 region of the Kindling Model of Epilepsy induced by corciaria lactone in rats]. *Sichuan da xue xue bao Yi xue ban = Journal of Sichuan University Medical science edition*. 2006 Jan;37(1):115-7.

Chen Y, Yu P, Lu D, Tagle DA, Cai T. A novel isoform of beta-spectrin II localizes to cerebellar Purkinje-cell bodies and interacts with neurofibromatosis type 2 gene product schwannomin. *Journal of molecular neuroscience : MN*. 2001 Aug;17(1):59-70.

Lavado A, He Y, Pare J, Neale G, Olson EN, Giovannini M, et al. Tumor suppressor Nf2 limits expansion of the neural progenitor pool by inhibiting Yap/Taz transcriptional coactivators. *Development*. 2013 Aug;140(16):3323-34.

Gronholm M, Teesalu T, Tyynela J, Piltti K, Bohling T, Wartiovaara K, et al. Characterization of the NF2 protein merlin and the ERM protein ezrin in human, rat, and mouse central nervous system. *Molecular and cellular neurosciences*. 2005 Apr;28(4):683-93.

Seo PS, Quinn BJ, Khan AA, Zeng L, Takoudis CG, Hanada T, et al. Identification of erythrocyte p55/MPP1 as a binding partner of NF2 tumor suppressor protein/Merlin. *Exp Biol Med (Maywood)*. 2009 Mar;234(3):255-62.

Stemmer-Rachamimov AO, Gonzalez-Agosti C, Xu L, Burwick JA, Beauchamp R, Pinney D, et al. Expression of NF2-encoded merlin and related ERM family proteins in the human central nervous system. *Journal of neuropathology and experimental neurology*. 1997 Jun;56(6):735-42.

England JD, Asbury AK. Peripheral neuropathy. *Lancet*. 2004 Jun 26;363(9427):2151-61.

Evans DG, Huson SM, Donnai D, Neary W, Blair V, Newton V, et al. A clinical study of type 2 neurofibromatosis. *The Quarterly journal of medicine*. 1992 Aug;84(304):603-18.

Sperfeld AD, Hein C, Schroder JM, Ludolph AC, Hanemann CO. Occurrence and characterization of peripheral nerve involvement in neurofibromatosis type 2. *Brain*. 2002 May;125(Pt 5):996-1004.

MacCollin M. Clinical aspects. Baltimore: Johns Hopkins University Press. 1999;Friedman JM, Gutmann DH, MacCollin M, Riccardi VM, editors(Neurofibromatosis type 2):299-326.

Grazzi L, Chiapparini L, Parati EA, Giombini S, D'Amico D, Leone M, et al. Type II neurofibromatosis presenting as quadriceps atrophy. *Italian journal of neurological sciences*. 1998 Apr;19(2):94-6.

Hagel C, Lindenau M, Lamszus K, Kluwe L, Stavrou D, Mautner VF. Polyneuropathy in neurofibromatosis 2: clinical findings, molecular genetics and neuropathological alterations in sural nerve biopsy specimens. *Acta Neuropathol*. 2002 Aug;104(2):179-87.

Baumer P, Mautner VF, Baumer T, Schuhmann MU, Tatagiba M, Heiland S, et al. Accumulation of non-compressive fascicular lesions underlies NF2 polyneuropathy. *Journal of neurology*. 2013 Jan;260(1):38-46.

Iwata A, Kunitomo M, Inoue K. Schwann cell proliferation as the cause of peripheral neuropathy in neurofibromatosis-2. *Journal of the neurological sciences*. 1998 Apr 1;156(2):201-4.

Iseki C, Takahashi Y, Wada M, Kawanami T, Kurita K, Kato T. [A case of neurofibromatosis type 2 (NF2) presenting with late-onset axonal polyneuropathy]. *Rinsho Shinkeigaku*. 2009 Jul;49(7):419-23.

Kuo HC, Chen SR, Jung SM, Wu Chou YH, Huang CC, Chuang WL, et al. Neurofibromatosis 2 with peripheral neuropathies: Electrophysiological, pathological and genetic studies of a Taiwanese family. *Neuropathology : official journal of the Japanese Society of Neuropathology*. 2010 Jan 26.

Bosch EP, Murphy MJ, Cancilla PA. Peripheral neurofibromatosis and peroneal muscular atrophy. *Neurology*. 1981 Nov;31(11):1408-14.

Overweg-Plandsoen WC, Brouwer-Mladin R, Merel P, de Vries L, Bijlsma EK. Neurofibromatosis type 2 in an adolescent boy with polyneuropathy and a mutation in the NF2 gene. *Journal of neurology*. 1996 Oct;243(10):724-6.

Perrot R, Berges R, Bocquet A, Eyer J. Review of the multiple aspects of neurofilament functions, and their possible contribution to neurodegeneration. *Mol Neurobiol*. 2008 Aug;38(1):27-65.

Bretscher A, Edwards K, Fehon RG. ERM proteins and merlin: integrators at the cell cortex. *Nature reviews Molecular cell biology*. 2002 Aug;3(8):586-99.

Corfas G, Velardez MO, Ko CP, Ratner N, Peles E. Mechanisms and roles of axon-Schwann cell interactions. *J Neurosci*. 2004 Oct 20;24(42):9250-60.

Hanemann CO. Magic but treatable? Tumours due to loss of merlin. *Brain*. 2008 Mar;131(Pt 3):606-15.

Denisenko N, Cifuentes-Diaz C, Irinopoulou T, Carnaud M, Benoit E, Niwa-Kawakita M, et al. Tumor suppressor schwannomin/merlin is critical for the organization of Schwann cell contacts in peripheral nerves. *J Neurosci*. 2008 Oct 15;28(42):10472-81.

Thaxton C, Bott M, Walker B, Sparrow NA, Lambert S, Fernandez-Valle C. Schwannomin/merlin promotes Schwann cell elongation and influences myelin segment length. *Molecular and cellular neurosciences*. 2011 May;47(1):1-9.

Jessen KR, Mirsky R. The origin and development of glial cells in peripheral nerves. *Nat Rev Neurosci*. 2005 Sep;6(9):671-82.

Michailov GV, Sereda MW, Brinkmann BG, Fischer TM, Haug B, Birchmeier C, et al. Axonal neuregulin-1 regulates myelin sheath thickness. *Science*. 2004 Apr 30;304(5671):700-3.

Taveggia C, Zanazzi G, Petrylak A, Yano H, Rosenbluth J, Einheber S, et al. Neuregulin-1 type III determines the ensheathment fate of axons. *Neuron*. 2005 Sep 1;47(5):681-94.

Scherer SS, JL. Axon-Schwann cell interactions during peripheral nerve degeneration and regeneration. *Glial cell development : basic principles and clinical relevance*. 2001(Oxford ; New York : Oxford University Press):165-96.

Gijtenbeek JM, Gabreels-Festen AA, Lammens M, Zwarts MJ, van Engelen BG. Mononeuropathy multiplex as the initial manifestation of neurofibromatosis type 2. *Neurology*. 2001 Jun 26;56(12):1766-8.

Fricker FR, Bennett DL. The role of neuregulin-1 in the response to nerve injury. *Future neurology*. 2011 Nov;6(6):809-22.

Denisenko-Nehrbass N, Goutebroze L, Galvez T, Bonnon C, Stankoff B, Ezan P, et al. Association of Caspr/paranodin with tumour suppressor schwannomin/merlin and beta1 integrin in the central nervous system. *Journal of neurochemistry*. 2003 Jan;84(2):209-21.

Zhang C, Susuki K, Zollinger DR, Dupree JL, Rasband MN. Membrane domain organization of myelinated axons requires betaII spectrin. *J Cell Biol*. 2013 Nov 11;203(3):437-43.

Salzer JL, Brophy PJ, Peles E. Molecular domains of myelinated axons in the peripheral nervous system. *Glia*. 2008 Nov 1;56(14):1532-40.

Gronholm M, Vossebein L, Carlson CR, Kuja-Panula J, Teesalu T, Alfthan K, et al. Merlin links to the cAMP neuronal signaling pathway by anchoring the R1beta subunit of protein kinase A. *J Biol Chem*. 2003 Oct 17;278(42):41167-72.

Yamauchi J, Miyamoto Y, Kusakawa S, Torii T, Mizutani R, Sanbe A, et al. Neurofibromatosis 2 tumor suppressor, the gene induced by valproic acid, mediates neurite outgrowth through interaction with paxillin. *Exp Cell Res*. 2008 Jul 1;314(11-12):2279-88.

Maeda M, Matsui T, Imamura M, Tsukita S. Expression level, subcellular distribution and rho-GDI binding affinity of merlin in comparison with Ezrin/Radixin/Moesin proteins. *Oncogene*. 1999 Aug 26;18(34):4788-97.

Schulz A, Kyselyova A, Baader SL, Jung MJ, Zoch A, Mautner VF, et al. Neuronal merlin influences ERBB2 receptor expression on Schwann cells through neuregulin 1 type III signalling. *Brain*. 2013 Dec 5.

Citri A, Skaria KB, Yarden Y. The deaf and the dumb: the biology of ErbB-2 and ErbB-3. *Exp Cell Res*. 2003 Mar 10;284(1):54-65.

Zanazzi G, Einheber S, Westreich R, Hannocks MJ, Bedell-Hogan D, Marchionni MA, et al. Glial growth factor/neuregulin inhibits Schwann cell myelination and induces demyelination. *J Cell Biol*. 2001 Mar 19;152(6):1289-99.

Sherman LS, Rizvi TA, Karyala S, Ratner N. CD44 enhances neuregulin signaling by Schwann cells. *J Cell Biol*. 2000 Sep 4;150(5):1071-84.

Thaxton C, Lopera J, Bott M, Fernandez-Valle C. Neuregulin and laminin stimulate phosphorylation of the NF2 tumor suppressor in Schwann cells by distinct protein

kinase A and p21-activated kinase-dependent pathways. *Oncogene*. 2008 Apr 24;27(19):2705-15.

Clark JJ, Provenzano M, Diggelmann HR, Xu N, Hansen SS, Hansen MR. The ErbB inhibitors trastuzumab and erlotinib inhibit growth of vestibular schwannoma xenografts in nude mice: a preliminary study. *Otology & neurotology : official publication of the American Otological Society, American Neurotology Society [and] European Academy of Otology and Neurotology*. 2008 Sep;29(6):846-53.

Ammoun S, Cunliffe CH, Allen JC, Chiriboga L, Giacotti FG, Zagzag D, et al. ErbB/HER receptor activation and preclinical efficacy of lapatinib in vestibular schwannoma. *Neuro-oncology*. 2010 Aug;12(8):834-43.

Parrinello S, Noon LA, Harrisingh MC, Wingfield Digby P, Rosenberg LH, Cremona CA, et al. NF1 loss disrupts Schwann cell-axonal interactions: a novel role for semaphorin 4F. *Genes Dev*. 2008 Dec 1;22(23):3335-48.

Joseph NM, Mosher JT, Buchstaller J, Snider P, McKeever PE, Lim M, et al. The loss of Nf1 transiently promotes self-renewal but not tumorigenesis by neural crest stem cells. *Cancer cell*. 2008 Feb;13(2):129-40.

James MF, Manchanda N, Gonzalez-Agosti C, Hartwig JH, Ramesh V. The neurofibromatosis 2 protein product merlin selectively binds F-actin but not G-actin, and stabilizes the filaments through a lateral association. *Biochem J*. 2001 Jun 1;356(Pt 2):377-86.

Xu HM, Gutmann DH. Merlin differentially associates with the microtubule and actin cytoskeleton. *J Neurosci Res*. 1998 Feb 1;51(3):403-15.

Hadfield KD, Smith MJ, Urquhart JE, Wallace AJ, Bowers NL, King AT, et al. Rates of loss of heterozygosity and mitotic recombination in NF2 schwannomas, sporadic vestibular schwannomas and schwannomatosis schwannomas. *Oncogene*. 2010 Nov 25;29(47):6216-21.

Stemmer-Rachamimov AO, Ino Y, Lim ZY, Jacoby LB, MacCollin M, Gusella JF, et al. Loss of the NF2 gene and merlin occur by the tumorlet stage of schwannoma development in neurofibromatosis 2. *Journal of neuropathology and experimental neurology*. 1998 Dec;57(12):1164-7.

Huang YY, Kandel ER, Varshavsky L, Brandon EP, Qi M, Idzerda RL, et al. A genetic test of the effects of mutations in PKA on mossy fiber LTP and its relation to spatial and contextual learning. *Cell*. 1995 Dec 29;83(7):1211-22.

Wassink TH, Brzustowicz LM, Bartlett CW, Szatmari P. The search for autism disease genes. *Mental retardation and developmental disabilities research reviews*. 2004;10(4):272-83.

Penzes P, Cahill ME, Jones KA, VanLeeuwen JE, Woolfrey KM. Dendritic spine pathology in neuropsychiatric disorders. *Nat Neurosci*. 2011 Mar;14(3):285-93.

Murakoshi H, Wang H, Yasuda R. Local, persistent activation of Rho GTPases during plasticity of single dendritic spines. *Nature*. 2011 Apr 7;472(7341):100-4.

Kimura J. *Electrodiagnosis in Diseases of Nerve and Muscle: Principles and Practice*: Oxford University Press, USA; 2001.

Hall A. G proteins and small GTPases: distant relatives keep in touch. *Science*. 1998 Jun 26;280(5372):2074-5.

Luo L. Rho GTPases in neuronal morphogenesis. *Nat Rev Neurosci*. 2000 Dec;1(3):173-80.

Flaiz C, Kaempchen K, Matthies C, Hanemann CO. Actin-rich protrusions and nonlocalized GTPase activation in Merlin-deficient schwannomas. *Journal of neuropathology and experimental neurology*. 2007 Jul;66(7):608-16.

6. Diskussion

Das Protein Merlin war 1993 als Tumorsuppressor in verschiedenen Gliazelltypen identifiziert und primär in diesem Kontext analysiert worden (Li *et al.*, 2012). Überdies konnten mehrere Studien zeigen, dass Merlin entscheidenden Einfluss auf die Morphologie und Motilität von Gliazellen, insbesondere von Schwann-Zellen ausüben kann (Pelton *et al.*, 1998; Gutmann *et al.*, 1999).

Lange Zeit war jedoch nicht bekannt, ob Merlin auch in Nervenzellen des PNS vorkommt. Trotz vereinzelter Hinweise auf eine Expression von Merlin auch in Neuronen (Yamauchi *et al.*, 2008; Gronholm *et al.*, 2003), konnte erst 2010 gezeigt werden, dass Merlin in Nervenzellen an der Neuromorphogenese und Neuritogenese wesentlich beteiligt ist (Schulz *et al.*, 2010).

Mit der vorliegenden Arbeit konnte die Relevanz von Merlin in Nervenzellen weiter verdeutlicht und untermauert werden. Wir konnten zeigen, dass Merlin Neuronen-intrinsisch die Aufrechterhaltung der axonalen Struktur bestimmt (Schulz *et al.*, 2013a). Durch die Aktivierung des kleinen G-Proteins RhoA und seiner assoziierten Kinase ROCK (engl. „Rho-associated kinase“) bewirkt es die Phosphorylierung von Neurofilamenten, die direkt die Stabilität der axonalen Fortsätze von Nervenzellen determiniert. Dabei konnte gezeigt werden, dass diese Funktion von Merlin durch die bisher wenig beachtete und kaum untersuchte Isoform 2 hervorgerufen wird.

Eine experimentell induzierte Reduktion der Expression von Merlin Isoform 2 führte in unseren *in vitro*- und *in vivo*-Versuchen zu einer verminderten Aktivierung des Schalterproteins RhoA und einer Hypophosphorylierung von Neurofilamenten. Eine irreguläre Neurofilament-Phosphorylierung wurde in früheren Studien mit axonaler Dysfunktion (Jackson *et al.*, 2005) und erhöhter axonaler Vulnerabilität gegenüber Schädigungen in Verbindung gebracht (Morrison *et al.*, 1987). Außerdem zeigen verschiedene Neuropathien veränderte Grade an Neurofilament-Phosphorylierungen (Perrot *et al.*, 2008). Basierend auf unseren Daten postulieren wir daher, dass die Reduktion der Merlin-Expression in Nervenzellen zu strukturellen Veränderungen führt, die die Entwicklung einer Neuropathie im Rahmen der Erkrankung NF2 begünstigen.

Axone von Mäusen, denen spezifisch Merlin Isoform 2 fehlt, sind weniger rund als die von Wildtyp-Kontrolltieren, zeigen also einen kleineren ‚solidity factor‘,

und weisen eine höhere Dichte zwischen einzelnen Neurofilamenten-Molekülen auf. In immunhistochemischen Färbungen ließ sich bei 8-Wochen-alten Mäusen jedoch keine floride Degeneration jener Axone nachweisen, weswegen wir unsere Resultate im Sinne einer axonalen Atrophie interpretieren (Elder *et al.*, 1999).

Nach der Etablierung eines geeigneten und reliablen Versuchsaufbaus führten wir darüber hinaus elektrophysiologische Untersuchungen an diesen genetisch veränderten Modellmäusen durch (Schulz *et al.*, 2014). Es zeigten sich erneut klare Hinweise für eine axonale Pathogenese der nachgewiesenen Neuropathie: Während die Nervenleitungsgeschwindigkeit durch den Knockout von Merlin Isoform 2 nicht kompromittiert wurde, resultierten deutlich reduzierte Muskelsummenaktionspotentiale (MSAP). Diese Parameterkonstellation spricht für einen axonalen jedoch keinen demyelinisierenden Prozess (Raynor *et al.*, 1995). Außerdem zeigten die gleichen Mäuse Störungen der motorischen Koordination im ‚Rotarod‘-Versuch sowie eine Thermhypästhesie im ‚Hotplate‘-Test (Crawley, 2007).

Im Zuge der Untersuchungen potentieller Signalwege Merlins in Axonen deuten unsere Ergebnisse darauf hin, dass Merlin direkt mit Neurofilamenten interagiert. Andererseits ist es aber auch in einem Komplex mit anderen Proteinen organisiert, die über die Aktivierung des kleinen G-Proteins RhoA entscheiden (Abbildung 5). Diese Moleküle (RhoGDI und p190RhoGAP) bestimmen, ob und in welchem Umfang RhoA-Proteine mit GTP beladen und dadurch biochemisch aktiviert werden (Boulter *et al.*, 2010). Somit legen unsere Daten nahe, dass die axonal exprimierte Isoform 2 von Merlin an der Feinregulierung von RhoA-Signalen in der örtlichen Nähe von Neurofilamenten beteiligt ist.

Hagel *et al.* berichteten im Jahr 2002, dass eine bestimmte Punktmutation innerhalb der Merlin-Sequenz – C784T – bei einem NF2-Patienten gefunden worden war, die offenbar eine schwerwiegende Neuropathie-Symptomatik verursachte (Hagel *et al.*, 2002). Dieses, aufgrund einer Verschiebung des Leserasters (‚Frameshift-Mutation‘), verkürzte Protein ist interessanterweise nicht mehr in der Lage eine Porteinbindung mit RhoGDI einzugehen. Wir konnten zeigen, dass dieses Proteinfragment folglich nicht in der Lage ist, RhoA zu aktivieren oder die Phosphorylierung von Neurofilamenten *in vitro* zu bewirken.

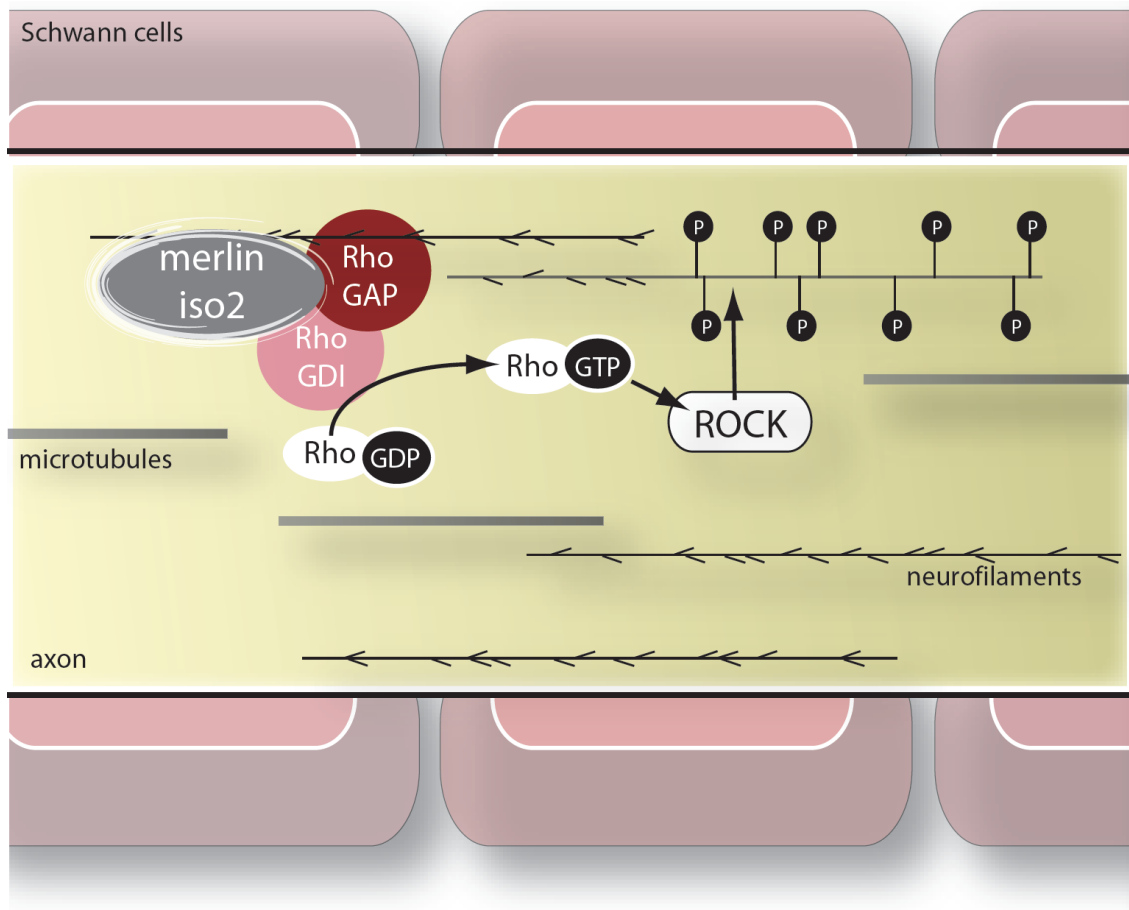


Abb. 5: Schematische Darstellung des Signalweges von Merlin in Axonen basierend auf den experimentellen Ergebnissen der vorliegenden Arbeit (eigene Abbildung).

Um die klinische Relevanz unserer Ergebnisse noch weiter zu untermauern, führten wir ultrastrukturelle Untersuchungen an Nervenbiopsien durch, die von NF2-Patienten entnommen wurden. Es zeigte sich dabei eine weitgehende Übereinstimmung unserer Ergebnisse aus Zellkulturversuchen, Experimenten mit gentechnisch veränderten Mäusen und den Analysen der Patientenbiopsien.

Die Reduktion der regulären Proteinmenge Merlins – bzw. der Verlust der Funktionstüchtigkeit Merlins durch Mutation – geht einher mit einem reduzierten Phosphorylierungsstatus der Neurofilamente. Dies wiederum hat eine signifikanten Abnahme der „interfilament distances“ zu Folge, also dem Abstand zwischen einzelnen, in der Längsachse der Axone gleichförmig orientierten Neurofilamenten. Höchstwahrscheinlich als direkte Konsequenz dieser Veränderungen stellte sich die geometrische Form der Axone in Nervenquerschnitten als entrundet und dysmorph dar, was mithilfe des ‚solidity factors‘ quantifiziert werden konnte.

Bei der qualitativen Analyse von Axonen zeigte sich, dass ein Verlust an Merlin Isoform 2 auch zur Akkumulation von kondensierten Mitochondrien in den Axonen führt. Dies könnte darauf hinweisen, dass zusätzlich zu den strukturellen Veränderungen der neuronalen Fortsätze auch eine Störung der axonalen Transportvorgänge besteht. Dies sollte allerdings nicht sonderlich verwundern, da der Phosphorylierungsgrad von Neurofilamenten selbst assoziiert ist mit der Geschwindigkeit des Transports von Vesikeln innerhalb von Axonen (Shea *et al.*, 2004). Ob allerdings eine pathologische Veränderung axonaler Transportvorgänge Folge oder Ursache der festgestellten axonalen Auffälligkeiten im Zuge von Merlin-Mutationen ist, müssen nachfolgende Untersuchungen klären.

Die in dieser Arbeit dargelegten Ergebnisse tragen zur mechanistischen Aufklärung bei, warum viele NF2-Patienten in Abwesenheit von potentiell Nervenschädigenden Schwann-Zell-Tumoren eine neuropathische Symptomatik entwickeln. Wir deuten unsere Ergebnisse im Sinne einer Neuronen-intrinsischen Pathogenese, die final in der Ausbildung einer ‚axonalen Atrophie‘ kulminiert. Ähnliches wurde zuvor bereits im Kontext von Neurofilament-Mutationen beschrieben (Elder *et al.*, 1999). Ob der hier identifizierte, Merlin-nachgeschaltete Signalweg – die Phosphorylierung von Neurofilamenten durch das G-Protein RhoA und die Kinase ROCK – noch bei anderen hereditären Neuropathie-Erkrankungen (z.B. Charcot-Marie-Tooth) eine Rolle spielt, ist bisher unbekannt, jedoch durchaus vorstellbar und sollte daher untersucht werden.

Die Kernaussage der Arbeit, d.h. dass die Entwicklung der Neuropathien bei NF2-Patienten (zumindest teilweise) Merlin-assoziierte axonale Ursachen hat, ist größtenteils als unerwartet und überraschend zu werten. Gleichzeitig zeigt es aber die Komplexität von Erkrankungen auf, bei denen mehrere Gewebe- oder Zelltypen auf verschiedene Weise durch denselben genetischen Defekt beeinträchtigt sind.

Darüber hinaus ist es erforderlich, die Bedeutung des Mikroumfelds (engl. „microenvironment“) innerhalb eines Gewebes hervorzuheben: Ein bestimmter Zelltyp kann nicht isoliert von dessen Umgebung betrachtet werden. Im vorliegenden Modell des peripheren Nervens sollten deshalb Schwann-Zellen immer auch in Abhängigkeit von bzw. Interaktion mit axonalen Nervenzellfortsätzen untersucht werden und vice versa (Olsson, 1990). Dies wird

auch durch die pathogenetische Forschung belegt, da bekanntermaßen im Rahmen von Erkrankungen der peripheren Nerven die Schädigung des einen Zelltyps unwiderruflich auch zu pathophysiologischen Veränderungen des anderen führt (Fricker and Bennett, 2011).

In einer weiterführenden Studie untersuchten wir deshalb, inwieweit der Verlust von Merlin in Axonen Auswirkungen auf das Verhalten von Schwann-Zellen hat. Unter Nutzung gentechnisch veränderter Mäuse, die einen Neuronen-spezifischen Verlust von Merlin aufwiesen, konnten wir u.a. zeigen, dass diese Axone stärker myelinisiert sind (Schulz *et al.*, 2013b). Dies deutet erneut daraufhin, dass Schwann-Zellen unter strenger Kontrolle von axonalen Signalen stehen – sowohl während der Entwicklung als auch im adulten Nervengewebe (Jessen and Mirsky, 2005). In dieser intimen und bidirektionalen Beziehung zwischen Schwann-Zellen und Axonen sind es maßgeblich die axonalen Fortsätze von Nervenzellen, durch die bestimmt wird, ob Schwann-Zellen ein myelinisierendes oder nicht- myelinisierendes Differenzierungsprogramm einschlagen (Corfas *et al.*, 2004; Taveggia *et al.*, 2005).

In den vergangenen Jahren konnte wiederholt gezeigt werden, dass Merlin in Schwann-Zellen neben seiner proliferationshemmenden Aufgabe als Tumorsuppressorprotein noch andere Funktionen hat. So spielt es eine wichtige Rolle bei der komplexen Etablierung der speziellen Zellkontakte zwischen Schwann-Zellen und Axonen (Denisenko *et al.*, 2008). Darüber hinaus bestimmt Merlin innerhalb von Schwann-Zellen die Länge der Myelinsegmente im Zuge der Myelinisierung peripherer Nerven (Thaxton *et al.*, 2011).

Zusätzlich konnten wir nun experimentell beweisen, dass auch neuronal-exprimiertes Merlin am Aufbau des Kontaktes zwischen axonalen Fortsätzen und Schwann-Zellen mitwirkt: Merlin in Nervenzellen ist in der Lage, die Expression des Oberflächenmoleküls Neuregulin 1 (Nrg1 type III) auf Axonen zu beeinflussen (Schulz *et al.*, 2013b), das die Proliferation, Differenzierung und Myelinisierung von Schwann-Zellen bestimmt (Michailov *et al.*, 2004; Birchmeier and Nave, 2008). Der auf Schwann-Zellen sitzende Rezeptor von Nrg1 type III-Liganden, ErbB2/3 (Brinkmann *et al.*, 2008) – ein bewährtes molekulares Target in der Therapie von Brustkrebs (Behr *et al.*, 2001) –, wird überexprimiert, wenn man die Proteinmenge von Merlin in Axonen verringert. Diese experimentellen Ergebnisse, die mithilfe von konditionellen Knockout-Mäusen gewonnen wurden, konnten wir

wiederum an Nervenbiopsien von NF2-Patienten bestätigen. Im Sinne einer holistischen Wirkungstheorie des Tumorsuppressor-Proteins Merlin lässt sich also feststellen, dass sowohl dessen Verlust in Nervenzellen (Schulz *et al.*, 2013b) und in Schwann-Zellen selbst (Lallemand *et al.*, 2009) eine gesteigerte Expression des ErbB2/3-Rezeptors auf Schwann-Zellen verursacht. Somit eröffnet eine Antikörper-Therapie gegen diese Rezeptor-Tyrosinkinase, z.B. durch Trastuzumab, eine mögliche Behandlungsoption für Patienten mit Neurofibromatose Typ 2 (Clark *et al.*, 2008).

7. Ausblick

Um Therapieoptionen für das Tumorsyndrom NF2 entwickeln zu können bedienen sich viele Forscher verschiedenartig konzipierter Mausmodelle (Gutmann and Giovannini, 2002). Das hiervon gebräuchlichste und weitverbreitetste Tiermodell ist das des konditionellen Knockouts von Merlin in Schwann-Zellen (Giovannini *et al.*, 2000), wodurch die für NF2 charakteristischen Schwannome entstehen. Jedoch berücksichtigt dieses Mausmodell nicht die Bedeutung der Zelltyp-spezifischen Interaktion (Konzept der „microenvironment“) innerhalb peripherer Nerven. Basierend auf unserer Erkenntnis, dass Merlin auch in Nervenzellen eine entscheidende Rolle spielt, wollen wir zukünftig Mäuse kreieren, bei denen Merlin in Schwann-Zellen und/oder Neuronen ausgeschaltet ist.

In einem weiterführenden Ansatz wollen wir der Frage nachgehen, ob nach experimentell gesetztem Nervenschaden im Rahmen eines gestörten Regenerationsablaufs das Auftreten von Schwann-Zell-Tumoren begünstigt wird. Ein axonaler Schaden induziert nämlich die rasche De-Differenzierung von Schwann-Zellen, die begleitet wird vom Abbau der Myelinschicht, dem zellulären ‚Ablösen‘ der Schwann-Zellen von ihren jeweiligen Axonen sowie anschließenden Proliferationsprozessen (Jessen and Richardson, 1997). Zudem zeigt bioptisch entnommenes Nervengewebe von NF2-Patienten typischerweise einen Verlust des Zellkontaktes zwischen Axonen und Schwann-Zellen im Bereich der gutartigen Schwannome (Corfas *et al.*, 2004). Bereits 2002 hatten Sperfeld *et al.* vermutet, dass die NF2-assoziierte Tumorbildung und die periphere Neuropathie zwei Ausprägungen des gleichen Problems sein könnten: der Unfähigkeit einer gewissen Fraktion von Schwann-Zellen im Nerven, den essentiellen Zellkontakt mit Axonen aufrecht zu erhalten (Sperfeld *et al.*, 2002). Wir hoffen, mit den in der Zwischenzeit begonnenen neuen Forschungsvorhaben hierzu weitere Beiträge liefern zu können.

8. Schlussfolgerungen

Auf Grundlage der in dieser Arbeit gezeigten Experimente und Resultate postulieren wir, dass das Tumorsuppressorprotein Merlin nicht nur eine wichtige Funktion in Gliazellen bei der Verhinderung von Tumoren hat, sondern auch die axonale Integrität im PNS entscheidend beeinflusst.

Die spezielle Isoform 2 von Merlin wird in axonalen Fortsätzen von Neuronen exprimiert und steuert die Aktivierung des kleinen G-Proteins RhoA. Dies hat schlussendlich entscheidenden Einfluss auf die Struktur und den Durchmesser von Axonen, indem es die Phosphorylierung von Neurofilamenten durch die Kinase ROCK reguliert.

Wir konnten mechanistisch aufklären, weshalb NF2-Patienten an peripherer Neuropathie erkranken. Aufgrund unserer experimentellen Befunde postulieren wir hierbei erstmals eine Neuronen-intrinsische Pathogenese für das Auftreten der neuropathischen Symptomatik auch ohne Druckschädigung der erkrankten Nerven durch Schwann-Zell-Tumore. Durch den von uns beschriebenen, nachgeschalteten Signalweg von Merlin in Axonen ergibt sich nun die Möglichkeit zur Entwicklung neuer Therapieoptionen zur Behandlung des erblichen Tumorsyndroms Neurofibromatose Type 2. Weiterhin sollte untersucht werden, ob die beteiligten Proteine bei anderen hereditären Neuropathie-Formen bisher unbekannter Genese beteiligt sind.

Weiterführende Experimente konnte unterdessen zeigen, dass neuronal exprimiertes Merlin indirekt bei der Entstehung von Schwannomen beteiligt sein könnte. Durch den spezifischen Verlust von Merlin in Nervenzellen, verstärkt sich die Expression des proliferationsfördernden Rezeptors ErbB2/3 auf Schwann-Zellen. Merlin hat ebenfalls Einfluss auf ein wichtiges Oberflächenmolekül auf Axonen, das u.a. der Etablierung und Aufrechterhaltung von Zellkontakten mit Schwann-Zellen dient. In diesem Sinne sollte in Zukunft eruiert werden, ob Merlin-Mutationen im Zuge von Regenerationsprozessen von peripheren Nerven dazu führen, dass Schwann-Zellen nach erfolgreicher De-Differenzierung und Proliferation sich evtl. nicht wieder suffizient an Axone anlagern können und somit in einem teilungsfreudigen Zustand verbleiben.

9. Literatur – und Quellenverzeichnis

- ASTHAGIRI, A. R., PARRY, D. M., BUTMAN, J. A., KIM, H. J., TSILOU, E. T., ZHUANG, Z. & LONER, R. R. 2009. Neurofibromatosis type 2. *Lancet*, 373, 1974-86.
- BASER, M. E., DG, R. E. & GUTMANN, D. H. 2003. Neurofibromatosis 2. *Curr Opin Neurol*, 16, 27-33.
- BASHOUR, A. M., MENG, J. J., IP, W., MACCOLLIN, M. & RATNER, N. 2002. The neurofibromatosis type 2 gene product, merlin, reverses the F-actin cytoskeletal defects in primary human Schwannoma cells. *Mol Cell Biol*, 22, 1150-7.
- BAUMER, P., MAUTNER, V. F., BAUMER, T., SCHUHMANN, M. U., TATAGIBA, M., HEILAND, S., KAESTEL, T., BENDSZUS, M. & PHAM, M. 2013. Accumulation of non-compressive fascicular lesions underlies NF2 polyneuropathy. *J Neurol*, 260, 38-46.
- BEHR, T. M., BEHE, M. & WORMANN, B. 2001. Trastuzumab and breast cancer. *N Engl J Med*, 345, 995-6.
- BENNETT, C. L. & CHANCE, P. F. 2001. Molecular pathogenesis of hereditary motor, sensory and autonomic neuropathies. *Curr Opin Neurol*, 14, 621-7.
- BERCIANO, J. 2011. Peripheral neuropathies: Molecular diagnosis of Charcot-Marie-Tooth disease. *Nat Rev Neurol*, 7, 305-6.
- BIRCHMEIER, C. & NAVE, K. A. 2008. Neuregulin-1, a key axonal signal that drives Schwann cell growth and differentiation. *Glia*, 56, 1491-7.
- BOSCH, E. P., MURPHY, M. J. & CANCELLA, P. A. 1981. Peripheral neurofibromatosis and peroneal muscular atrophy. *Neurology*, 31, 1408-14.
- BOULTER, E., GARCIA-MATA, R., GUILLUY, C., DUBASH, A., ROSSI, G., BRENNWALD, P. J. & BURRIDGE, K. 2010. Regulation of Rho GTPase crosstalk, degradation and activity by RhoGDI1. *Nat Cell Biol*, 12, 477-83.
- BRANDT, T., STEINBECK, G. & PAUMGARTNER, G. 2005. *Therapie innerer Krankheiten*, Springer.
- BRINKMANN, B. G., AGARWAL, A., SEREDA, M. W., GARRATT, A. N., MULLER, T., WENDE, H., STASSART, R. M., NAWAZ, S., HUMML, C., VELANAC, V., RADYUSHKIN, K., GOEBBELS, S., FISCHER, T. M., FRANKLIN, R. J., LAI, C., EHRENREICH, H., BIRCHMEIER, C., SCHWAB, M. H. & NAVE, K. A. 2008. Neuregulin-1/ErbB signaling serves distinct functions in myelination of the peripheral and central nervous system. *Neuron*, 59, 581-95.
- CLARK, J. J., PROVENZANO, M., DIGGELMANN, H. R., XU, N., HANSEN, S. S. & HANSEN, M. R. 2008. The ErbB inhibitors trastuzumab and erlotinib inhibit growth of vestibular schwannoma xenografts in nude mice: a preliminary study. *Otol Neurotol*, 29, 846-53.
- CORFAS, G., VELARDEZ, M. O., KO, C. P., RATNER, N. & PELES, E. 2004. Mechanisms and roles of axon-Schwann cell interactions. *J Neurosci*, 24, 9250-60.
- CRAWLEY, J. N. 2007. *What's Wrong With My Mouse: Behavioral Phenotyping of Transgenic and Knockout Mice*, Wiley.
- DAHNERT, W. 2003. Radiology Review Manual 5th edition. *Lippincott, Williams & Wilkins*.
- DE WAEGH, S. M., LEE, V. M. & BRADY, S. T. 1992. Local modulation of neurofilament phosphorylation, axonal caliber, and slow axonal transport by myelinating Schwann cells. *Cell*, 68, 451-63.
- DENISENKO, N., CIFUENTES-DIAZ, C., IRINOPOULOU, T., CARNAUD, M., BENOIT, E., NIWA-KAWAKITA, M., CHAREYRE, F., GIOVANNINI, M.,

- GIRAULT, J. A. & GOUTEBROZE, L. 2008. Tumor suppressor schwannomin/merlin is critical for the organization of Schwann cell contacts in peripheral nerves. *J Neurosci*, 28, 10472-81.
- DIENER, H. & WEIMAR, C. 2012. Leitlinien für Diagnostik und Therapie in der Neurologie. *Thieme Verlag*.
- ELDER, G. A., FRIEDRICH, V. L., JR., MARGITA, A. & LAZZARINI, R. A. 1999. Age-related atrophy of motor axons in mice deficient in the mid-sized neurofilament subunit. *J Cell Biol*, 146, 181-92.
- ENGLAND, J. D. & ASBURY, A. K. 2004. Peripheral neuropathy. *Lancet*, 363, 2151-61.
- ETIENNE-MANNEVILLE, S. & HALL, A. 2002. Rho GTPases in cell biology. *Nature*, 420, 629-35.
- EVANS, D. G., HUSON, S. M., DONNAI, D., NEARY, W., BLAIR, V., NEWTON, V. & HARRIS, R. 1992. A clinical study of type 2 neurofibromatosis. *Q J Med*, 84, 603-18.
- FRICKER, F. R. & BENNETT, D. L. 2011. The role of neuregulin-1 in the response to nerve injury. *Future Neurol*, 6, 809-822.
- GIOVANNINI, M., ROBANUS-MAANDAG, E., VAN DER VALK, M., NIWAKAWAKITA, M., ABRAMOWSKI, V., GOUTEBROZE, L., WOODRUFF, J. M., BERNIS, A. & THOMAS, G. 2000. Conditional biallelic Nf2 mutation in the mouse promotes manifestations of human neurofibromatosis type 2. *Genes Dev*, 14, 1617-30.
- GRAZZI, L., CHIAPPARINI, L., PARATI, E. A., GIOMBINI, S., D'AMICO, D., LEONE, M. & BUSSONE, G. 1998. Type II neurofibromatosis presenting as quadriceps atrophy. *Ital J Neurol Sci*, 19, 94-6.
- GRONHOLM, M., VOSSEBEIN, L., CARLSON, C. R., KUJA-PANULA, J., TEESALU, T., ALFTHAN, K., VAHERI, A., RAUVALA, H., HERBERG, F. W., TASKEN, K. & CARPEN, O. 2003. Merlin links to the cAMP neuronal signaling pathway by anchoring the R1beta subunit of protein kinase A. *J Biol Chem*, 278, 41167-72.
- GUTMANN, D. H. & GIOVANNINI, M. 2002. Mouse models of neurofibromatosis 1 and 2. *Neoplasia*, 4, 279-90.
- GUTMANN, D. H., SHERMAN, L., SEFTOR, L., HAIPEK, C., HOANG LU, K. & HENDRIX, M. 1999. Increased expression of the NF2 tumor suppressor gene product, merlin, impairs cell motility, adhesion and spreading. *Hum Mol Genet*, 8, 267-75.
- GUTMANN, D. H., WRIGHT, D. E., GEIST, R. T. & SNIDER, W. D. 1995. Expression of the neurofibromatosis 2 (NF2) gene isoforms during rat embryonic development. *Hum Mol Genet*, 4, 471-8.
- HAGEL, C., LINDENAU, M., LAMSZUS, K., KLUWE, L., STAVROU, D. & MAUTNER, V. F. 2002. Polyneuropathy in neurofibromatosis 2: clinical findings, molecular genetics and neuropathological alterations in sural nerve biopsy specimens. *Acta Neuropathol*, 104, 179-87.
- HANEMANN, C. O., DIEBOLD, R. & KAUFMANN, D. 2007. Role of NF2 haploinsufficiency in NF2-associated polyneuropathy. *Brain Pathol*, 17, 371-6.
- HOFFMAN, P. N., GRIFFIN, J. W. & PRICE, D. L. 1984. Control of axonal caliber by neurofilament transport. *J Cell Biol*, 99, 705-14.
- HUVENEERS, S. & DANEN, E. H. 2009. Adhesion signaling - crosstalk between integrins, Src and Rho. *J Cell Sci*, 122, 1059-69.
- IWATA, A., KUNIMOTO, M. & INOUE, K. 1998. Schwann cell proliferation as the cause of peripheral neuropathy in neurofibromatosis-2. *J Neurol Sci*, 156, 201-4.

- JACKSON, S. J., PRYCE, G., DIEMEL, L. T., CUZNER, M. L. & BAKER, D. 2005. Cannabinoid-receptor 1 null mice are susceptible to neurofilament damage and caspase 3 activation. *Neuroscience*, 134, 261-8.
- JESSEN, K. R. & MIRSKY, R. 2005. The origin and development of glial cells in peripheral nerves. *Nat Rev Neurosci*, 6, 671-82.
- JESSEN, K. R. & RICHARDSON, W. D. 1997. Glial Cell Development: basic principles and clinical relevance. *Oxford University Press, USA*, 2 edition (December 15, 2001).
- KIM, J. H., KIM, I. S., KWON, S. Y., JANG, B. C., SUH, S. I., SHIN, D. H., JEON, C. H., SON, E. I. & KIM, S. P. 2006. Mutational analysis of the NF2 gene in sporadic meningiomas by denaturing high-performance liquid chromatography. *Int J Mol Med*, 18, 27-32.
- KNUDSON, A. G., JR. 1971. Mutation and cancer: statistical study of retinoblastoma. *Proc Natl Acad Sci U S A*, 68, 820-3.
- KUO, H. C., CHEN, S. R., JUNG, S. M., WU CHOU, Y. H., HUANG, C. C., CHUANG, W. L., WEI, K. C. & RO, L. S. 2010. Neurofibromatosis 2 with peripheral neuropathies: Electrophysiological, pathological and genetic studies of a Taiwanese family. *Neuropathology*.
- LALLEMAND, D., MANENT, J., COUVELARD, A., WATILLIAUX, A., SIENA, M., CHAREYRE, F., LAMPIN, A., NIWA-KAWAKITA, M., KALAMARIDES, M. & GIOVANNINI, M. 2009. Merlin regulates transmembrane receptor accumulation and signaling at the plasma membrane in primary mouse Schwann cells and in human schwannomas. *Oncogene*, 28, 854-65.
- LI, W., COOPER, J., KARAJANNIS, M. A. & GIANCOTTI, F. G. 2012. Merlin: a tumour suppressor with functions at the cell cortex and in the nucleus. *EMBO Rep*, 13, 204-15.
- LI, W., YOU, L., COOPER, J., SCHIAVON, G., PEPE-CAPRIO, A., ZHOU, L., ISHII, R., GIOVANNINI, M., HANEMANN, C. O., LONG, S. B., ERDJUMENT-BROMAGE, H., ZHOU, P., TEMPST, P. & GIANCOTTI, F. G. 2010. Merlin/NF2 suppresses tumorigenesis by inhibiting the E3 ubiquitin ligase CRL4(DCAF1) in the nucleus. *Cell*, 140, 477-90.
- LIEM, R. K. & MESSING, A. 2009. Dysfunctions of neuronal and glial intermediate filaments in disease. *J Clin Invest*, 119, 1814-24.
- LUO, L. 2000. Rho GTPases in neuronal morphogenesis. *Nat Rev Neurosci*, 1, 173-80.
- LUTCHMAN, M. & ROULEAU, G. A. 1996. Neurofibromatosis type 2: a new mechanism of tumor suppression. *Trends Neurosci*, 19, 373-7.
- MACCOLLIN, M. & MAUTNER, V. F. 1998. The diagnosis and management of neurofibromatosis 2 in childhood. *Semin Pediatr Neurol*, 5, 243-52.
- MANI, T., HENNIGAN, R. F., FOSTER, L. A., CONRADY, D. G., HERR, A. B. & IP, W. 2011. FERM domain phosphoinositide binding targets merlin to the membrane and is essential for its growth-suppressive function. *Mol Cell Biol*, 31, 1983-96.
- MARTYN, C. N. & HUGHES, R. A. 1997. Epidemiology of peripheral neuropathy. *J Neurol Neurosurg Psychiatry*, 62, 310-8.
- MCCLATCHEY, A. I. & FEHON, R. G. 2009. Merlin and the ERM proteins--regulators of receptor distribution and signaling at the cell cortex. *Trends Cell Biol*, 19, 198-206.
- MCLEOD, J. G. 2000. Sural nerve biopsy. *J Neurol Neurosurg Psychiatry*, 69, 431.
- MICHAILOV, G. V., SEREDA, M. W., BRINKMANN, B. G., FISCHER, T. M., HAUG, B., BIRCHMEIER, C., ROLE, L., LAI, C., SCHWAB, M. H. & NAVE, K. A. 2004. Axonal neuregulin-1 regulates myelin sheath thickness. *Science*, 304, 700-3.

- MORRISON, H., SHERMAN, L. S., LEGG, J., BANINE, F., ISACKE, C., HAIPEK, C. A., GUTMANN, D. H., PONTA, H. & HERRLICH, P. 2001. The NF2 tumor suppressor gene product, merlin, mediates contact inhibition of growth through interactions with CD44. *Genes Dev*, 15, 968-80.
- MORRISON, H., SPERKA, T., MANENT, J., GIOVANNINI, M., PONTA, H. & HERRLICH, P. 2007. Merlin/neurofibromatosis type 2 suppresses growth by inhibiting the activation of Ras and Rac. *Cancer Res*, 67, 520-7.
- MORRISON, J. H., LEWIS, D. A., CAMPBELL, M. J., HUNTLEY, G. W., BENSON, D. L. & BOURAS, C. 1987. A monoclonal antibody to non-phosphorylated neurofilament protein marks the vulnerable cortical neurons in Alzheimer's disease. *Brain Res*, 416, 331-6.
- MURANEN, T., GRONHOLM, M., LAMPIN, A., LALLEMAND, D., ZHAO, F., GIOVANNINI, M. & CARPEN, O. 2007. The tumor suppressor merlin interacts with microtubules and modulates Schwann cell microtubule cytoskeleton. *Hum Mol Genet*, 16, 1742-51.
- MURANEN, T., GRONHOLM, M., RENKEMA, G. H. & CARPEN, O. 2005. Cell cycle-dependent nucleocytoplasmic shuttling of the neurofibromatosis 2 tumour suppressor merlin. *Oncogene*, 24, 1150-8.
- NIESEL, H. C. & VAN AKEN, H. 2006. Lokalanästhesie, Regionalanästhesie, Regionale Schmerztherapie. *Thieme Verlag*.
- NIKOLIC, M. 2002. The role of Rho GTPases and associated kinases in regulating neurite outgrowth. *Int J Biochem Cell Biol*, 34, 731-45.
- OLSSON, Y. 1990. Microenvironment of the peripheral nervous system under normal and pathological conditions. *Crit Rev Neurobiol*, 5, 265-311.
- OVERWEG-PLANDSOEN, W. C., BROUWER-MLADIN, R., MEREL, P., DE VRIES, L. & BIJLSMA, E. K. 1996. Neurofibromatosis type 2 in an adolescent boy with polyneuropathy and a mutation in the NF2 gene. *J Neurol*, 243, 724-6.
- PAREYSON, D. & MARCHESI, C. 2009. Diagnosis, natural history, and management of Charcot-Marie-Tooth disease. *Lancet Neurol*, 8, 654-67.
- PELTON, P. D., SHERMAN, L. S., RIZVI, T. A., MARCHIONNI, M. A., WOOD, P., FRIEDMAN, R. A. & RATNER, N. 1998. Ruffling membrane, stress fiber, cell spreading and proliferation abnormalities in human Schwannoma cells. *Oncogene*, 17, 2195-209.
- PERROT, R., BERGES, R., BOCQUET, A. & EYER, J. 2008. Review of the multiple aspects of neurofilament functions, and their possible contribution to neurodegeneration. *Mol Neurobiol*, 38, 27-65.
- PYKETT, M. J., MURPHY, M., HARNISH, P. R. & GEORGE, D. L. 1994. The neurofibromatosis 2 (NF2) tumor suppressor gene encodes multiple alternatively spliced transcripts. *Hum Mol Genet*, 3, 559-64.
- RAMESH, V. 2004. Merlin and the ERM proteins in Schwann cells, neurons and growth cones. *Nat Rev Neurosci*, 5, 462-70.
- RAYNOR, E. M., ROSS, M. H., SHEFNER, J. M. & PRESTON, D. C. 1995. Differentiation between axonal and demyelinating neuropathies: identical segments recorded from proximal and distal muscles. *Muscle Nerve*, 18, 402-8.
- REINHARDT, F. & GREHL, H. 2012. *Checkliste Neurologie*, Thieme.
- ROULEAU, G. A., MEREL, P., LUTCHMAN, M., SANSON, M., ZUCMAN, J., MARINEAU, C., HOANG-XUAN, K., DEMCZUK, S., DESMAZE, C., PLOUGASTEL, B. & ET AL. 1993. Alteration in a new gene encoding a putative membrane-organizing protein causes neuro-fibromatosis type 2. *Nature*, 363, 515-21.

- SCHMUCKER, B., TANG, Y. & KRESSEL, M. 1999. Novel alternatively spliced isoforms of the neurofibromatosis type 2 tumor suppressor are targeted to the nucleus and cytoplasmic granules. *Hum Mol Genet*, 8, 1561-70.
- SCHULZ, A., BAADER, S. L., NIWA-KAWAKITA, M., JUNG, M. J., BAUER, R., GARCIA, C., ZOCH, A., SCHACKE, S., HAGEL, C., MAUTNER, V. F., HANEMANN, C. O., DUN, X. P., PARKINSON, D. B., WEIS, J., SCHRODER, J. M., GUTMANN, D. H., GIOVANNINI, M. & MORRISON, H. 2013a. Merlin isoform 2 in neurofibromatosis type 2-associated polyneuropathy. *Nat Neurosci*.
- SCHULZ, A., GEISLER, K. J., KUMAR, S., LEICHSENING, G., MORRISON, H. & BAADER, S. L. 2010. Merlin inhibits neurite outgrowth in the CNS. *J Neurosci*, 30, 10177-86.
- SCHULZ, A., KYSELYOVA, A., BAADER, S. L., JUNG, M. J., ZOCH, A., MAUTNER, V. F., HAGEL, C. & MORRISON, H. 2013b. Neuronal merlin influences ERBB2 receptor expression on Schwann cells through neuregulin 1 type III signalling. *Brain*.
- SCHULZ, A., WALTHER, C., MORRISON, H. & BAUER, R. 2014. In Vivo Electrophysiological Measurements on Mouse Sciatic Nerves. e51181.
- SCOLES, D. R. 2008. The merlin interacting proteins reveal multiple targets for NF2 therapy. *Biochim Biophys Acta*, 1785, 32-54.
- SCOLES, D. R., HUYNH, D. P., CHEN, M. S., BURKE, S. P., GUTMANN, D. H. & PULST, S. M. 2000. The neurofibromatosis 2 tumor suppressor protein interacts with hepatocyte growth factor-regulated tyrosine kinase substrate. *Hum Mol Genet*, 9, 1567-74.
- SHEA, T. B., YABE, J. T., ORTIZ, D., PIMENTA, A., LOOMIS, P., GOLDMAN, R. D., AMIN, N. & PANT, H. C. 2004. Cdk5 regulates axonal transport and phosphorylation of neurofilaments in cultured neurons. *J Cell Sci*, 117, 933-41.
- SHERMAN, L., XU, H. M., GEIST, R. T., SAPORITO-IRWIN, S., HOWELLS, N., PONTA, H., HERRLICH, P. & GUTMANN, D. H. 1997. Interdomain binding mediates tumor growth suppression by the NF2 gene product. *Oncogene*, 15, 2505-9.
- SPERFELD, A. D., HEIN, C., SCHRODER, J. M., LUDOLPH, A. C. & HANEMANN, C. O. 2002. Occurrence and characterization of peripheral nerve involvement in neurofibromatosis type 2. *Brain*, 125, 996-1004.
- STEMMER-RACHAMIMOV, A. O., INO, Y., LIM, Z. Y., JACOBY, L. B., MACCOLLIN, M., GUSELLA, J. F., RAMESH, V. & LOUIS, D. N. 1998. Loss of the NF2 gene and merlin occur by the tumorlet stage of schwannoma development in neurofibromatosis 2. *J Neuropathol Exp Neurol*, 57, 1164-7.
- TAVEGGIA, C., ZANAZZI, G., PETRYLAK, A., YANO, H., ROSENBLUTH, J., EINHEBER, S., XU, X., ESPER, R. M., LOEB, J. A., SHRAGER, P., CHAO, M. V., FALLS, D. L., ROLE, L. & SALZER, J. L. 2005. Neuregulin-1 type III determines the ensheathment fate of axons. *Neuron*, 47, 681-94.
- THAXTON, C., BOTT, M., WALKER, B., SPARROW, N. A., LAMBERT, S. & FERNANDEZ-VALLE, C. 2011. Schwannomin/merlin promotes Schwann cell elongation and influences myelin segment length. *Mol Cell Neurosci*, 47, 1-9.
- THIAGALINGAM, S., LAKEN, S., WILLSON, J. K., MARKOWITZ, S. D., KINZLER, K. W., VOGELSTEIN, B. & LENGAUER, C. 2001. Mechanisms underlying losses of heterozygosity in human colorectal cancers. *Proc Natl Acad Sci U S A*, 98, 2698-702.
- YAMAUCHI, J., MIYAMOTO, Y., KUSAKAWA, S., TORII, T., MIZUTANI, R., SANBE, A., NAKAJIMA, H., KIYOKAWA, N. & TANOUE, A. 2008.

Neurofibromatosis 2 tumor suppressor, the gene induced by valproic acid, mediates neurite outgrowth through interaction with paxillin. *Exp Cell Res*, 314, 2279-88.

ZHU, Q., COUILLARD-DESPRES, S. & JULIEN, J. P. 1997. Delayed maturation of regenerating myelinated axons in mice lacking neurofilaments. *Exp Neurol*, 148, 299-316.

10. Lebenslauf

■ Persönliche Daten

Name: Alexander Schulz
Akademischer Titel: Dr. med., M.Sc.
Geburtsdatum: 30. November 1985 in Pößneck
Private Anschrift: Kronfeldstraße 16, 07745 Jena
Telefon: 03641 / 7959485
Familienstand: ledig
Schulausbildung: Gymnasium „Am Weißen Turm“ in Pößneck
Abschluss: Abitur
Zivildienst: Thüringen-Kliniken Pößneck (2004 bis 2005)

■ Ausbildung

Medizinstudium

10/2005 Beginn des Studiums der Humanmedizin an der Friedrich-Schiller-Universität Jena
08/2007 1. Staatsexamen Medizin
10/2009 - 09/2010 Beurlaubung vom Studium zum Zwecke der Forschung
08/2011 - 07/2012 Praktisches Jahr

- Unfallchirurgie (Thüringen-Kliniken „Georgius Agricola“ Pößneck)
- Neurologie (Hans-Berger-Klinik für Neurologie, Friedrich-Schiller-Universität Jena)
- Kardiologie (Katholisches Krankenhaus „St. Johann Nepomuk“ Erfurt)

11/2012 2. Staatsexamen Medizin
01/2013 Approbation als Arzt

Masterstudiengang „Molecular Medicine“

10/2012 Beginn des Masterstudiengangs „Molecular Medicine“ an der Friedrich-Schiller-Universität Jena
05/2013 Abschluss als „Master of Science“
Thema: „Neuronal merlin regulates ErbB2 receptor expression on Schwann cells via Neuregulin 1 type III signaling “

Neurobiologie

06/2013 – 07/2013 Neurobiologischer Kurs am Marine Biological Laboratory (Woods Hole, Massachusetts, USA)
Direktoren: Dr. Graeme Davis und Dr. Timothy Ryan

■ Wissenschaftlicher Tätigkeit

2007 – 2008	Medizinischer Doktorand Arbeitsgruppe Prof. Dr. rer. nat. Stephan Baader Neurobiologie Institut für Anatomie I Friedrich-Schiller-Universität, Jena
seit 2008	Medizinischer und biologischer Doktorand Arbeitsgruppe Dr. rer. nat. Helen Morrison Neuro- und Tumorbologie Leibniz-Institut für Altersforschung Fritz-Lipmann-Institut, Jena
12/2012	Promotion zum Dr. med. mit Auszeichnung Prädikat „Summa cum laude“ Thema: „Das Tumorsuppressorprotein Merlin inhibiert das Neuritenwachstum im ZNS“

■ Auszeichnungen und Stipendien

2012	Young Investigator Award Children's Tumor Foundation (New York, USA)
2013	MBL Scholarship Award Marine Biological Laboratory (Woods Hole, Massachusetts, USA)
2013	Travel Grant (Boehringer Ingelheim Fonds)
2013	Promotionspreis Medizinische Fakultät der Friedrich-Schiller-Universität Jena
2013	NeuroWiss Forschungspreis („Grundlagenforschung“) NeuroWiss e.V. Frankfurt am Main, Deutschland

■ Publikationen

1. **Schulz A**, Geissler KJ, Kumar S, Leichsenring G, Morrison H, Baader SL. Merlin inhibits neurite outgrowth in the CNS. *J. Neurosci.* 2010. 30:10177-10186.
2. Hayn-Leichsenring G, Liebig C, Miething A, **Schulz A**, Kumar S, Schwalbe M, Eiberger B, Baader SL. Cellular distribution of metastasis suppressor 1 and the shape of cell bodies are temporarily altered in Engrailed-2 overexpressing cerebellar Purkinje cells. *Neuroscience.* 2011. 189:68-78.
3. **Schulz A**, Baader SL, Niwa-Kawakita M, Bauer R, Garcia C, Zoch A, Jung MJ, Gutmann DH, Hagel C, Mautner VF, Hanemann CO, Weis J, Schröder JM, Giovannini M, Morrison H. The role of merlin isoform 2 in neurofibromatosis type 2-associated polyneuropathy. *Nat. Neurosci.* 2013. 4:426-33.
4. **Schulz A**, Kyselyova A, Baader SL, Jung MJ, Zoch A, Mautner VF, Hagel C, Morrison H. Neuronal merlin influences ErbB2 receptor expression on Schwann cells via neuregulin 1 type III signalling. *Brain.* 2013. 137:420-32.
5. **Schulz A**, Walther C, Morrison H, Bauer R. In vivo Electrophysiological Measurements on Mouse Sciatic Nerves. *J. Vis. Exp.* 2014. e51181.
6. **Schulz A**, Zoch A, Morrison H. The tumor suppressor protein merlin in neurons. (under review)

11. Danksagung

Mein besonderer Dank soll an dieser Stelle an alle direkt und indirekt Beteiligten der Erstellung dieser Arbeit ergehen.

An erster Stelle möchte ich meiner Chefin Dr. Helen Morrison für ihre uneingeschränkte Unterstützung und freundschaftliche Betreuung bedanken. Ihr beständiges Vertrauen in mutige Projekte und Ideen während unserer langen Zusammenarbeit hat mich sehr geprägt.

Auch unseren langjährigen Kooperationspartnern bin ich zu besonderem Dank verpflichtet, insbesondere und namentlich Prof. Dr. Stephan Baader, der mich initial für die Wissenschaft begeistert hat sowie Prof. Dr. Reinhard Bauer und Prof. Dr. Christian Hagel.

Des Weiteren möchte ich allen Koautoren der in dieser Dissertation enthaltenen Veröffentlichungen danken. Ohne ihre Hilfe und Kontributionen wären die Projekte nicht in diesem Umfang realisierbar gewesen.

Außerdem soll ein herzliches Dankschön an alle Mitglieder meiner Arbeitsgruppe am Fritz-Lipmann-Institut Jena unter der Leitung von Dr. Helen Morrison ergehen.

Schlussendlich möchte ich mich bei meiner Familie, meiner Verlobten und meinem Freundeskreis bedanken, die mich stets bedingungslos unterstützten.

12. Ehrenwörtliche Erklärung

Hiermit erkläre ich, dass

mir die Promotionsordnung der Medizinischen Fakultät der Friedrich-Schiller-Universität bekannt ist,

ich die Dissertation selbst angefertigt habe und alle von mir benutzten Hilfsmittel, persönlichen Mitteilungen und Quellen in meiner Arbeit angegeben sind,

mich folgende Personen bei der Auswahl und Auswertung des Materials sowie bei der Herstellung des Manuskripts unterstützt haben:

Prof. Dr. Stephan Baader (Universität Bonn), Dr. Michiko Niwa-Kawakita (Universität Paris), Prof. Dr. Marco Giovannini (Universität Kalifornien), Prof. Dr. Reinhard Bauer (Universität Jena), Cynthia Garcia und Prof. Dr. David Gutmann (Universität Washington), Dr. Ansgar Zoch, Marie Juliane Jung, Stephan Schacke, Dr. Helen Morrison (FLI Jena) Dr. Xing-Pen, Dr. David Parkinson, Prof. Dr. Oliver Hanemann (Universität Plymouth), Prof. Dr. Christian Hagel, Prof. Dr. Victor-Felix Mautner (Universität Hamburg), Prof. Dr. Joachim Weis, Prof. Dr. Michael Schröder (Universität Aachen) und Christian Walther (Universität Jena),

die Hilfe eines Promotionsberaters nicht in Anspruch genommen wurde und dass Dritte weder unmittelbar noch mittelbar geldwerte Leistungen von mir für Arbeiten erhalten haben, die im Zusammenhang mit dem Inhalt der vorgelegten Dissertation stehen,

dass ich die Dissertation noch nicht als Prüfungsarbeit für eine staatliche oder andere wissenschaftliche Prüfung eingereicht habe und dass ich die gleiche, eine in wesentlichen Teilen ähnliche oder eine andere Abhandlung nicht bei einer anderen Hochschule als Dissertation eingereicht habe.

Jena, am 25. April 2014

Alexander Schulz